The University Of Sheffield.

A JOURNEY DOWN THE RABBIT HOLE: PONDERING PREFERENTIAL ATTACHMENT MODELS WITH LOCATION

By: Mark Alexander Yarrow

A thesis submitted in partial fulfillment
of the requirements for the degree of
Doctor of Philosophy

University of Sheffield
Faculty of Science
School of Mathematics and Statistics
Applied Probability

Copyright

Student: **Dr Mark A Yarrow**
Signature: _____
Date: _____

Supervisor: **Dr Jonathan H Jordan**
Signature: _____
Date: _____

Abstract

We investigate the use of stochastic approximation as a method of identifying conditions necessary to facilitate condensation and coexistence. We did this for a variety of preferential attachment models which are growing by way of some predetermined selection criteria.

The main results presented in this thesis concern the choice of r model. This growth method uses preferential attachment to select r vertices from a graph at time n. These r vertices are subsequently ranked according to fixed location assigned at each of their creations and used as an extra level of comparison between vertices. A new vertex is then attached to one of these r selected vertices according to a predetermined vector of probabilities corresponding to this ranking. We have shown that condensation can occur for any of these vectors, if we can find at least two stable fixed points to the corresponding set of stochastic approximation equations. Following this we investigate the degree distribution and complexity associated to the introduction of a higher dimensional location coefficient.

Our concluding chapter investigates the coexistence between vertices in preferential attachment networks where vertices posses different types and locations. Using similar methods as in the choice of r model we have shown that coexistence can occur in location type models with phase transitions helping to classify different cases.

Acknowledgements

I would like to express my deepest gratitude to both my supervisor Dr Jonathan Jordan and my adviser Dr Nic Freeman for both their guidance academically and personal support throughout my studies. I can say with confidence that if I had not had Jonathan's enthusiasm and kind personality spurring me on, I would not have completed my studies. I would like to thank all of the members of the University of Sheffield's School of Mathematics and Statistics for their continued support during my degree.

I would like to thank my boyfriend Daniel Stevens, mother Suzanne Garrett and grandfather Donald Garrett for their continued motivation of which I am extremely grateful.

Lastly, but by no means least; I would like to thank The Absolut Company who contributed more than they will ever know.

CONTENTS

Page

LIST OF FIGURES

LIST OF TABLES

1. INTRODUCTION

Large scale networks are observable in many different aspects of society, from internet pages connected via hyperlinks, friends or followers in social networks, or even publication networks whereby articles form directed edges to others via citations.

Preferential attachment networks are stochastic models used to simulate complex networks involving noise. Gaining particular notoriety in the early 2000's, the Barabási and Albert [BA99] model of preferential attachment forms the basis for many extensions and adaptations devised to study a multitude of different phenomena. An example which many of these networks exhibit is that of a scale free property present in the distribution of degrees. That is there are a small proportion of high degree vertices which typically possess a larger potential for growth than the more common low degree vertices.

There are a number of standard assumptions which are made when using preferential attachment as a model throughout this thesis. Some of these hold in general whereas some are elsewhere in the literature. The first of these we discuss is that vertices arrive one by one in discrete time with increments between any two vertices being ignored and assumed not influential to the overall network growth. A further assumption we discuss is that the attractiveness of the vertex joining the network has no impact on where it will form edges to. The validity of this assumption depends on the network being modelled. In the Twitter social network, for example, the formation of a (directed) edge can be modelled as one sided based on the attractiveness of existing vertices in the network. The same could be said about the citation network but not so much about some other social networks such as Facebook where an edge

is two sided. The third and final assumption involves the formation of edges. We define $\mathbb{P}(v_{n+1} \sim v)$ as the conditional probability on the graph G_n at time $n+1$ an edge is formed between the new vertex v_{n+1} and a pre-existing vertex in the network $v \in V(G_n)$, as preferential attachment models grow by way of a new vertex v_{n+1} joining G_n. It follows from this that $\mathbb{P}(v_{n+1} \sim v) > 0$, however, in our models an edge between two existing vertices in G_n cannot be formed, i.e. $\mathbb{P}(v_i \sim v_j) = 0$ such that $v_i, v_j \in V(G_n)$. This quality is included in other models in various ways. Similarly to the previously discussed assumption two, whether this condition is met is dependent on the type of network we are trying to model. If we consider the citation network, the formation of edges between pre-existing vertices is rare and can be ignored. This assumption is somewhat unrealistic when considering some networks such as social networks though entirely plausible when considering others including the citation network. The fourth and final assumption, more specific to models discussed in this thesis, is that we do not include death in our network, vertex or edge.

The chapter following this explores the background of preferential attachment, relevant models and introduces important techniques we use to conduct our analysis. We outline general notation used throughout subsequent chapters. In particular we define vertex location as a fixed coefficient assigned at birth allowing for the comparison between vertices in the network disjoint of degree.

During this thesis we discuss two particular models of preferential attachment whereby new vertices make a choice where to form edges based on a sample of existing vertices taken from G_n. The model discussed in Chapters 3-5, evolves in discrete time by sampling r vertices from G_n by way of a generalised preferential attachment kernel. An edge is then formed between the new vertex and a member of this sample according to a predetermined selection criterion based on a ranking on locations of sampled vertices. The first iteration of this model, outlined in Chapter 3, explores a family of models for conditions which we can impose on model parameters which allow for condensation to occur. Condensation occurs when there is asymptotically linear growth in the degree of a vertex (or subset of vertices of size $o(n)$.) Condensation is important in the study of networks for a number of reasons; an interesting

one is in securing the popularity of a vertex as a network grows. From a marketing point of view, investors are interested in the longevity of a product or personality (vertex). Using methods outlined in Section 2.3 we give conditions on whether or not condensation can occur based on the strength of the preferential attachment kernel and model parameters. We show the existence of phase transitions in our model, most notably in relation to the occurrence or lack of condensation.

Chapter 4 explores the degree distribution associated to the model discussed in Chapter 3 in the non-condensation phase. We cannot identify a specific distribution for the condensation phase due to a discontinuity in the limit caused by the condensate. The degree distribution here indeed follows a power law distribution whereby the mass found in the tail correlates directly with the predetermined selection rule.

The model described in chapter 3 is based around the growth of networks by choice based on one dimensional location values. In reality it is fairly unrealistic to assume that a real world network grows wholly based on a choice involving a single attribute. Chapter 5 explores extending the location assigned to each vertex at birth to a multidimensional vector. Due to the complexity of this model we reduced the complexity in order to prove the existence of a phase transition existing between the condensation and non-condensation phases.

The concluding chapter, Chapter 6, explores a different model to that discussed in Chapters 3-5. We have vertices occupying two locations, decided at birth; vertices are then assigned one of two types based on a predetermined classification rule. This classification rule involves the m edges formed between the new vertex and vertices in G_n selected using preferential attachment involving a biasing coefficient where relevant. We detail conditions we can implement on the strength of the biasing coefficient to allow for coexistence between subsets of the four combinations of types and locations; identifying phase transitions between the coexistence and non-coexistence phases. Coexistence is where a positive proportion of the edge mass exists at sets of vertices possessing different types in the limit as $n \to \infty$.

2. BACKGROUND

2.1 Preferential attachment

The late 1950's saw the publication of the first notable random graph models by Erdős and Rényi [ER59, ER60] and Gilbert [Gil59]. A description of the Erdős-Rényi random graph model is as follows. We have an undirected graph $G_{n,N}$ on n labelled vertices $\{v_1, v_2, \ldots, v_n\}$ and a subset of N edges contained in the edge set $E(G_{n,N})$. Here $E(G_{n,N})$ contains exactly one copy of all $\frac{n(n-1)}{2}$ possible edges in $G_{n,N}$. Concisely, the Erdős-Rényi model explores the probability of the graph $G_{n,N}$ occurring whereby each of the $\binom{\binom{n}{2}}{N}$ possible graphs are equally likely to occur. Soon after the publication of the Erdős-Rényi random graph model Gilbert [Gil59] proposed the Binomial random graph model. Here Gilbert examines graphs on n vertices and N edges denoted by $G_{n,p}$. The probability p is assigned to the event of each of the $\binom{n}{2}$ edges existing in $G_{n,p}$. An alternative definition could be starting with the edge-less graph on n vertices and forming an edge between each pair of vertices independently of each other according to a Bernoulli random variable with probability p. Gilbert [Gil59] fails to specify the the independence of the appearance of eadges

There is no question both the Erdős-Rényi and Binomial random graph models are inaccurate representations of growing networks, firstly because they both model static (non-growing) random graphs and secondly because they treat the existence of every edge as equally likely. It is observable in most growing networks that this simply isn't true; moreover vertices with higher degree tend to have a greater potential for growth. An example of this is the Twitter social network where those members

with the highest number of followers tend to remain in the top spots as time passes, sometimes regardless of activity. We show this type of behaviour in Figure 2.1 which depicts the current highest five followed people on the social network. Looking back over seven years we can see they have remained in similar positions. This is particularly interesting when considering the other 320 million members of the network, many of which are more active than those depicted in Figure 2.1.

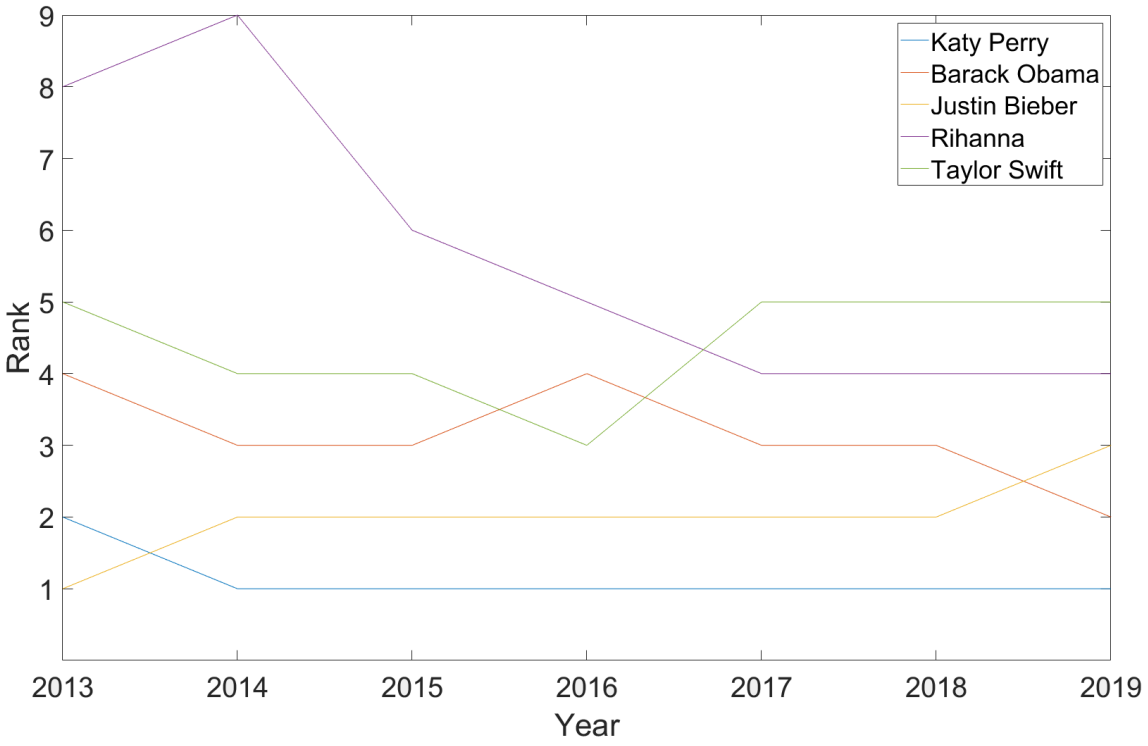

Fig. 2.1: A graph depicting the rankings of the current five most followed members of Twitter over the past seven years. Data collected from the following sites: friendorfollow.com/twitter/most-followers/,thenewdaily.com.au/entertainment/celebrity/2018/03/29/instagram-twitter-most-followers, /buytwitterfollowersreview.org/10-followed-accounts-twitter, time.com/4591951/top-twitter-celebrities-2016, www.forbes.com/sites/maddieberg/2015/06/29/twitters-most-followed-celebrities-retweets-dont-always-mean-dollars, blog.twitter.com/en_gb/a/en-gb/2014/2014-the-year-on-twitteranddavidpapp.com/2013/10/16/top-10-twitter-accounts-by-most-followers-as-of-october-16-2013.

It is clear the vertex degree distribution associated to a growing networks such as social networks, sexual networks or citation networks should approximately follow a Pareto "Power law" distribution. Though these preferential attachment based networks should follow a power law distribution, suggested by [Arn15], showing evidence

of this property in data via a log-log scale is not enough evidence to conclude this definitively. Moreover, it is not true that a network growing by preferential attachment is necessarily a good model for growing networks. This power law distribution takes into consideration the rarity of vertices with high degree compared with the more common vertices with lower degrees. The general form of power law distribution governing the proportion of degree k vertices in G_n denoted by p_k is given by

$$p_k \sim \beta k^{-\gamma} \tag{2.1}$$

as $k \to \infty$, here the degree $k \in \mathbb{N}$. Both β and γ are constants approximated by way of an algorithm such as maximum likelihood or MCMC to fit a Yule-Simon distribution to observed data. Figure 2.2 below depicts the typical power law trend observable in real world networks.

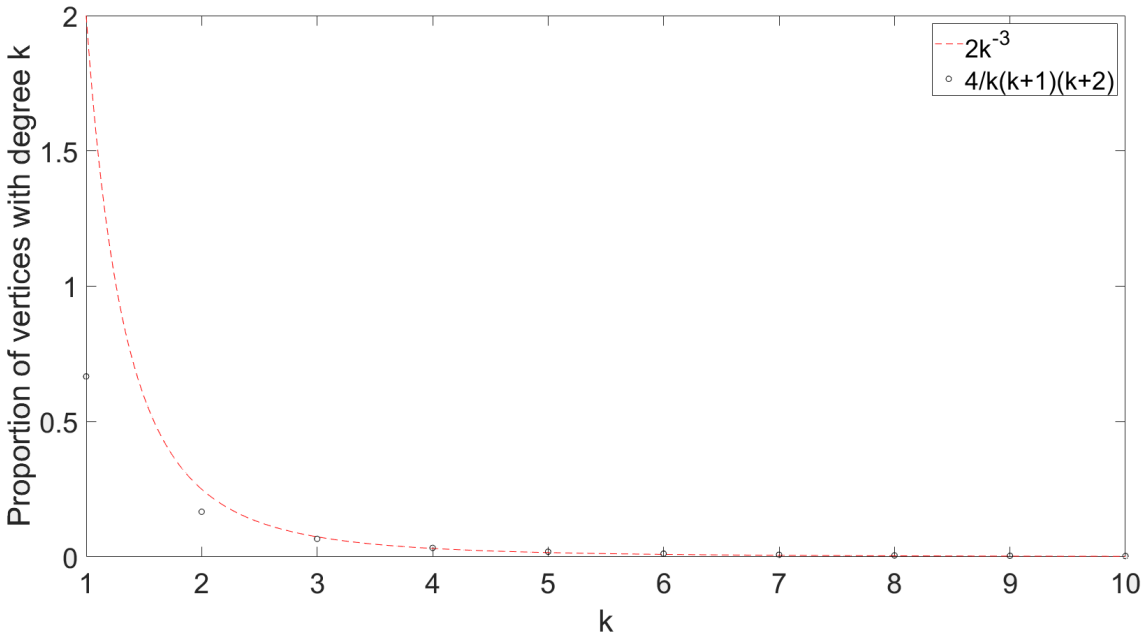

Fig. 2.2: The proportion of vertices of degree k plotted both using the Barabási-Albert models degree distribution given by (2.3) for $m = 1$ and as approximated by the power law distribution given by (2.1).

A number of studies have been conducted into the power law index of real world

networks. Typically they found that $\gamma \in (2,3)$ such as [CDMG06] where it was found that the income distribution in Australia and Italy follows a power law distribution with approximately $\gamma = 2.3 \pm 0.2$ and $\gamma = 2.5 \pm 0.1$ respectively. The name "scale-free" was given to networks which possesses a degree distribution following a power law.

Shortly before the turn of the millennium the first widely used model of scale-free networks was devised. The Barabási-Albert [BA99] preferential attachment model which has similarities to models devised by Yule [Yul25] and Simon [Sim55], gave birth to a whole new way of describing network growth. Here, authors proposed a model of evolving networks where edges were formed by new vertices at time $n+1$ and existing vertices in the graph based on the state of the graph at time n, G_n. Networks growing in this way favour vertices possessing higher degree at time n.

More formally the preferential attachment process starts with a graph G_0 on n_0 vertices labelled $\{v_{-(n_0-1)}, v_{-(n_0-2)}, \ldots, v_{-1}, v_0\}$. We define preferential attachment by way of a growing tree, i.e. $m = 1$, where m is the number of edges each new vertex brings to the network. Let $Y_{n+1,i}$ be the event that the edge $v_{n+1} \sim v_i$ is formed such that $v_i \in V(G_n)$. The next graph in the sequence, G_{n+1}, is constructed by the addition of vertex v_{n+1} by way of preferential attachment (independently with replacement if extended to $m > 1$) according to

$$\mathbb{P}(Y_{n+1,i}) = \frac{\deg_{G_n}(v_i)}{\sum_{j=1-n_0}^{n} \deg_{G_n}(v_j)}. \tag{2.2}$$

conditionally independent on previous additions to the graph. We have expressed the preferential attachment kernel here as if it were only applicable to growing trees. It is simple to extend this to include a fixed $m \in \mathbb{N}$ whereby we redefine $Y_{n+1,i}^{(j)}$ to be the event the j^{th} new edge of the m edges adjacent to v_{n+1} at time $n+1$ follows $v_{n+1}^{(j)} \sim v_i$. Here, edges v_{n+1} forms with G_n are not included in calculations related to probabilities until v_{n+2} joins the network.

Let W_n be the event a vertex chosen from the graph where each vertex in G_n is

equally likely to be selected. It is shown by Bollobás, Riordan, Spencer and Tusnády in [BRST01] that the degree distribution of the Barabási-Albert model is expressed by

$$\lim_{k\to\infty} \mathbb{P}(W_n = k) \to \frac{2m(m+1)}{k(k+1)(k+2)}. \tag{2.3}$$

We see, as $k \to \infty$ that

$$\frac{\lim_{k\to\infty} \mathbb{P}(W_n = k)}{k^{-3}} \to \beta.$$

When considering these networks it is typically more common to study the tail index as the approximation is more accurate for large k (this is observable in Figure 2.2) and it gives an insight into the frequency of higher degree vertices. Examples of where the study into degree distributions of complex networks is important include the growth of online networks [KBM13] and the spread of diseases [JH03, JCLX15].

Shortly after the formalization of the Barabási-Albert model an adaption to equation (2.2) was introduced by Dorogovtsev, Mendes and Samukhin in [DMS00] whereby a constant $\alpha \in (-1, \infty)$ was introduced to form

$$\mathbb{P}(Y_{n+1,i}) = \frac{\deg_{G_n}(V_i) + \alpha}{\sum_{j=1-n_0}^{n} \left(\deg_{G_n}(V_j) + \alpha\right)} \tag{2.4}$$

allowing for greater flexibility in the model. Here α allows us to inhibit or suppress the effect the addition a new edge has on the probabilities used to calculate where future edges form. It can be seen that Barabási-Albert preferential attachment model is the Dorogovtsev, Mendes and Samukhin model if $\alpha = 0$. Figure 2.3 depicts three simulations of the preferential attachment model each with different values of α.

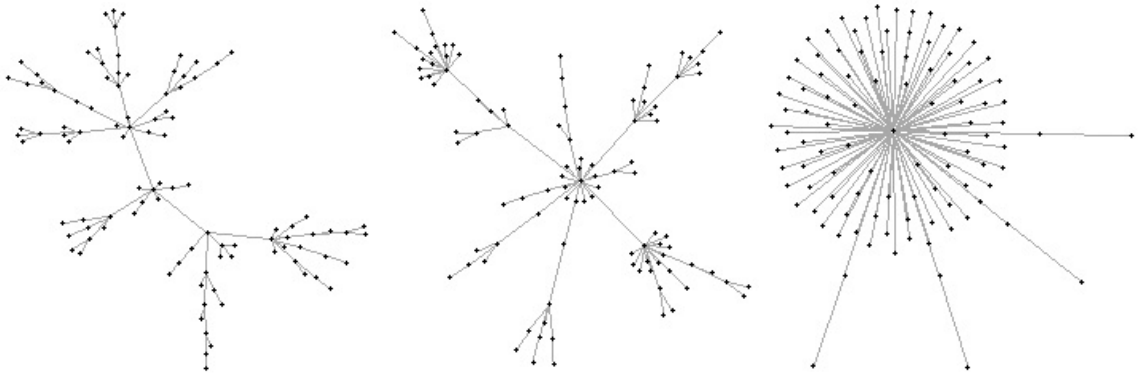

(a) $\alpha = \frac{1}{2}$ (b) $\alpha = 0$ (c) $\alpha = -\frac{1}{2}$

Fig. 2.3: Three simulations of preferential attachment on 100 vertices with different values of α.

It is observable from Figure 2.3 that as $\alpha \downarrow -1$ the number of hubs become fewer and more dominant. It can be seen that a change in α results in a change of the overall degree distribution by way of changes to β and γ in equation (2.1). An adaptation to (2.1) was found by [DMS00] to include this value α describing how γ varies with α effects the overall degree distribution.

In subsequent chapters, when referring to preferential attachment we are referring to the form given by equation (2.4).

Early 2006 in [RTV07] saw a further extension of [BA99] whereby the preferential attachment mechanism governing growth given by equation (2.2) was modified to become

$$\mathbb{P}(Y_{n+1,i}) = \frac{w\left(\deg_{G_n}(V_i)\right)}{\sum_{j=1-n_0}^{n} w\left(\deg_{G_n}(V_j)\right)}. \tag{2.5}$$

Here $w(\cdot)$ is a predetermined nonlinear function associated to the attachment rule. It is a clear that equation (2.2) is a special case of (2.5) such that $w(x) = x$. The authors prove a number of results in regards to the limiting distribution of this model [RTV07] in both the sub-tree generated by selecting a random vertex and the network as a whole. For this selection rule, the asymptotic degree distribution was found for a randomly selected vertex.

2.2 Fitness, choice and condensation

Though the Barabási-Albert model of preferential attachment was found to be an appropriate basis for some real world systems it failed to capture important aspects of network growth. As discussed in Section 2.1, evolution in a network growing by way of preferential attachment favours vertices with higher degree. This implies older vertices have a greater potential to attract new edges than new ones. Though this assumption is appropriate in regards some networks this is not entirely true for others such as social networks. Many observable networks are comprised of vertices which have an inherent growth potential disjoint of their degrees. Some examples where old vertices do not necessarily have an advantage over new ones include: citation networks, social media followers and elections.

At the turn of the millennium Bianconi and Barabási [BB01] proposed a model which allows for an extra level of competition between vertices. Here the authors combined the Barabási-Albert [BA99] model with the concept of vertex fitness. The model begins with an initial graph G_0 on n_0 vertices where each of the n_0 vertices are coupled with a fitness drawn from some distribution $\rho(\eta)$. In other words a vertex v_i has fitness η_i drawn independently from $\rho(\eta)$. Similarly to in the Barabási-Albert model [BA99] with $m = 1$, let $Y_{n+1,i}$ be the event that the edge $v_{n+1} \sim v_i$ is formed where $v_i \in \{v_{-(n_0-1)}, v_{-(n_0-2)}, ..., v_0, v_1, ...v_n\}$. For the Bianconi-Barabási [BB01] we modify equation (2.2) to become

$$\mathbb{P}(Y_{n+1,i}) = \frac{\eta_i \deg_{G_n}(V_i)}{\sum_{j=1-n_0}^{n} \eta_j \deg_{G_n}(V_j)}. \tag{2.6}$$

For this model G_{n+1} is formed by way of a new vertex v_{n+1} joining G_n with its own fitness $\eta_{n+1} \sim \rho(\eta)$. A size $m = 1$ sample of vertices are taken from G_n with replacement according to equation (2.6) to form edges with v_{n+1}. Which of this sample is chosen as the candidate for attachment is based on a model attachment rule.

We see from equation (2.6) that vertices which have high degree combined with high

fitness have greater probability of attaching new edges. Using this method of growth the authors found the time dependence of the vertex's connectivity depends on the fitness of the vertex. This is to be expected as the time needed for a vertex with lower fitness to grow to a certain size will be longer than if the vertex was to have higher fitness. It should be clear that if every vertex had the same fitness (i.e. $\rho(\eta)$ is a Dirac mass) then no vertex has an advantage over another in this regard, as a consequence these cases reduce to the Barabási-Albert model discussed earlier.

Long term behaviour has always been of interest to those studying growing networks, in particular what phenomena can be observed as the number of vertices $n \to \infty$. One of these phenomena we study is that of condensation, in the sense of growing networks condensation is where a subset of vertices attracts a positive proportion of new edge ends as $n \to \infty$. There exists $\mathbb{S}_n \subset V(G_n)$ for all $\epsilon > 0$ such that $|\mathbb{S}_n| = o(n)$, as $n \to \infty$ and $\mathbb{E}\left(\sum_{v \in \mathbb{S}_n} deg_{G_n}(v) \geq\right) \epsilon n$ for sufficiently large n.

The existence of condensation in a network is useful in predicting the longevity of a vertex's potential to attract new edges. If we consider a social network whereby a vertex gaining a new edge represents a new follower, condensation at a vertex represents a member gaining a constant proportion of new followers as time progresses. This concept is attractive from a marketing point of view as the non-existence of condensation implies that eventually a new, more attractive vertex joins the graph causing the rate of edges attaching to previously fit vertices to decline.

Much analysis has been conducted in the area of preferential attachment with fitness. Notable articles include Borgs, Chayes, Daskalakis and Roch [BCDR07] where authors define phases categorising the growth dynamics of a model for different distributions generating fitness coefficients. More specifically authors showed that the asymptotic fitness distribution is absolutely continuous in the non-condensation phase however does include a discontinuity in the condensation phase. In the limit of the condensation phase a positive proportion of mass is centred on vertices whose fitness falls into a specific region allowing for condensation to occur. Further analysis by Dereich and Ortgiese in [DO14] looked into the connection between degree and

the fitness distribution of a uniformly chosen vertex in the network. Condensation has been studied further in relation to a number of more applied network models, for example the Kingman model of genetic variation by [DM13].

Condensation is observable in two important forms; non-extensive and extensive. Non-extensive as seen in [DMM17] is where the set of vertices which condensation is orientated around $|\mathbb{S}_n| \to \infty$ for any choice of $\mathbb{S}_n$. Extensive condensation is where for some choice of $|\mathbb{S}_n|$ does not follow this definition. Vertices attracting extensive condensation can change over time. A clear example of this is [FJ18] where condensation occurs at the vertex in G_n with the highest fitness which clearly changes over time as new, more fit vertices arrive. Persistent hub condensation is a special case of extensive condensation whereby the condensate occurs at a single vertex which does not change as $n \to \infty$.

Much work has been conducted on the topic of preferential attachment networks with fitness where the fitnesses are used to scale the preferential attachment kernel. We introduce the notion of choice. By this we mean, that as a new vertex joins the network a two-step process is started. Step one, the vertex chooses a sample of vertices using preferential attachment typically given by equation (2.4). Step two, a selection criterion is imposed on this set of vertices to decide which vertex/vertices our new vertex will attach to. This selection criterion is typically predetermined before the graph begins to grow and remains fixed for the duration of the process.

We first explore some models which incorporate choice into their selection process however do not contain a fitness aspect. The first we discuss is that of Krapivsky and Redner [KR14]. This model evolves as follows: begin with a graph G_0 on n_0 vertices, $V(G_{n+1}) = V(G_n) \cup \{v_{n+1}\}$. As a new vertex joins the graph and uses a linear preferential attachment kernel as expressed by equation (2.4) to sample a subset of vertices from G_n with repetition. After this step, an edge is formed between the vertex in the sample with the highest degree and v_{n+1}. This 'greedy' algorithm for deciding on new edge connections effectively doubles down on the rich-get-richer mentality hiding behind preferential attachment. We see the parameters of this model

can be configured to match that of the Barabási-Albert model by setting $\alpha = 0$ and the size of the sampled vertices from G_n to be one. As one might expect from this model, the authors found there are a number of different outcomes dependent on the selected preassigned attachment rule, though there exists one scenario whereby a single dominant hub forms with degree of size order n. This implies the existence of both the condensation phenomena and a phase transition in the model. A phase transition π for a given parameter Π occurs in a model when the behaviour of a model is qualitatively different when $\Pi > \pi$ as opposed to when $\Pi < \pi$. For example, in the Krapivsky and Redner model [KR14] it was found that this critical value $\alpha_c = s - 2$ where s vertices are sampled to form a potential edge to. This means if $\alpha \geq \alpha_c$, there is no presence of a single macroscopic hub, however if $\alpha < \alpha_c$ a hub forms in the network with probability 1. Clearly as s increases, the likelihood of a hub forming similarly increases. This is logical as it means our sample size increases the likelihood of selecting the vertex of highest degree.

Similar variations of the Krapivsky and Redner model have been studied, in particular by Malyshkin and Paquette in [MP15, MP14]. The first of these two, [MP15], adapts [KR14] in that as a new vertex joins G_n two vertices are sampled. An edge is formed from the new vertex to the member of the pair with the smallest degree. This method of growth, though different to [KR14] continues to value older vertices over newer vertices. Though it is highly plausible that the highest degree vertex is selected twice the authors found that the highest degree vertex in the network is

$$\max_i(\deg_{G_n}(v_i)) = \frac{\ln\left(\ln\left(\sum_{1-n_0}^{n} \deg_{G_n}(v_i)\right)\right)}{\ln(2)} + \Theta(1) \tag{2.7}$$

with high probability. Comparing this with [KR14] who calculated

$$\max_i(\deg_{G_n}(v_i)) = \frac{n}{\ln(n)\ln(n)} + \Theta(1) \tag{2.8}$$

we can generate Table 2.1.

	10^3	10^4	10^5	10^6
equation (2.7)	2.93	3.31	3.61	3.86
equation (2.8)	21	118	754	5239

Tab. 2.1: A comparison of the expected highest degree vertices in the Malyshkin and Paquette [MP15] and Krapivsky and Redner [KR14] models.

We see from Table 2.1 this alteration from attaching to the highest of a sample [KR14] to attaching to the lowest of two [MP15] is dramatic. A further adaptation by Haslegrave and Jordan [HJ16] looked into the evolution of graphs whereby for a fixed r and s, a sample of r vertices is taken from G_n. The new edge is formed between the new vertex and the member of the sample with the s^{th} highest degree. The authors here found that if $s = 1$ a condensation like behaviour can be observed which could be seen for $s > 1$ for large enough r.

We have discussed many methods of choice which utilize a two-step method both of which involve the degree of vertices to decide on new attachments. In later chapters we discuss models whereby new vertices have a competitive edge against older vertices with higher degrees.

2.3 Stochastic approximation

There are many techniques used in the analysis of growing networks; a key method we utilize is that of stochastic approximation. Derived by Robbins and Monro in [RM51] and analysed further by Kiefer and Wolfowitz in [KW52] stochastic approximation is a method of proving convergence of a sequence of random variables occuring in a noisy environment [Sim55]. Stochastic approximation as a method is one in which takes in a noisy process and approximates it to a differential equation [RM51, KW52]. This iterative process operates in a discrete setting using the current state of a dynamical system to approximate the next step. The aim of this process is to force the flow of the dynamical system towards a stable equilibrium.

A crude example of a dynamical system converging to a stable equilibrium is that

of a pendulum. The notion of stable and unstable equilibria can be expressed using figure 2.4. Here weights are attached to rigid rods fixed to a rotation plate suspended on a wall.

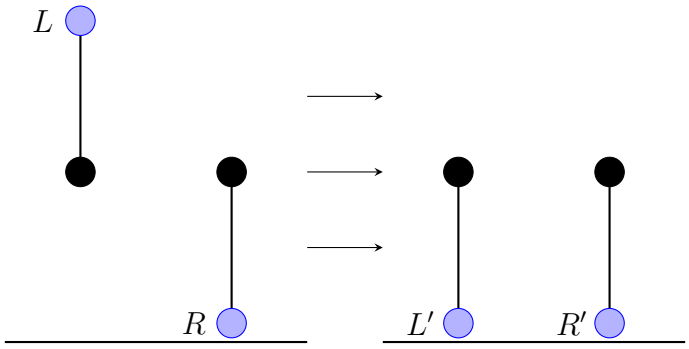

Fig. 2.4: (Left) two pendulums in equilibrium labeled L and R prior to a perturbation. (Right) two pendulums in equilibrium labeled L' and R' after a small perturbation.

Figure 2.4 shows that both diagrams are in equilibrium. Upon applying a small perturbation of equal size to each of pendulums L and R. Pendulum R will begin swinging until becoming stationary in the same state as before the perturbation given by R'. Pendulum L on the other hand will swing out of equilibrium and begin converging to L' which is at the same position as R'. We describe pendulum L in Figure 2.4; state of equilibrium as unstable whereas pendulums R, R' and L' are in states of stable equilibrium.

We formalize the notation needed for stochastic approximation using notation in Pemantle [Pem07]. Let the n dimensional vector $\mathbf{X}_n$ be a random process in $\mathbb{R}^n$ and $\mathcal{F}_n$ be the filtration generated by the process up to time n. Suppose that

$$\mathbf{X}_{n+1} - \mathbf{X}_n = \gamma_n(F(\mathbf{X}_n) + \xi_{n+1} + R_n), \tag{2.9}$$

where the remainder term R_n and noise ξ_{n+1} satisfy both $\sum_{n=1}^{\infty} \gamma_n |R_n| < \infty$ and $\mathbb{E}(\xi_{n+1}|\mathcal{F}_n) = 0$ respectively. The value γ_n is a normalization constant satisfying

both

$$\sum_n \gamma_n = \infty \text{ and } \sum_n \gamma_n^2 < \infty.$$

The function $F(\cdot)$ is a vector field evaluated at a random points $\mathbf{X}_n$, controlling the flow of the dynamical system.

Due to theory summarized in [Pem07] we have a collection of sufficient conditions to classify the roots of $F(\mathbf{X}_n)$ as stable or unstable. Pemantle [Pem07] outlines results which, if satisfied, tell us whether our dynamical system converges to a stable point or not. Theorem 2.8 of [Pem07] outlines conditions in which a dynamical system converges to a stable equilibrium with probability one. Similarly Theorem 2.9 of [Pem07] proves non-convergence to unstable equilibria.

2.3.1 Example of stochastic approximation: Pólya's Urn

A classic example of where stochastic approximation equations can be applied are generalised Pólya urn processes as detailed in [CCL13, Dri08, Pol14] which explores calculating limiting proportion of balls in urns. For this example, consider a simple urn process whereby an urn contains b_0 blue, g_0 green and r_0 red balls at time 0. At each time step we select a ball from the urn, observe its colour, placing it back in the urn along with a ball of the same colour with probability p or a ball of a different colour with probability $\frac{1-p}{2}$ each. Let us define three random variables: let B_k be the proportion of blue balls in the urn at time k and a similar definition for G_k and R_k. Clearly we have that

$$B_k = \frac{b_k}{b_k + g_k + r_k},\ G_k = \frac{g_k}{b_k + g_k + r_k} \text{ and } R_k = \frac{r_k}{b_k + g_k + r_k}.$$

We define the filtration $\mathcal{F}_n$ as the natural σ-algebra generated by the sequence of balls removed and added up to time n. Using our model description we formulate three approximation equations describing the proportion of balls of each type at time

$k+1$ as

$$B_{k+1} = \gamma_{n+1}\left(\gamma_k^{-1}B_k + pB_k + \frac{(1-p)}{2}(R_k+G_k) + \xi_{k+1}^{(B)}\right)$$
$$G_{k+1} = \gamma_{n+1}\left(\gamma_k^{-1}G_k + pG_k + \frac{(1-p)}{2}(B_k+R_k) + \xi_{k+1}^{(G)}\right)$$
$$R_{k+1} = \gamma_{n+1}\left(\gamma_k^{-1}R_k + pR_k + \frac{(1-p)}{2}(B_k+G_k) + \xi_{k+1}^{(R)}\right)$$

where $\gamma_{n+1}^{-1} = b_{k+1} + g_{k+1} + r_{k+1}$ and $\xi_{k+1}^{(B)}, \xi_{k+1}^{(G)}, \xi_{k+1}^{(R)}$ are the associated noise distributed with zero expectation. We first rearrange these into the form outlined in [Pem07] given in equation (2.9)

$$\begin{pmatrix} B_{k+1} \\ G_{k+1} \\ R_{k+1} \end{pmatrix} - \begin{pmatrix} B_k \\ G_k \\ R_k \end{pmatrix} = \gamma_{n+1}\begin{pmatrix} \frac{1}{2}(1-p)(-2B_k+R_k+G_k) \\ \frac{1}{2}(1-p)(B_k-2R_k+G_k) \\ \frac{1}{2}(1-p)(B_k+R_k-2G_k) \end{pmatrix} + \gamma_{n+1}\begin{pmatrix} \xi_{k+1}^{(B)} \\ \xi_{k+1}^{(G)} \\ \xi_{k+1}^{(R)} \end{pmatrix}.$$

This can be simplified using $B_k + R_k + G_k = 1$ to form

$$\begin{pmatrix} B_{k+1} \\ G_{k+1} \\ R_{k+1} \end{pmatrix} - \begin{pmatrix} B_k \\ G_k \\ R_k \end{pmatrix} = \gamma_{n+1}\begin{pmatrix} \frac{1}{2}(1-p)(1-3B_k) \\ \frac{1}{2}(1-p)(1-3R_k) \\ \frac{1}{2}(1-p)(1-3G_k) \end{pmatrix} + \gamma_{n+1}\begin{pmatrix} \xi_{k+1}^{(B)} \\ \xi_{k+1}^{(G)} \\ \xi_{k+1}^{(R)} \end{pmatrix}.$$

From here we calculate the stationary points of this system by solving

$$\frac{1}{2}(1-p)(1-3B_k) = \frac{1}{2}(1-p)(1-3R_k) = \frac{1}{2}(1-p)(1-3G_k) = 0$$

to get

$$B_k = R_k = G_k = \frac{1}{3}$$

for $p \in [0,1)$ and any viable combination of B_k, G_k and R_k for $p = 1$. Pemantle [Pem07] states that a solution to a system of stochastic approximation equations is stable if all the eigenvalues of the Jacobian matrix of partial derivitives describing the flow are strictly negative when evaluated at that solution. The three eigenvalues

of our system are all equal given by

$$\lambda = \frac{3}{2}(p-1)$$

which is negative for any value $p \in [0,1)$ which allows us to conclude that $B_k = R_k = G_k = \frac{1}{3}$ is the only stable equilibrium. In order for this argument to hold we must check conditions on the noise outlined in Section 2 of [Pem07]; though we ommitted these here.

2.4 Vertex types and coexistence

Graph theory, more specifically, evolutionary graph theory is studied as a model of real world systems. The inclusion of vertex fitness was an important step in developing these models, allowing for inherent growth potential among vertices despite vertex age. However, this method of growth only works under the assumption that a vertex in G_n is perceived equally attractive to each new vertex when forming G_{n+1}. This is not necessarily true in many real world systems. It is clear in a two party voting system, the distribution of votes when plot on a graph is not uniform. Figure 2.5 depicts a colour map representing the way states voted in a US bipartisan presidential elections from 1972-2016. There is clear non-uniformity among the voting patterns; a general trend is the middle states vote republican (red) and the coastal states vote democrat (blue).

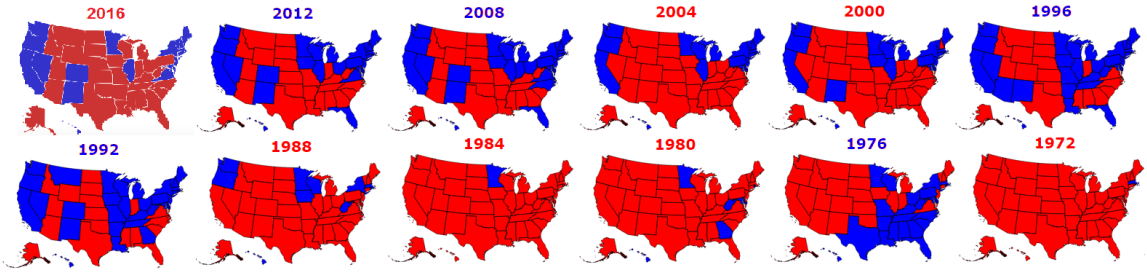

Fig. 2.5: US presidential election timeline depicting how states voted by colour, red represents Republican and blue Democrat. Image 2016 from https://www.realclearpolitics.com/elections/live_results/2016_general/president/map.html and images from 1972-2012 are from http://metrocosm.com/us-presidential-elections/.

Figure 2.5 gives evidence to support the notion of where someone is born correlating with their political affiliation. This does not mean people in a state which historically votes Republican (Alaska) or Democrat (Minnesota) will not vote for the opposing party. We can translate this macro observation to a micro observation and model these networks using graphs.

The idea of vertices possessing 'types' which behave differently to one another is one which has been studied recently. Austin and Rodgers [AR03] looked at the case where vertices are allocated one of two growth rates; type A with probability $\mathbb{P}(t)$ and type B with probability $1 - \mathbb{P}(t)$ where $\mathbb{P}(t)$ is either constant or variable based on initial input parameters. The authors discuss two models in [AR03]; the first where different types evolve by way of preferential attachment with different rates. The second, only one type grows by way of preferential attachment, the other at a constant rate. Austin and Rodgers were interested in the behaviour of the degree distribution of the model, moreover whether the models followed power law distributions as in [BA99]. They found that both models considered adhered to a power law distribution in their degree sequences in the limit.

2.4.1 Coexistence tri-colour example

The following, along with Figures 2.6a-2.6d, depict a crude example of coexistence. This model evolves as follows: vertices join a network with a two dimensional fitness $\binom{X_1}{X_2}$ chosen according to some distribution. At time $n+1$ a new vertex joins the network evaluating its surroundings and uses a predetermined selection rule to decide its type. This could be something with low complexity such as nearest neighbour or it could be decided based on a sampling of the network favouring closer vertices. In this example we use the colours red, blue and purple to visualise the three vertex types.

We define the proportion of the n vertices of colour j by $Y_n^{(j)}$ so that both $Y_n^{(j)} \in [0,1]$ and $\sum_j Y_n^{(j)} = 1$. As $n \to \infty$ the proportion of vertices of each colour satisfies

$$\lim_{n\to\infty} Y_n^{(j)} = Y^{(j)}.$$

Coexistence is where $1 > Y^{(j)} > 0$ for at least two different colours. Figure 2.6a shows example initial conditions for this model where $n = 1750$ split into three groups (red, blue and purple.) Vertices are placed according to one of three bivariate normal distributions; a new vertex joins the network using one of these distributions to generate its location. A nearest neighbour algorithm is then used to sample a subset of existing vertices; the new vertex's colour is then assigned based on the colours of these sampled vertices using a predetermined attachment rule.

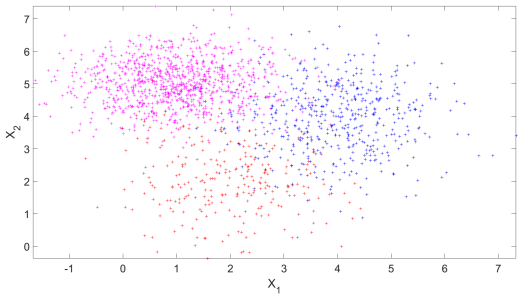

(a) Model initial conditions: 250 red vertices, 1000 blue and 1000 purple

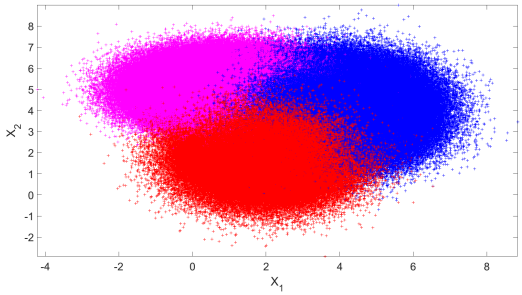

(b) Evidence of coexistence between the three colours.

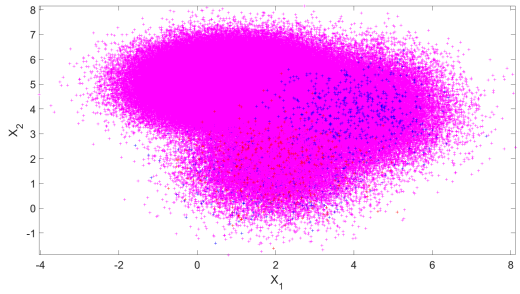

(c) Evidence of purples domination in the network.

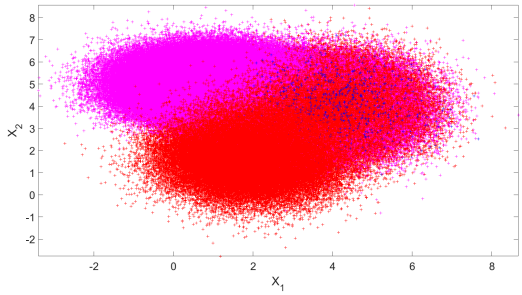

(d) Evidence of coexistence between the purple and red and domination over blue.

Fig. 2.6: Three sets of data where points are denoted by $Z_{i,j}$ where $j \in \{R, B, P\}$ and $i \in \{1, 2, \dots\}$. Points distributed according to $Z_{i,j} \sim N_2(\mu_j, \Sigma_j)$.

We clearly see in Figure 2.6a a dense population of purple vertices, a sparse number of red vertices and a moderate density of blue vertices with evidence of regional hubs. In the following Figures we explore a number of different outcomes which arise when we let the number of vertices in this model grow. Figure 2.6b gives evidence of coexistence between vertices of each of the three colours. This doesn't necessarily mean they are equal proportions but moreover $\lim_{n\to\infty} Y_n^{(R)} = Y^{(R)}$, $\lim_{n\to\infty} Y_n^{(B)} = Y^{(B)}$ and $\lim_{n\to\infty} Y_n^{(P)} = Y^{(P)}$ such that $1 > Y^{(R)}, Y^{(B)}, Y^{(P)} > 0$ and $Y^{(R)} + Y^{(B)} + Y^{(P)} = 1$. Figure 2.6c shows dominance of purple vertices over the other two colours, i.e. $Y^{(R)} = Y^{(B)} = 0$ and $Y^{(P)} = 1$ providing evidence of domination over red and blue. Finally, Figure 2.6d provides evidence of coexistence between vertices of red and purple in that $Y^{(R)} = k$, $Y^{(B)} = 0$ and $Y^{(P)} = 1 - k$

where $|k| + |1 - k| = 1$.

2.4.2 Coexistence results

Section 2.4.1 outlines key signs which point towards the emergence of coexistence in a preferential attachment network. Similarly to the search for condensation, we use stochastic approximation techniques [Pem07] to derive conditions on model parameters to allow for coexistence to occur in a network.

The Antunović, Mossel and Rácz model [AMR16] begins with an initial graph G_0 on n_0 vertices where each vertex has a preassigned type. In this model we specify there are two types which are both represented in G_0. To form G_{n+1} a new vertex v_{n+1} joins G_n selecting m vertices independently from G_n using standard preferential attachment. Our new vertex then is assigned a type based on those of the vertices it has formed edges to. This is done in a number of different ways. Given the two type case we define $k \in \mathbb{Z}^+$ such that $0 \leq k \leq m$ as the number of type 1 vertices adjacent to v_{n+1} and ρ_k as the probability v_{n+1} selects type 1. A few interesting selection criteria include:

1. The majority wins model; here $\rho_k = 1$ if $k > \frac{m}{2}$ and $\rho_k = 0$ if $k < \frac{m}{2}$. In the event of a tie a fair coin is flipped.
2. The linear model; here $\rho_k = \frac{k}{m}$.
3. The coin flip model; here $\rho_0 = 0$, $\rho_m = 1$ and $\rho_k = c$ for $k \notin \{0, m\}$.

Let us define the proportion of vertices of each type at time n by A_n and B_n and the proportion of edge ends adjacent to vertices of each type at time n be denoted by X_n and Y_n respectively. Using these the authors formulated a two dimensional system of stochastic approximation equations. The authors studied these models and found the possible limiting proportions of vertices of each types. They found that often competing types can coexist and occupy a positive proportion of the total number of vertices in the network. The work of [AMR16] was extended by Jordan [Jor18] to include vertex fitness in order to verify whether or not the results

of [AMR16] extended. Jordan [Jor18] proved that coexistence can occur in these fitness models. Further work by Haslegrave and Jordan [HJ18] was conducted to explore how an increased number of types changed the behaviour of the network and provide detailed examples showing behaviour which could not occur in the two type case. This extension increases the models complexity as it is no longer true that v_{n+1} takes on type one with probability ρ_k and type two with probability $1-\rho_k$. It is straightforward to see how increasing the types above three as in [HJ18] increases the model complexity dramatically by creating a more complex set of stochastic approximation equations which would require solving. They found in this case that the limit of the type proportions does not converge, moreover behaving in a cyclic motion where each type takes turns to dominate.

3. LOCATION BASED CHOICE MODEL: CONDENSATION

This chapter focuses on a new model of preferential attachment which could be described as a generalization of [FJ18]. The network described in [FJ18] grows by selecting a varying number of vertices denoted by r using preferential attachment (2.4). The new vertex then forms an edge between itself and the member of the selection which is categorized as the fittest. Though our model is thought of as a generalization of a special case of [FJ18] (why will become clear shortly) we maintain that exactly r vertices are sampled at each time step with replacement.

The contents of this chapter are as follows. We start by describing the model and defining key notation in Section 3.1. Section 3.2 discusses our methods, results relating to condensation in this model and outlining our proofs. Finally section 3.3 outlines four specific examples which showcase these results and relate them to relevant other models in the literature.

The content for this chapter has been adapted into [HJY19] which has been accepted to appear in Random Structures and Algorithms.

3.1 Model description

Fix an initial model parameter $r \in \mathbb{N}$ such that $r \geq 2$, a vector $\Xi \in \mathbb{R}^r$ such that $\Xi_i \in [0,1]$ and $\sum_{i=1}^{r} \Xi_i = 1$, and a real number $\alpha > -1$. We specify an initial graph G_0 on $n_0 \geq 2$ vertices where each vertex $v_i \in V(G_0)$ has its own distinct i.i.d. location generated according to $x_i \sim \text{Uni}(0,1)$. Though we place this condition on our network it is noted that this is done to tidy up calculations using the known

structure of trees. The results are not expected to be different if we were to remove this condition.

A new graph G_{n+1} is formed from G_n at time $n+1$ by the addition of a new vertex v_{n+1} via a single edge as to maintain the tree structure. This new vertex joins with its own i.i.d. uniform random variable denoted by $x_{n+1} \sim \text{Uni}[0,1]$. Where v_{n+1} attaches to is decided by selecting a sample of r vertices with replacement by preferential attachment according to equation (2.4). We denote the r selected vertices sampled from G_n as $\left\{v_1^{(n+1)}, v_2^{(n+1)}, \ldots, v_r^{(n+1)}\right\}$ reordering appropriately such that the locations of these r selected vertices $x_1^{(n+1)}, \ldots, x_r^{(n+1)}$ follow $x_1^{(n+1)} \geq \cdots \geq x_r^{(n+1)}$. Specifically let vertex $v_k^{(n+1)}$ be the vertex with the k^{th} highest location of the r sampled vertices from G_n.

For completeness, if two vertices or more are sampled with the same location we rank them in the order they were sampled. Note that with probability 1 the only way this occurs is if the same vertex is selected multiple times. The probability that v_{n+1} forms an edge between itself and $v_i^{(n+1)}$ is given by Ξ_i; this choice is made irrespective of vertices selected in this or any previous step.

An example of this model which we revisit in Section 3.3.3 is the middle of three model described by the vector $\Xi = (0,1,0)$. Here our network grows by new vertices sampling a subset $r = 3$ of existing vertices from G_n with replacement by preferential attachment forming an edge between itself and the vertex in the selected set corresponding to the median location/rank 2.

3.2 Results

We begin by defining notation describing aspects of this model we would like to track. Let the random variable $\Psi_n(x)$ be the probability under preferential attachment according to equation (2.4) that vertex v_{n+1} selects a vertex for attachment from G_n

which has location less than or equal to x, that is

$$\Psi_n(x) = \frac{1}{(n+n_0-1)(2+\alpha)+\alpha} \sum_{v_i \in V(G_n)} \mathbb{1}_{\{x_i \leq x\}} \left(\deg_{G_n}(v_i) + \alpha\right).$$

We see the normalisation constant used is the sum of weighted degree mass in G_n

$$\sum_{j=1-n_0}^{n} \left(\deg_{G_n}(v_j) + \alpha\right) = (n+n_0-1)(2+\alpha)+\alpha.$$

We have that $\Psi_n(0) = 0$ as there is probability 0 of a vertex at location 0 and $\Psi_n(1) = 1$. We think of Ψ_n as being the distribution function of the normalised empirical measure on the location space given by weighting the location of each vertex of the graph by its degree plus α; we label this measure ν_n. Let $\mathcal{F}_n$ be the σ-algebra generated by the graphs G_n and the locations of the vertices contained within up until time n, $\mathcal{F}_n = \sigma(G_i, x_j; i, j \leq n)$.

We define $e_{k,r}$ as the situation when $\Xi_k = 1$ and $\Xi_i = 0$ for all $i \in \{1, 2, \ldots, k-1, k+1, \ldots, r\}$. Upon selecting r vertices using preferential attachment the probability of attaching to a vertex in G_n with location in $[0, x]$ is equal to

$$g_k(\Psi_n(x); e_{k,r}) = \sum_{i=k}^{r} \binom{r}{i} \Psi_n(x)^i (1-\Psi_n(x))^{r-i}.$$

The equation $g_k(\Psi_n(x); e_{k,r})$ leads to a more general equation describing the probability of v_{n+1} attaching to a vertex which has location at most x with respect to any attachment vector Ξ

$$g(\Psi_n(x); \Xi) = \sum_{k=1}^{r} \Xi_k g_k(\Psi_n(x); e_{k,r}). \tag{3.1}$$

We formulate a stochastic approximation equation associated to our model. If G_0 has n_0 vertices and e_0 edges, G_n has $n_0 + n$ vertices and $e_0 + n$ edges, giving the normalising constant $\gamma_n = \left(2\left(e_0+n\right) + \alpha\left(n_0+n\right)\right)^{-1}$. Assuming G_0 is a tree, which

we do, we have the simpler form $\gamma_n = ((n + n_0 - 1)(2 + \alpha) + \alpha)^{-1}$.

Lemma 3.2.1. *For a fixed $\alpha \in (-1, \infty)$, $x \in [0, 1]$ and $\Xi \in \mathbb{R}^r$, it follows that*

$$\Psi_{n+1}(x) - \Psi_n(x) = \gamma_{n+1}\left(F_1(\Psi_n(x); x, \alpha, \Xi) + \xi_{n+1}\right), \tag{3.2}$$

where

$$F_1(y; x, \alpha, \Xi) = x(1 + \alpha) - (2 + \alpha)y + g(y; \Xi),$$

for $y \in [0, 1]$. Here $g(y; \Xi)$ is defined in equation (3.1) and ξ_{n+1} is given by $\xi_{n+1} = \gamma_{n+1}^{-1}\left(\Psi_{n+1}(x) - \mathbb{E}(\Psi_{n+1}(x)|\mathcal{F}_n)\right)$ and satisifes $\mathbb{E}(\xi_{n+1}|\mathcal{F}_n) = 0$.

Proof. We begin by fixing $x \in [0, 1]$. Let us say that v_{n+1} attaches to w_{n+1} which has location at most x with probability $g(\Psi_n(x); \Xi)$ from equation (3.1) as the probability of attaching to each of the r selections. We note that at time n the total weighted edge mass in the interval $[0, x]$ is given by

$$\sum_{j=1-n_0}^{n} \mathbb{1}_{\{x_j \le x\}}\left(\deg_{G_n}(v_j) + \alpha\right) = \gamma_n^{-1}\Psi_n(x).$$

We wish to calculate the total change to $\gamma_n^{-1}\Psi_n(x)$ when v_{n+1} joins G_n. The expected addition to the system arising from the location of the new vertex is $x(\deg_{G_n}(v_{n+1}) + \alpha) = x(1 + \alpha)$. The total expected addition is given by

$$\begin{aligned}
\mathbb{E}(\gamma_{n+1}^{-1}\Psi_{n+1}(x)\,|\mathcal{F}_n) &= \gamma_n^{-1}\Psi_n(x) + x(1 + \alpha) + g(\Psi_n(x); \Xi) \\
&= \gamma_{n+1}^{-1}\Psi_n(x) + x(1 + \alpha) - (2 + \alpha)\Psi_n(x) + g(\Psi_n(x); \Xi) \\
&= \gamma_{n+1}^{-1}\Psi_n(x) + F_1(\Psi_n(x); x, \alpha, \Xi).
\end{aligned}$$

Stochastic approximation, as specified in [Pem07] allows for a remainder term R_n provided it satisfies specific convergence criteria; in our case we have that $R_n = 0$ which indeed satisfies these. Our function maps y to $F_1(y; x, \alpha, e_{k,r})$; clearly γ_n possesses the properties required to allow for convergence therefore it is required to

show ξ_{n+1} is suitably defined. This information leads to

$$\mathbb{E}(\Psi_{n+1}(x)\,|\mathcal{F}_n) = \Psi_n(x) + \gamma_{n+1}F_1\left(\Psi_n(x)\,; x, \alpha, \Xi\right)$$

which is in the same form as equation (3.2.1). We define

$$\xi_{n+1} = \gamma_{n+1}^{-1}\left(\Psi_{n+1}(x) - \mathbb{E}(\Psi_{n+1}(x)|\mathcal{F}_n)\right). \tag{3.3}$$

It is clear from equation (3.3) that $\mathbb{E}(\Psi_{n+1}(x)|\mathcal{F}_n) = 0$. □

As a summary of what was discussed in Chapter 2 we outline necessary and sufficient conditions in order for a system of random variables X_n to converge to a stable point or touchpoint of the vector field in which X_n is embedded. We say that a root $p \in [0,1]$ of $F_1(y; x, \alpha, \Xi)$ is stable if $F_1(p; x, \alpha, \Xi) = 0$ and there exists an $\epsilon > 0$ such that for $y \in (p-\epsilon, p)$ then $F_1(y; x, \alpha, \Xi) > 0$ and when $y \in (p, p+\epsilon)$ we have $F_1(y; x, \alpha, \Xi) < 0$. Alternatively we say a root $p \in [0,1]$ of $F_1(y; x, \alpha, \Xi)$ is unstable if $F_1(p; x, \alpha, \Xi) = 0$ for some ϵ such that for $y \in (p-\epsilon, p)$ then $F_1(y; x, \alpha, \Xi) < 0$ and when $y \in (p, p+\epsilon)$ we have $F_1(y; x, \alpha, \Xi) > 0$. Finally, if a root p of $F_1(y; x, \alpha, \Xi)$ is strictly positive or strictly negative on both $(p-\epsilon, p)$ and $(p, p+\epsilon)$ it is classified as a touchpoint. Given our function F is bounded and continuous, $\mathbb{E}(\xi_{n+1}|\mathcal{F}_n) \leq K$ must be satisfied for some finite K, and say that X_n converges almost surely to a root of F and that any stable root or touchpoint has a positive probability of being a limit. Furthermore [Pem07] requires both $\mathbb{E}(\xi_{n+1}^{+}|\mathcal{F}_n)$ and $\mathbb{E}(\xi^{-}|\mathcal{F}_n)$ be bounded above and below by positive numbers around a neighbourhood of an unstable root p; in this case we conclude that p is almost surely not the limit.

Remark 3.2.2. *Since $F_1(y; x, \alpha, \Xi)$ is a polynomial, every root in $[0,1]$ is either a stable root, an unstable root or a touchpoint. Also, for $x \in (0,1)$ we have*

$$F_1(0; x, \alpha, \Xi) > 0 > F_1(1; x, \alpha, \Xi)$$

, so 0 and 1 are not roots.

Theorem 3.2.3. *For a fixed $x \in (0,1)$ the sequence of random variables $\Psi_n(x)$ converges almost surely to a stable root p of $F_1(y; x, \alpha, \Xi)$. Any stable root $p \in [0,1]$ has a positive probability of being the limit. An unstable root has probability root of being the limit. We denote the limit of $\Psi_n(x)$ as Ψ.*

Proof. First we note that $F_1(0; x, \alpha, \Xi) = x(\alpha + 1) > 0$ and $F_1(1; x, \alpha, \Xi) = (1 + \alpha)(1 - x) < 0$. Therefore there must be at least one root of $F_1(y; x, \alpha, \Xi)$ in the interval $[0, 1]$.

Since $F_1(y; x, \alpha, \Xi)$ is a polynomial in y, it is continuously differentiable on $[0, 1]$. We therefore only need check that ξ_{n+1} satisfies.

The results for stable and unstable roots follow from Corollary 2.7, Theorem 2.8 and Theorem 2.9 of Pemantle [Pem07], as we have that $F_1(y; x, \alpha, \Xi)$ is continuous and γ_n^{-1} linear in n. To apply Corollary 2.7 and Theorem 2.8 we must to check that there exists a value $C \in \mathbb{R}^+$ such that $\mathbb{E}(\xi_{n+1}^2 | \mathcal{F}_n) \leq C$. For Theorem 2.9 we require the noise components $\mathbb{E}(\xi_{n+1}^+ | \mathcal{F}_n)$ and $\mathbb{E}(\xi_{n+1}^- | \mathcal{F}_n)$ are bounded above and below by positive numbers. Recall that ξ_{n+1} is the difference between $\gamma_{n+1}^{-1}\Psi_{n+1}(x)$ and $\gamma_{n+1}^{-1}\mathbb{E}(\Psi_{n+1}(x)|\mathcal{F}_n)$. We first bound the variance of the noise.

We have the vertex v_{n+1} with location x_{n+1} and the vertex w_{n+1} such that $v_{n+1} \sim w_{n+1}$ in G_{n+1} has location z_{n+1}. Given the filtration $\mathcal{F}_n$ the total increase in weight depends entirely on v_{n+1} and w_{n+1} resulting in $\gamma_{n+1}^{-1}\Psi_{n+1}(x) \in [\gamma_n^{-1}\Psi_n(x), \gamma_n^{-1}\Psi_n(x) + 2+\alpha]$ thus $\gamma_{n+1}^{-1}\mathbb{E}(\Psi_{n+1}(x)|\mathcal{F}_n)$ is in this interval. Clearly it is true that $\mathbb{E}(|\xi_{n+1}||\mathcal{F}_n) \leq 2 + \alpha$.

We consider bounds on the noise. Since $|\xi_n| = \xi_n^- + \xi_n^+$ we know that both components are bounded above. For an unstable root $p \in (0,1)$ we let ϵ satisfy $0 < p - \epsilon < p + \epsilon < 1$. If $\Psi_n(x) \in (p - \epsilon, p + \epsilon)$ then it is true that $\mathbb{P}(x_{n+1}, z_{n+1} \leq x | \mathcal{F}_n) = xg(\Psi_n(x); \Xi)$ which is bounded away from 0, similarly for $\mathbb{P}(x_{n+1}, z_{n+1} > x | \mathcal{F}_n)$

It follows that $\gamma_{n+1}^{-1}\mathbb{E}(\Psi_{n+1}(x)|\mathcal{F}_n)$ is bounded away from $\gamma_n^{-1}\Psi_n(x)$ but remaining the same value with positive probability, this gives a lower bound on $\mathbb{E}(\xi_{n+1}^- | \mathcal{F}_n)$; a similar bound can be found for ξ_n^+.

All the results described above apply in this setting, giving almost sure convergence to the root set, positive probability of convergence to each stable root or touchpoint, and zero probability of convergence to each unstable root. □

Lemma 3.2.4. *Let $x \in (0,1)$ and Ξ be selected such that there exists a touchpoint p satisfying*

$$F_1(p; x, \alpha, \Xi) = F_1'(p; x, \alpha, \Xi) = 0$$

Then there exists a positive probability $\Psi_n(x)$ converges to p.

Proof. As an extension of Theorem 3.2.3 in the case when p is a touchpoint, we apply the result stated as Theorem 2.5 in Antunović, Mossel and Rácz [AMR16] based on work by Pemantle in [AR03]; the bounds on our noise immediately given in the proof of Theorem 3.2.3 imply that the conditions needed are met, and so convergence to the touchpoint happens with positive probability. □

Corollary 3.2.5. *The sequence of measures defined by Ψ_n converges weakly, almost surely, to a limit defined by a (possibly random) distribution function $\Psi : [0,1] \to [0,1]$.*

Proof. By definition, we have that for each n, Ψ_n is a non-decreasing cadlag function with $\Psi_n(1) = 1$ and, almost surely, $\Psi_n(0) = 0$. We apply Theorem 3.2.3 to a countably dense set of $x \in (0,1)$ and for x in this set we define $\hat{\Psi}(x) = \lim_{n\to\infty} \Psi_n(x)$. Then define a cadlag function Ψ by $\Psi(x) = \inf_{y>x} \hat{\Psi}(y)$ for $x \in [0,1)$, $\Psi(x) = 0$ for $x < 0$ and $\Psi(x) = 1$ for $x \geq 1$. By this construction, the probability measure with distribution function Ψ is a weak limit of the sequence of probability measures with distribution functions Ψ_n. □

We have shown it is possible our process converges to a stable root or touchpoint of $F_1(y; x, \alpha, \Xi)$. The next step is to examine whether condensation can occur in our model. This happens when our process "jumps" from converging from one stable

root to another. This jump represents a discontinuity in the limit caused by the condensate which otherwise would not have been there based on initial distributions.

Dependent on the parameters of the specific model (α and x) the limit to which our sequence of random variables $\Psi_n(x)$ converges can either be continuous or discontinuous. A discontinuity in the limit Ψ of $\Psi_n(x)$ corresponds to a condensation phenomena occurring in the graph. As discussed in Section 2.2, this is where a proportionally small number of vertices $\mathbb{S}_n \subset V(G_n)$ have a positive probability of attracting an approximately constant proportion of new neighbours as $n \to \infty$.

This "jump" in the convergence represents a discontinuity in the limit of $\Psi_n(x)$ and could be down to a single vertex; though this is not necessarily the case. Referring back to the middle of three example discussed further in Section 3.1 when $\Xi = (0, 1, 0)$. The function $F_1(y; x, \alpha, \Xi)$ is a cubic polynomial allowing for a maximum of three real roots dependent on different input values of α and x. If three distinct real roots exist then there exist exactly two stable roots. We will talk more about this case in Section 3.3.3.

In order to examine whether a limit discontinuity is down to a single vertex becoming a persistent hub we introduce a second random variable tracking the evolution of a specific vertex; namely v_1. Without loss of generality, we study the vertex v_1 as it is present in the graph from the start of the process. We denote the location of v_1 as z in order to distinguish it from the others. For a graph G_n on $n + n_0$ vertices and a fixed value $\alpha \in (-1, \infty)$, the probability of selecting v_1 for attachment is derived from equation (2.4) as

$$D_n = \frac{\alpha + \deg_{G_n}(v_1)}{\sum_{i=1-n_0}^{n}(\alpha + \deg_{G_n}(v_i))},$$

by conditioning on the location of vertex one being equal to z. To do this we form a two dimensional stochastic approximation for $(\Psi_n(z), D_n)$ and consider whether vertex v_1 shows qualities of a persistent hub by attracting linear growth; alternatively whether $D_n \to 0$ as $n \to \infty$ as this indicates the degree of vertex one not growing at

a linear rate.

Let χ_n be the location of a selected vertex under preferential attachment from G_n. Assuming vertex one is the only vertex at location z, which is true almost surely, we have

$$\mathbb{P}(\chi_n = z|\mathcal{F}_n) = D_n,\ \mathbb{P}(\chi_n < z|\mathcal{F}_n) = \Psi_n(z) - D_n \text{ and } \mathbb{P}(\chi_n > z|\mathcal{F}_n) = 1 - \Psi_n(z).$$

The probability of selecting this vertex at location z for attachment conditional on the vertex being of rank k is given by

$$h_k(\Psi_n(z), D_n; e_{k,r}) = \left(\sum_{j=0}^{k-1} \sum_{i=k}^{r} \binom{r}{i} \binom{i}{j} (\Psi_n(z) - D_n)^j D_n^{i-j} (1 - \Psi_n(z))^{r-i} \right). \quad (3.4)$$

This is the sum of all of the combinations of the probabilities $\mathbb{P}(\chi_n = z)$, $\mathbb{P}(\chi_n > z)$ and $\mathbb{P}(\chi_n < z)$ which, when ranked by their locations ensures a vertex in the k^{th} position with location z.

Lemma 3.2.6. *For a fixed $\alpha \in (-1, \infty)$, the stochastic approximation equation related to D_n is given by*

$$D_{n+1} - D_n = \gamma_{n+1} \left(F_2(\Psi_n(z), D_n; \alpha, \Xi) + \zeta_{n+1} \right), \quad (3.5)$$

where

$$F_2(y, d; \alpha, \Xi) = -(2 + \alpha)d + \sum_{k=1}^{r} \Xi_k h_k(y, d; e_{k,r})$$

and ζ_{n+1} is the noise incurred such that $\mathbb{E}(\zeta_{n+1}|\mathcal{F}_n) = 0$.

Proof. Similarly to how we found equation (3.2) we use (3.4) to obtain the form outlined in Pemantle [Pem07].

$$\mathbb{E}(\gamma_{n+1}^{-1} D_{n+1}|\mathcal{F}_n) = \gamma_n^{-1} D_n + \sum_{k=1}^{r} \Xi_k h_k(y, d; e_{k,r})$$

$$
\begin{aligned}
&= \gamma_{n+1}^{-1} D_n - (2+\alpha) D_n + x(1+\alpha) + h\left(\Psi_n(x), D_n; \Xi\right) \\
&= \gamma_{n+1}^{-1} D_n + F_2\left(\Psi_n(x), D_n; \Xi\right),
\end{aligned}
$$

We therefore have the stochastic approximation equation for D_n in the form

$$
D_{n+1} - D_n = \gamma_{n+1}\left(F_2(\Psi_n(z), D_n; \Xi) + \zeta_{n+1}\right).
$$

We define ζ_{n+1} as

$$
\zeta_{n+1} = \gamma_{n+1}^{-1}\left(D_{n+1} - \mathbb{E}(D_{n+1}|\mathcal{F}_n)\right).
$$

It follows immediately that $\mathbb{E}(\zeta_{n+1}|\mathcal{F}_n) = 0$. □

We have formed a two dimensional system of stochastic approximation equations represented by

$$
\begin{pmatrix} \Psi_{n+1}(z) \\ D_{n+1} \end{pmatrix} - \begin{pmatrix} \Psi_n(z) \\ D_n \end{pmatrix} = \gamma_{n+1} \begin{pmatrix} F_1(\Psi_n(z); z, \alpha, \Xi) \\ F_2(\Psi_n(z), D_n; \alpha, \Xi) \end{pmatrix} + \gamma_{n+1} \begin{pmatrix} \xi_{n+1} \\ \zeta_{n+1} \end{pmatrix}.
$$

The following relationship between F_1 and F_2 is useful in solving our two dimensional set of stochastic approximation equations to find the stationary points of our vector field.

Theorem 3.2.7. *We have that*

$$
F_1(y-d; x, \alpha, e_{k,r}) = F_1(y; x, \alpha, e_{k,r}) - F_2(y, d; \alpha, e_{k,r}). \tag{3.6}
$$

Proof. In order to prove this result we use induction on k. For $k = 1$

$$
\begin{aligned}
F_1(y-d; x, \alpha, e_{1,r}) =& 1 - (1-y+d)^r - (2+\alpha)(y-d) + x(\alpha+1) \\
&- \left(-(2+\alpha)d + \sum_{i=1}^{r} \binom{r}{i} d^i (1-y)^{r-i}\right) \\
=& \left(-(2+\alpha)y + x(\alpha+1) + \sum_{i=1}^{r} \binom{r}{i} y^i (1-y)^{r-i}\right)
\end{aligned}
$$

$$=F_1(y;x,\alpha,e_{1,r})-F_2(y,d;\alpha,e_{1,r})$$

We show that the statement holds true for $F_1(y-d;x,e_{k+1,r})$ using equation (3.6) as the assumption step.

$$F_1(y-d;x,\alpha,e_{k+1,r})=x(\alpha+1)-(2+\alpha)(y-d)+\sum_{i=k+1}^{r}\binom{r}{i}(y-d)^i(1-y+d)^{r-i}$$

$$=F_1(y-d;x,\alpha,e_{k,r})-\binom{r}{k}(y-d)^k(1-y+d)^{r-k}$$

$$=F_1(y;x,\alpha,e_{k,r})-F_2(y,d;\alpha,e_{k,r})-\binom{r}{k}(y-d)^k(1-y+d)^{r-k},\text{ (by the induction hypothesis.)}$$

$$=F_1(y;x,\alpha,e_{k+1,r})-F_2(y,d;\alpha,e_{k,r})$$
$$-\binom{r}{k}(y-d)^k(1-y+d)^{r-k}+\binom{r}{k}y^k(1-y)^{r-k}$$

$$=F_1(y;x,\alpha,e_{k+1,r})-(2+\alpha)d-\left(\sum_{j=0}^{k-1}\sum_{i=k}^{r}\binom{r}{i}\binom{i}{j}(y-d)^jd^{i-j}(1-y)^{r-i}\right)$$
$$-\left(\sum_{i=k}^{r}\binom{r}{i}\binom{i}{k}(y-d)^kd^{i-k}(1-y)^{r-i}\right)$$
$$+\left(\sum_{j=0}^{k}\binom{r}{k}\binom{k}{j}(y-d)^jd^{k-j}(1-y)^{r-k}\right)$$

$$=F_1(y;x,\alpha,e_{k+1,r})-\left(\sum_{j=0}^{k-1}\sum_{i=k}^{r}\binom{r}{i}\binom{i}{j}(y-d)^jd^{i-j}(1-y)^{r-i}\right)-(2+\alpha)d$$
$$-\left(\sum_{j=k}^{k}\sum_{i=k}^{r}\binom{r}{i}\binom{i}{j}(y-d)^jd^{i-j}(1-y)^{r-i}\right)$$
$$+\left(\sum_{j=0}^{k}\sum_{i=k}^{k}\binom{r}{i}\binom{i}{j}(y-d)^jd^{i-j}(1-y)^{r-i}\right)$$

$$=F_1(y;x,\alpha,e_{k+1,r})-\left(\left(\sum_{j=0}^{k}\sum_{i=k+1}^{r}\binom{r}{i}\binom{i}{j}(y-d)^jd^{i-j}(1-y)^{r-i}\right)+(2+\alpha)d\right)$$

$$=F_1(y;x,\alpha,e_{k+1,r})-F_2(y,d;\alpha,e_{k+1,r})$$

completing the proof. □

Corollary 3.2.8. *Given the probability vector* $\Xi=(\Xi_1,\Xi_2,\ldots,\Xi_r)$ *associated to our model where* Ξ_k *is the probability associated with forming an edge between* v_{n+1} *and* v_k *we deduce from Theorem 3.2.7 that*

$$F_1(y-d;x,\alpha,\Xi)=F_1(y;x,\alpha,\Xi)-F_2(y,d;\alpha,\Xi)$$

Proof. By definition

$$\begin{aligned}F_1(y-d;x,\alpha,\Xi)=&\sum_{k=1}^{r}F_1(y-d;x,\alpha,e_{k,r})\\=&\sum_{k=1}^{r}\left(F_1(y;x,\alpha,e_{k,r})-F_2(y,d;\alpha,e_{k,r})\right)\\=&\sum_{k=1}^{r}(F_1(y;x,\alpha,e_{k,r}))-\sum_{k=1}^{r}(F_2(y,d;\alpha,e_{k,r}))\\=&F_1(y;x,\alpha,\Xi)-F_2(y,d;\alpha,\Xi)\end{aligned}$$

□

It follows from Theorem 3.2.8 that if $F_1\left(y_i;z,\alpha,\Xi\right)=F_1\left(y_j;z,\alpha,\Xi\right)=0$ then $F_2\left(y_i,y_i-y_j;z,\alpha,\Xi\right)=0$ and the solutions to $F_1\left(y;z,\alpha,\Xi\right)=F_2\left(y,d;\alpha,\Xi\right)=0$ all take the form $(y,d)=(y_i,y_i-y_j)$ where $i,j\in\{1,2,\ldots,r\}$.

We investigate the stability conditions of our two dimensional system by way of the Jacobian matrix given by

$$M=\begin{bmatrix}\frac{\partial}{\partial y}F_1\left(y_i;z,\alpha,\Xi\right) & \frac{\partial}{\partial d}F_1\left(y_i;z,\alpha,\Xi\right)\\ \frac{\partial}{\partial y}F_2\left(y,d;\alpha,\Xi\right) & \frac{\partial}{\partial d}F_2\left(y,d;\alpha,\Xi\right)\end{bmatrix}$$

We observe that M is an upper triangular matrix as $F_1(y; x, \alpha, \Xi)$ does not vary with D_n. We have that the eigenvalues of our system are given by

$$\lambda_1^{(k)}(y; \alpha, e_{k,r}) = \left(\sum_{i=k}^{r} \binom{r}{i} y^{i-1}(1-y)^{r-i-1}(i-r) \right) - (2+\alpha),$$
$$\lambda_2^{(k)}(y, d; \alpha, e_{k,r}) = \left(\sum_{j=0}^{k-1} \sum_{i=k}^{r} \binom{r}{i}\binom{i}{j} Q_{i,j}(y,d) y^{j-1} d^{i-j-1}(1-y)^{r-i-1} \right) - (2+\alpha),$$

where $Q_{i,j}(y,d) = (y-d)(i - iy + rd - id) + j(1-y)(2d-y)$. The eigenvalues associated to our full model with respect to Ξ are given by

$$\lambda_1(y; \alpha, \Xi) = \sum_{k=1}^{r} \Xi_k \frac{\partial}{\partial y} F_1(y; x, \alpha, e_{k,r}) = \sum_{k=1}^{r} \Xi_k \lambda_1^{(k)}(y; \alpha, e_{k,r})$$

and

$$\lambda_2(y, d; \alpha, \Xi) = \sum_{k=1}^{r} \Xi_k \frac{\partial}{\partial d} F_2(y, d; \alpha, e_{k,r}) = \sum_{k=1}^{r} \Xi_k \lambda_1^{(k)}(y-d; \alpha, e_{k,r}).$$

Here $y \in \{y_1, y_2, \ldots, y_r\}$ which is the set of solutions to equation $F_1(y; x, \alpha, \Xi) = 0$. If $F_1(y_i; x, \alpha, \Xi) = 0$ then by using equation (3.6) and equating terms we see that $F_2(y_i, y_i - y_j; \alpha, \Xi) = 0$.

It follows from Theorem 3.2.7 that if

$$F_1(y_i; x, \alpha, e_{k,r}) = F_1(y_j; x, \alpha, e_{k,r}) = 0$$

then

$$F_2(y_i, y_i - y_j; x, \alpha, \Xi) = 0. \tag{3.7}$$

We see from (3.7) that the solutions of $F_1(y; x, \alpha, \Xi) = F_2(y, d; \alpha, \Xi) = 0$ take the form $(y_i, y_i - y_j)$ where $i, j \in \{1, 2, \ldots, r\}$. Using intuition we deduce that some of these solutions are not feasible. For example, solutions where $y_j > y_i$ are clearly infeasible as they cause D_n to be negative which is impossible based on its definition.

Lemma 3.2.9. *If both $y_i - y_j > 0$ such that*

$$F_1(y_i; x, \alpha, e_{k,r}) = F_1(y_j; x, \alpha, e_{k,r}) = 0$$

and

$$\frac{\partial}{\partial y} F_1(y; x, \alpha, \Xi) = \lambda_1(y; \alpha, \Xi) < 0$$

are satisfied then for both y_i,y_j $(y_i, y_i - y_j)$ is a stable stationary point of the vector field described by equations (3.2) and (3.5).

Proof. By rearranging equation (3.6) we see that

$$F_2(y, d; \alpha, \Xi) = F_1(y; x, \alpha, \Xi) - F_1(y - d; x, \alpha, \Xi)$$

and deduce that $\lambda_2(y, d; \alpha, \Xi) = \frac{\partial}{\partial d}\left(F_1(y; x, \alpha, \Xi) - F_1(y - d; x, \alpha, \Xi)\right)$, here because $F_1(y; x, \alpha, \Xi)$ does not depend on d it follows that $\frac{\partial}{\partial y} F_1(y; x, \alpha, \Xi) = 0$. It is observable that $\lambda_2(y, d; \alpha, \Xi) = -\frac{\partial}{\partial d} F_1(y - d; x, \alpha, \Xi) = \lambda_1(y - d; \alpha, \Xi)$. All roots of $F_1(y; x, \alpha, \Xi) = F_2(y, d; \alpha, \Xi) = 0$ are of the form $(y_i, y_i - y_j)$. If we evaluate our eigenvalues at this point we get $\lambda_1(y_i; \alpha, \Xi)$ and $\lambda_2(y_i, d_i; x, \alpha, \Xi) = \lambda_1(y_j; \alpha, \Xi)$, which by referring to our initial conditions are both negative. Therefore the pair y_i and y_j form the possible limit $(y_i, y_i - y_j)$. □

Corollary 3.2.10. *As a direct consequence of Lemma 3.2.9; if we have two stable fixed points in the one dimensional system $y_i, y_j \in \{y_1, y_2, \ldots, y_r\}$ such that $y_i \geq y_j$ then there is a positive probability that $(\Psi_n(x), D_n) \to (y_i, y_i - y_j)$ is a limit as $n \to \infty$ of the stochastic process resulting in the potential for condensation to occur at vertices which have a location in the region which produced y_i and y_j.*

Proof. Lemma 3.2.9 states that $(y_i, y_i - y_j)$ is a stationary point of the vector field given by $(F_1(\cdot), F_2(\cdot))$. It follows from Theorem 2.16 of [Pem07] that it suffices to show convergence to this stable point cannot happen if there is no t for which $(\Psi_{n+t}(z), D_{n+t})_{n \geq 0}$, as $(F_1(\cdot), F_2(\cdot))$ almost surely avoids some neighbourhood of

$(y_i, y_i - y_j)$. It is true that both $\deg_{G_{t+n}}(v_0) \in (\deg_{G_0}(v_0), \deg_{G_0}(v_0) + t + n)$ and $D_{t+n} \in \left[0, \frac{1}{2+\alpha}\right]$ for sufficiently large n. We can use similar arguments for $\Psi_{n+t}(z)$, to show $(\Psi_{n+t}(z), D_{n+t})_{n\geq 0}$ approaches $(y_i, y_i - y_j)$ arbitrarily close so long as $0 \leq y_i \leq 1$ and $0 \leq y_i - y_j \leq \frac{1}{2+\alpha}$. Both of these conditions hold assuming $y_i \geq y_j$ as $y_i - y_j = d_i$ satisfying $d_i \in \left[0, \frac{1}{2+\alpha}\right]$ and noting that

$$\frac{(1+\alpha)x}{2+\alpha} \leq y \leq \frac{1}{2+\alpha} + \frac{(1+\alpha)x}{2+\alpha}.$$

□

A natural question to discuss is whether there could be more than one point of condensation in the model corresponding to more than one discontinuity in the limit Ψ. The following result outlines that in the situation when v_{n+1} always attaches to the member of the seleced r vertices with the k^{th} highest location ($e_{k,r} = 1$) then it is impossible to have two (or more) points of condensation.

Theorem 3.2.11. *When we sample r vertices using preferential attachment forming an edge between the new vertex v_{n+1} and the vertex in the sample with rank k with probability 1, it is impossible to have more than one point of condensation.*

Proof. Note that

$$\begin{aligned}
\frac{\partial}{\partial y} g(y; e_{k,r}) =& \frac{\partial}{\partial y} \sum_{i=k}^{r} \binom{r}{i} y^i (1-y)^{r-i} \\
=& \sum_{i=k}^{r} i \binom{r}{i} y^{i-1} (1-y)^{r-i} - \sum_{i=k}^{r-1} (r-i) \binom{r}{i} y^i (1-y)^{r-i-1} \\
=& \sum_{i=k}^{r} r \binom{r-1}{i-1} y^{i-1} (1-y)^{r-i} - \sum_{i=k}^{r-1} r \binom{r-1}{i} y^i (1-y)^{r-i-1} \\
=& r \binom{r-1}{k-1} y^{k-1} (1-y)^{r-k},
\end{aligned}$$

by way of a teloscopic sum. Therefore

$$\frac{\partial}{\partial y}F_1(y;x,\alpha,e_{k,r}) = r\binom{r-1}{k-1}y^{k-1}(1-y)^{r-k} - (2+\alpha)\,.$$

If $k=r$ then $\frac{\partial^2}{\partial y^2}F_1(y;x,\alpha,e_{k,r})$ is positive on $(0,1)$, and if $k=1$ then it is negative on $(0,1)$. Otherwise,

$$\begin{aligned}\frac{\partial^2}{\partial y^2}F_1(y;x,\alpha,e_{k,r}) =& r\binom{r-1}{k-1}\big((k-1)(1-y)-(r-k)y\big)y^{k-2}(1-y)^{r-k-1}\\ =& r\binom{r-1}{k-1}y^{k-2}(1-y)^{r-k-1}\big((k-1)-(r-1)y\big),\end{aligned}$$

which is positive for $y\in(0,\frac{k-1}{r-1})$ and negative for $y\in(\frac{k-1}{r-1},1)$. It follows that the equation $\frac{\partial}{\partial y}F_1(y;x,\alpha,e_{k,r})=0$ has at most two roots in $(0,1)$, and further that if it has exactly two roots $z_1<z_2$ then $\frac{\partial}{\partial y}F_1(y;x,\alpha,e_{k,r})>0$ in the range $z_1<y<z_2$. Consequently, the equation $F_1(y;x,\alpha,e_{k,r})=0$ has at most three roots in $[0,1]$. By Theorems 3.2.9 the two dimensional system associated to a vertex with location z in which condensation can occur has the form (y_i, y_i-y_j) such as $y_i-y_j>0$; here y_i, y_j are roots of $F_1(y;x,\alpha,e_{k,r})=0$ and $\frac{\partial}{\partial y}F_1(y_i;x,\alpha,e_{k,r})$, $\frac{\partial}{\partial y}F_1(y_j;x,\alpha,e_{k,r})<0$. □

3.3 Examples

During this section we outline four cases that occur from different attachment vectors $\Xi=(\Xi_1,\Xi_2,\ldots,\Xi_r)$ which highlight different traits of results proved in Section 3.2. All four of the following examples follow the same initial process as outlined in Section 3.1. Starting with a tree G_0 on n_0 vertices, at each step we add one vertex to G_n, in order to maintain the tree property we have set the number of edges the new vertex brings to G_n to one. To obtain G_{n+1} we use preferential attachment on G_n to select r vertices from $V(G_n)$ with replacement according to equation (2.4). Our new vertex then attaches based on a fixed vector of probabilities Ξ.

If we choose $r=1$ we have regular preferential attachment as outlined in Section 3.1.

If we chose $r = 2$ the options are $\Xi = (0, 1)$ and $\Xi = (1, 0)$ which fall into the highest of r case by definition or symmetry, likewise for the highest and lowest case when $r = 3$. The general case for $r = 2$ is explored in Section 3.3.2 where $\Xi = (\Xi_1, \Xi_2)$. The simplest case where attachment is always to a particular ranked vertex ($\Xi_k = 1$) in which we expect different results from the highest of r case is the middle of three denoted by the vector $\Xi = (0, 1, 0)$ explored in section 3.3.3. Finally in Section 3.3.4 we discuss the situation where $\Xi = \left(0, \frac{1}{2}, 0, 0, 0, \frac{1}{2}, 0\right)$ as this case exhibits interesting properties.

3.3.1 Largest of r

This case corresponds to the vector $\Xi = (0, \ldots, 0, 1)$ where the new vertex v_{n+1} attaches to the member of the r selected vertices which corresponds to the highest location. By using equation (3.1) to attain $g(y; e_{r,r}) = y^r$ we formulate the stochastic approximation equation

$$F_1(y; x, \alpha, e_{r,r}) = y^r - (2 + \alpha)y + x(1 + \alpha).$$

Figure 3.1 below shows the behaviour of this model at a fixed $\alpha = -\frac{1}{2}$ for four values of r. Each figure is evaluated at three values of x namely $\left\{0, \frac{1}{2}, 1\right\}$, (bottom, middle, top lines of each respectively.)

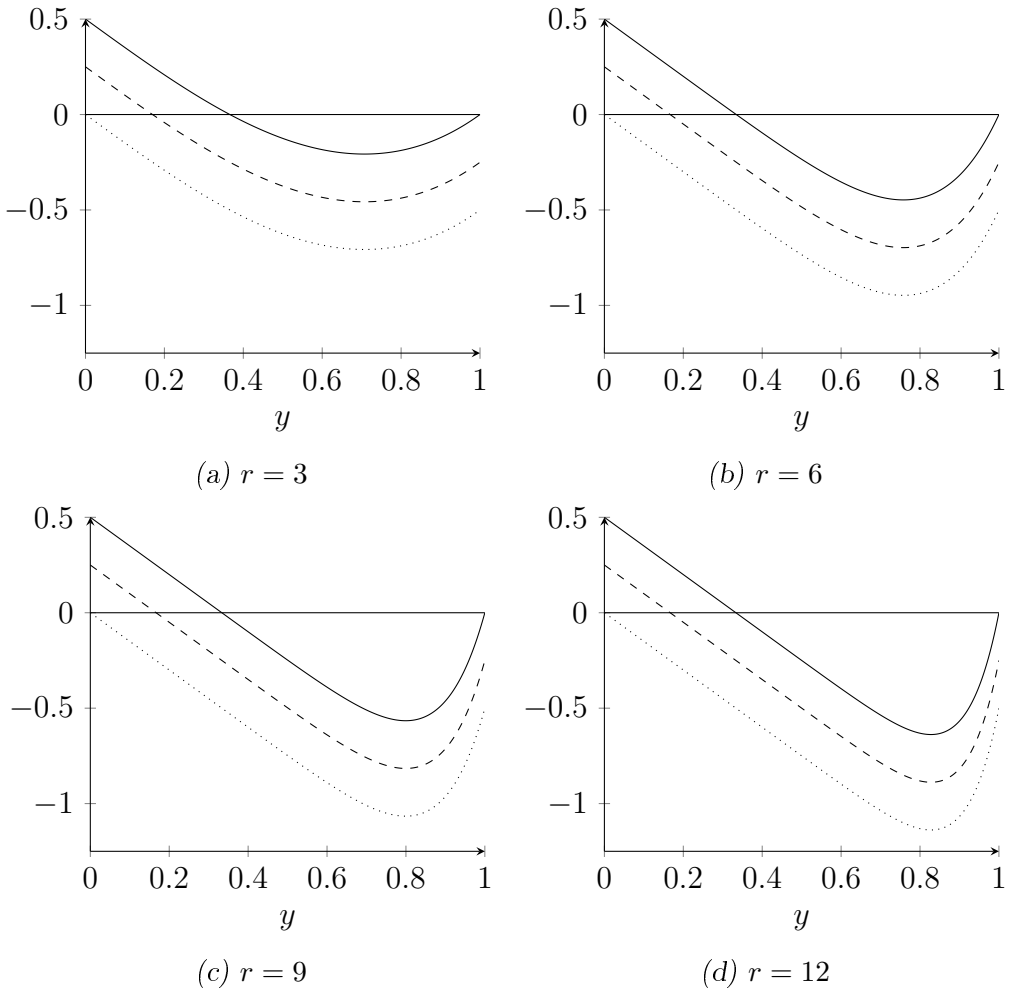

(a) $r = 3$ (b) $r = 6$

(c) $r = 9$ (d) $r = 12$

Fig. 3.1: A depiction of how an increase in r varies the stochastic approximation equation for a fixed value of $\alpha = -\frac{1}{2}$ evaluated at each of $x \in \{0, \frac{1}{2}, 1\}$.

Here we observe that as r increases the turning point inside $y \in [0, 1]$ increases while its vertical component decreases. Figure 3.2 plot below gives the behaviour of our stochastic approximation equation as α decreases for a fixed value of r. (Again all figures are evaluated at $x \in \{0, \frac{1}{2}, 1\}$.)

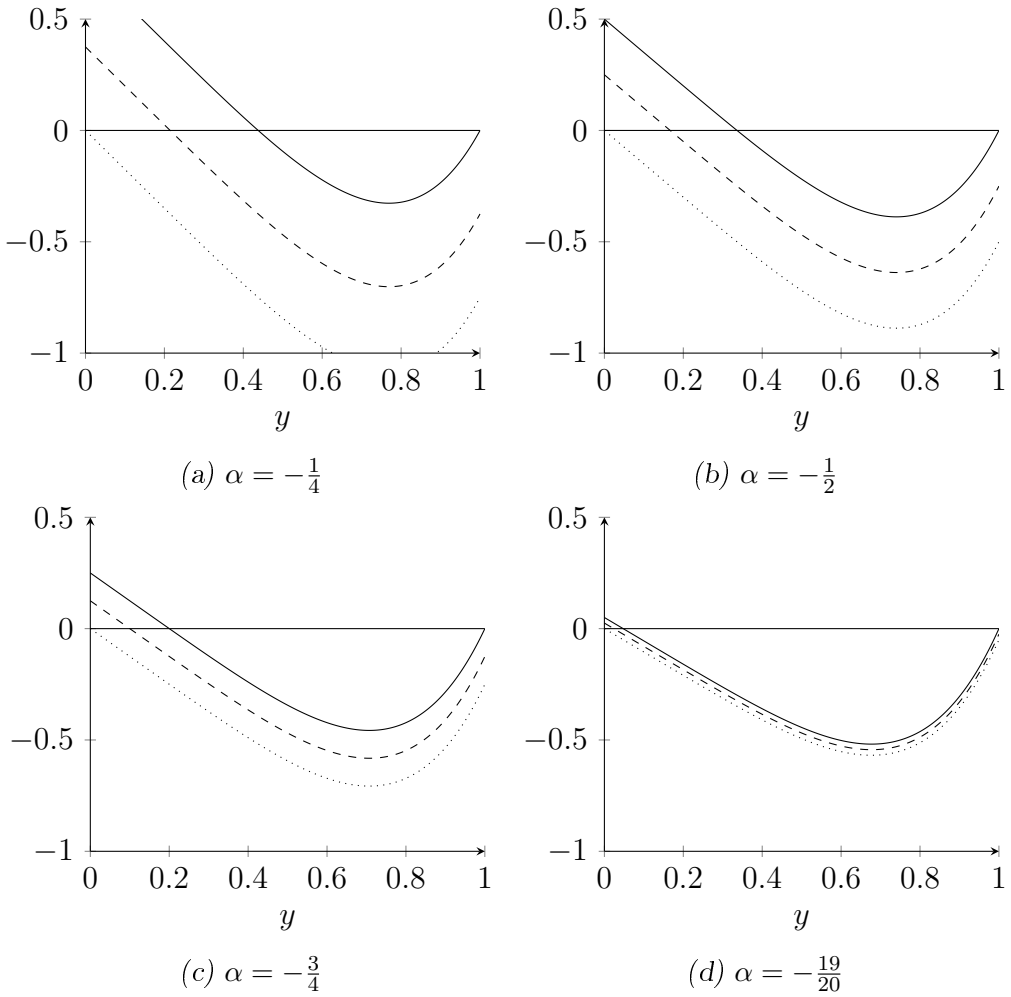

(a) $\alpha = -\frac{1}{4}$ (b) $\alpha = -\frac{1}{2}$

(c) $\alpha = -\frac{3}{4}$ (d) $\alpha = -\frac{19}{20}$

Fig. 3.2: Graphs to show how a decrease in α effects the stochastic approximation equation for a fixed value of $r = 5$.

Here we see that as α decreases towards -1, the turning point is tending towards $\left(r^{-\frac{1}{r-1}}, (r-1)r^{-\frac{1}{r-1}}\right)$.

In order to analyze this model we first fix $x \in (0,1)$. We see that $F_1(0; x, \alpha, e_{r,r}) = x(\alpha+1) > 0$ and $F_1(0; x, \alpha, e_{r,r}) = (x-1)(\alpha+1) < 0$ for all $\alpha \in (-1, \infty)$. We calculate the turning points as $y \in \left\{\pm \sqrt[r-1]{\frac{2+\alpha}{r}}\right\}$ and disregarding the negative value

as it is never satisfies $y \in [0,1]$. We can see that

$$\frac{\partial^2}{\partial y^2} F_1\left(\left(\frac{2+\alpha}{r}\right)^{\frac{1}{r-1}}; x, \alpha, e_{r,r}\right) = r(r-1)\left(\frac{2+\alpha}{r}\right)^{\frac{r-2}{r-1}}$$

is positive and strictly monotonic for all integers $r \geq 2$ and $\alpha \in (-1, \infty)$. There exists exactly one solution of $F_1(y; x, \alpha, e_{r,r}) = 0$ for $y \in [0,1]$. The turning point of which is at $y = \left(\frac{2+\alpha}{r}\right)^{\frac{1}{r-1}}$ satisfying $0 \leq \left(\frac{2+\alpha}{r}\right)^{\frac{1}{r-1}} \leq 1$ when $-2 \leq \alpha \leq r-2$ which we can refine to $-1 < \alpha \leq r-2$ to include the definition of α.

Pulling all of this together we study how $F_1'(y; \alpha, e_{r,r})$ behaves in the region $y \in [0,1]$. It is easy to show that $y = 0$ and $y = 1$ are roots of $F_1(y; x, \alpha, e_{r,r}) = 0$ for all $r \in \mathbb{N}$ when evaluated at $x = 0$ and $x = 1$ respectively. The gradient of $F_1'(0; \alpha, e_{r,r}) = -(2+\alpha) < 0$, is always negative for any values of r and α. Whereas $F_1'(1; \alpha, e_{r,r}) > 0$ for each $r \in \mathbb{N}$ when $r > (2+\alpha)$.

When $\alpha \in (-1, r-2]$ there exists a turning point when $y \in [0,1]$ implying $F_1(1; x, e_{r,r})$ is an increasing function which allows for condensation. When $\alpha > r-2$ there is no turning point in $[0,1]$ therefore $F_1(1; x, \alpha, e_{r,r})$ is a decreasing function. If

$$\frac{\partial}{\partial y} F_1(y; x, \alpha, e_{r,r})\Big|_{y=0} < 0,$$

then $r \leq 2+\alpha$. When satisfied, there is no discontinuity in the limit, hence no condensation. Further results on this model can be found in [FJ18] where the authors explore this model further allowing for an r of random size.

3.3.2 Choice of two

In this section we look at the natural extension of the highest/lowest of two model which both follow the structure of the highest of r case previously discussed. We examine the selection vector $\Xi = (\Xi_1, \Xi_2)$ where neither Ξ_1 or Ξ_2 equal 1. An example of when a model like this might be used is a binary voting system, specifically when the attractiveness to one candidate is higher than the other. Here we want to study

whether two candidates could gain a positive proportion of votes in the limit.

The associated stochastic approximation equations are found using Lemmas 3.2.1 and 3.2.6 to be:

$$F_1(y; x, \alpha, \Xi) = (1 - 2\Xi_1)y^2 - (2 + \alpha - 2\Xi_1)y + x(\alpha + 1) \tag{3.8}$$

and

$$F_2(y, d; \alpha, \Xi) = d(2d\Xi_1 - d + 2y - 4\Xi_1 y - 2 - \alpha + 2\Xi_1).$$

Figure 3.3 displays how $F_1\left(y; \frac{1}{2}, \alpha, \Xi\right)$ behaves as α decreases. Here we see an initial

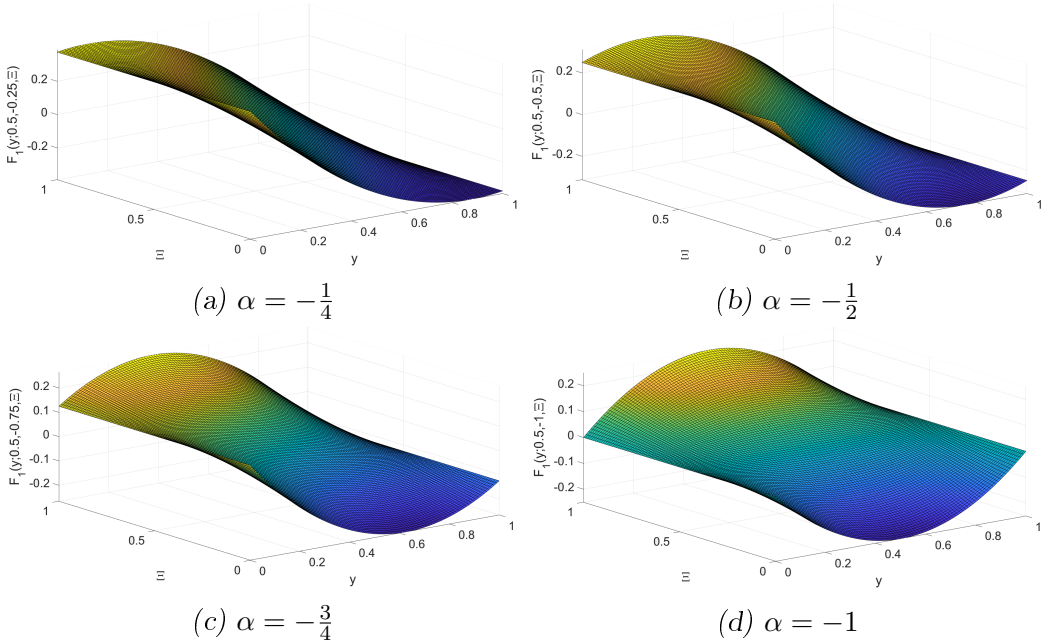

(a) $\alpha = -\frac{1}{4}$ (b) $\alpha = -\frac{1}{2}$

(c) $\alpha = -\frac{3}{4}$ (d) $\alpha = -1$

Fig. 3.3: The function $F_1\left(y; \frac{1}{2}, \alpha, \Xi\right)$ evaluated at four different values of α.

bias towards values of y on the lower end of its range. This bias clearly weakens as $\alpha \to -1$. As equation (3.8) is a quadratic we solve it attaining the solutions

$$\psi_+(x), \psi_-(x) = \frac{(2 + \alpha - 2\Xi_1)}{2(1 - 2\Xi_1)} \pm \frac{\sqrt{(2 + \alpha - 2\Xi_1)^2 - 4x(\alpha + 1)(1 - 2\Xi_1)}}{2(1 - 2\Xi_1)}, \tag{3.9}$$

for $\Xi_1 \neq \frac{1}{2}$. The case where $\Xi = \frac{1}{2}$ is uninteresting as it reduces the model to regular preferential attachment as the ranking of the sampled vertex's locations pays no part in the formation of edges. This statement remains true in the general case where each entry of the length r vector Ξ is equal to $\frac{1}{r}$. For either solution of equation (3.9) we solve $F_2(\psi_i(x), d_j; \alpha, \Xi)$ for d as

$$d_1 = 0 \text{ and } d_2 = 2\psi_i(x) - 1 - \frac{\alpha + 1}{1 - 2\Xi_1}.$$

We look for the stable roots of this model using the Jacobian matrix or the general form found in Section 3.2 to find the eigenvalues

$$\lambda_1 = 2y(1 - 2\Xi_1) - (2 + \alpha - 2\Xi_1) \tag{3.10}$$

and

$$\lambda_2 = 4d\Xi_1 - 2d + 2y - 4y\Xi_1 - 2 - \alpha + 2\Xi_1 = 4d(\Xi_1 - 1) + \lambda_1 = -4d(1 - \Xi_1) + \lambda_1.$$

It is clear that if λ_1 is negative then λ_2 must also be negative. By rearranging equation (3.10) we see that λ_1 is negative if

$$y < \frac{2 + \alpha - 2\Xi_1}{2(1 - 2\Xi_1)}$$

which is the first term of equation (3.9). We therefore need only solve

$$0 = \frac{\sqrt{(2 + \alpha - 2\Xi_1)^2 - 4x(\alpha + 1)(1 - 2\Xi_1)}}{2(1 - 2\Xi_1)} \tag{3.11}$$

in order to find a critical point in the stability of the first eigenvalue. Equation (3.11) is satisfied when

$$x = \frac{(2 + \alpha - 2\Xi_1)^2}{4(\alpha + 1)(1 - 2\Xi_1)}$$

which we denote by x_{crit}. If $x < x_{crit}$ it follows that $\psi_+(x)$ is stable. We conclude that $\psi_-(x)$ is stable when $x > x_{crit}$. We look into necessary conditions on α and Ξ_1

to ensure $x_{crit} \in (0,1)$,

$$\begin{aligned} 0 <& x_{crit} < 1 \\ 0 <& \frac{(2+\alpha-2\Xi_1)^2}{4(\alpha+1)(1-2\Xi_1)} < 1 \\ 0 <& 1 + \frac{(\alpha+2\Xi_1)^2}{4(\alpha+1)(1-2\Xi_1)} < 1. \end{aligned}$$

Which we rearrange to formulate expressions based on whether $\Xi_1 < \frac{1}{2}$ or $\Xi_1 > \frac{1}{2}$. We first look at the case when $\Xi_1 < \frac{1}{2}$:

$$\begin{aligned} 0 < 1 + \frac{(\alpha+2\Xi_1)^2}{4(\alpha+1)(1-2\Xi_1)} < 1 \\ -4(\alpha+1)(1-2\Xi_1) < (\alpha+2\Xi_1)^2 < 0. \end{aligned}$$

We see that there are no combinations of $\alpha > -1$ and $\Xi_1 \in (0,1)$ which satisfy $(\alpha+2\Xi_1)^2 < 0$. We look at the situation when $\Xi_1 > \frac{1}{2}$:

$$\begin{aligned} 0 < 1 + \frac{(\alpha+2\Xi_1)^2}{4(\alpha+1)(1-2\Xi_1)} < 1 \\ 0 < 1 - \frac{(\alpha+2\Xi_1)^2}{4(\alpha+1)(2\Xi_1-1)} < 1 \\ -4(\alpha+1)(1-2\Xi_1) < -(\alpha+2\Xi_1)^2 < 0. \end{aligned}$$

We see that $-(\alpha+2\Xi_1)^2 < 0$ is always true for $\alpha > -1$ and $\Xi_1 \in (0,1)$. We examine the lower limit of this which is never satisfied.

$$\begin{aligned} -4(\alpha+1)(1-2\Xi_1) < -(\alpha+2\Xi_1)^2 \\ (2\Xi_1-\alpha-2)^2 < 0. \end{aligned}$$

As our one dimensional stochastic approximation equation given by equation (3.8) is a degree two polynomial we cannot have two distinct stable roots, therefore cannot attract condensation occurring in this model for any $x \in (0,1)$.

For completeness we examine the cases where $x = 0$ and $x = 1$ to see if condensation could occur at vertices with these locations. It remains true that if $\lambda_1 < 0$ then $\lambda_2 < 0$. We look at the $x = 0$ case. We use equation (3.9) to show that

$$\psi_-(x) = 0$$

and

$$\psi_+(x) = \frac{2 + \alpha - 2\Xi_1}{1 - 2\Xi_1}.$$

When we evaluate the eigenvalues of our system at each of these points we get that $\psi_-(x)$ is stable when $\Xi_1 < \frac{2+\alpha}{2}$ and $\psi_+(x)$ is stable when $\Xi_1 > \frac{2+\alpha}{2}$. This means we have a phase transition occurring at $\Xi_1 = \frac{2+\alpha}{2}$.

For the case when $x = 1$ we find the roots of the first stochastic approximation equation to be

$$\psi_+(x) = 1$$

and

$$\psi_-(x) = \frac{1 + \alpha}{1 - 2\Xi_1}.$$

Similarly we evaluate λ_1 at these points and find that $\psi_+(x)$ is stable when $-\frac{\alpha}{2} < \Xi_1$ and $\psi_-(x)$ when $-\frac{\alpha}{2} > \Xi_1$ meaning this phase transition occurs when $\Xi_1 = -\frac{\alpha}{2}$.

These two results are interesting as if we let $\alpha = -1$ (which is not possible as $\alpha > -1$) then both of these phase transitions equal $\frac{1}{2}$. Therefore as $\alpha > -1$ a bias occurs in our model. If the new vertex favours attachment to vertices with lower locations then $\psi_+(x)$ is stable and if higher locations are more favourable then $\psi_-(x)$ is stable. This can be seen in Figure 3.3. Condensation can occur at $x = 0$ if $\alpha < -2(1 - \Xi_1)$ and at $x = 1$ if $\alpha < -2\Xi_1$.

3.3.3 *Middle of three*

In previous examples we have examined simple cases where it is beneficial for a vertex to have a location close to 0 or 1. We will now explore a situation where this is not

the case. This section characterizes the behaviour of the simplest case in which we expect different results to previous sections. In this middle of three model it is no longer beneficial to have a location close to 0 or 1. This model behaves as follows; the new vertex v_{n+1} joins the graph G_n selecting three ($r = 3$) vertices using preferential attachment. An edge is formed between itself and the selected vertex which has the median location of the three with probability 1. Using notation described in Section 3.1 we describe this as $\Xi = (0, 1, 0) = e_{2,3}$.

Using the setting we described in Lemmas 3.2.1 and 3.2.6 we express our functions $F_1(y; x, \alpha, e_{k,r})$ and $F_2(y, d; \alpha, e_{k,r})$ as

$$F_1(y; x, \alpha, e_{2,3}) = -2y^3 + 3y^2 - (2 + \alpha)y + x(\alpha + 1)$$

and

$$F_2(y, d; \alpha, e_{2,3}) = -2d^3 + 6d^2y - 3d^2 - 6dy^2 + 6dy - d(2 + \alpha).$$

Figure 3.4 shows the behaviour of $F_1(y; x, \alpha, e_{2,3})$ as α decreases for $x, y \in [0, 1]$. This Figure gives us an indication of the general structure of the solution set of this system for four different values of x. Figure 3.5 displays a cross sectional view of Figure 3.3c for $x = \frac{1}{2}$ in which there exist three real roots. Otherwise there exists exactly one real root.

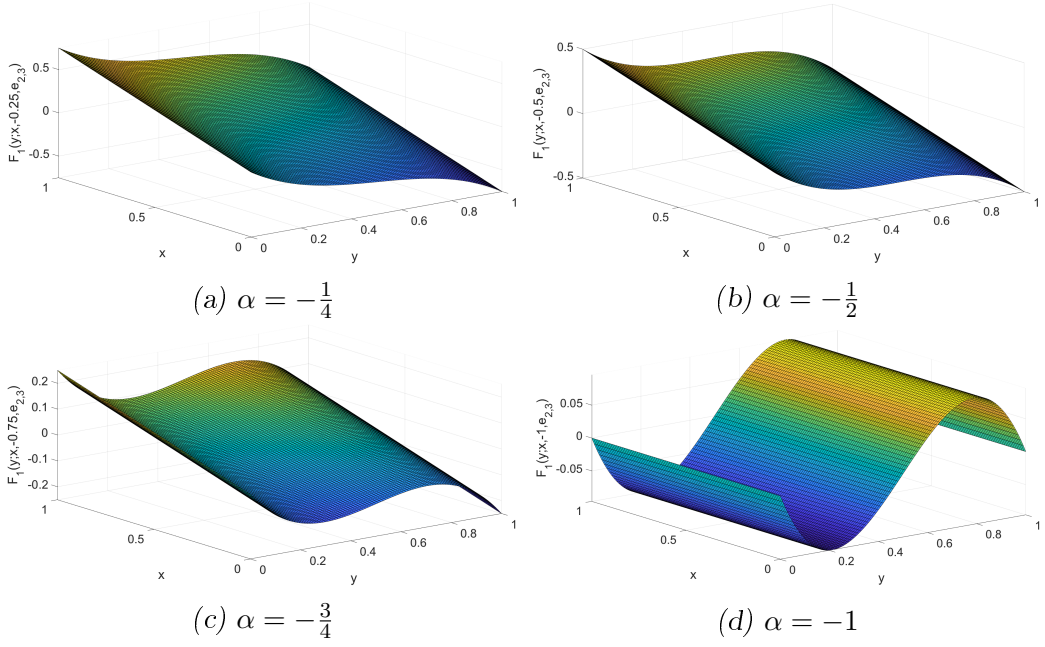

(a) $\alpha = -\frac{1}{4}$ (b) $\alpha = -\frac{1}{2}$

(c) $\alpha = -\frac{3}{4}$ (d) $\alpha = -1$

Fig. 3.4: The function $F_1(y; x, \alpha, e_{2,3})$ evaluated at different values of α and x.

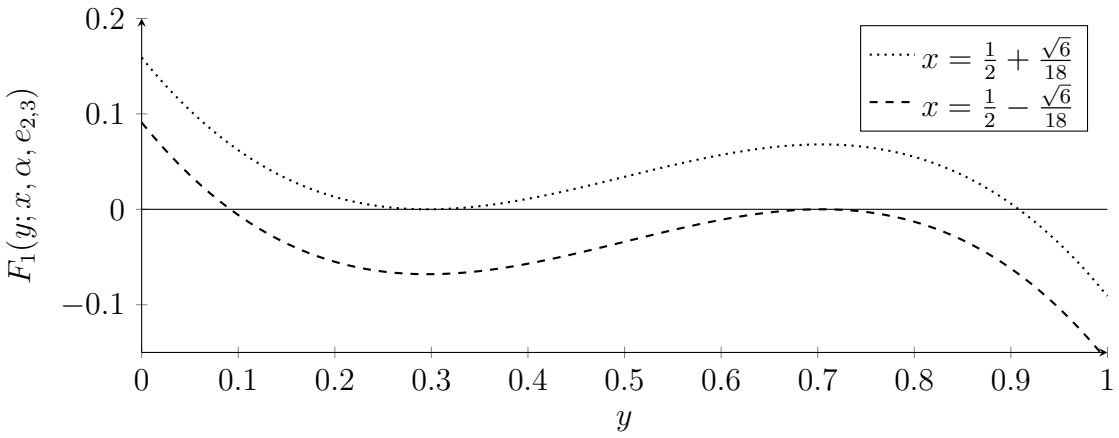

Fig. 3.5: $F_1\left(y; x, -\frac{3}{4}, e_{2,3}\right)$ evaluated at both $x = \frac{1}{2} \pm \frac{\sqrt{6}}{18}$.

Using Figure 3.5 we create a new diagram that depicts the frequency of roots of $F_1(y; x, \alpha, e_{2,3})$ as x increases from 0 to 1. The vertical axis expresses the value of the root or roots at any given $x \in [0, 1]$.

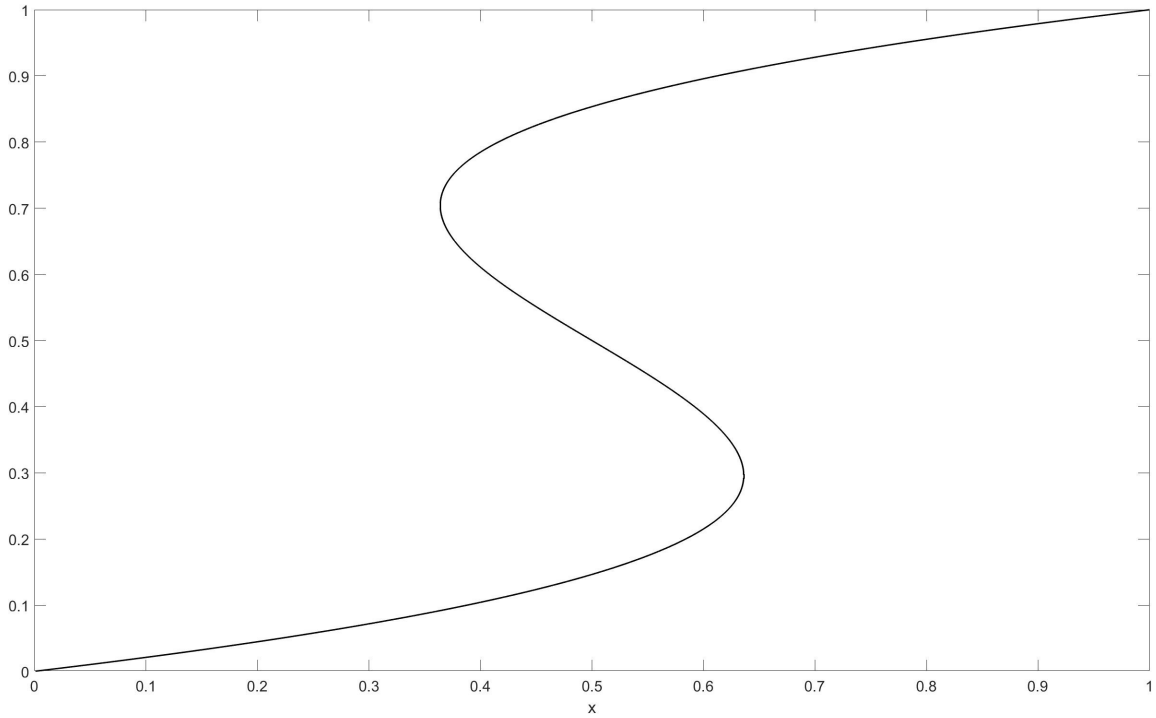

Fig. 3.6: Frequency plot of the roots of $F_1(y; x, 3/4, e_{2,3}) = 0$ against x.

It is clear to see from Figures 3.5 and 3.6 that there exists exactly one real root when $x \in \left\{\left[0, \frac{9+\sqrt{6}}{18}\right) \cup \left(\frac{9-\sqrt{6}}{18}, 1\right]\right\}$ and three real roots when $x \in \left[\frac{9-\sqrt{6}}{18}, \frac{9+\sqrt{6}}{18}\right]$.

For $x \in (0,1)$ $F_1(y; x, \alpha, e_{2,3}) = 0$ is a cubic; let us denote $\{\psi_1(x), \psi_2(x), \psi_3(x)\}$ such that $\psi_1(x) \leq \psi_2(x) \leq \psi_3(x)$ as the three real roots of $F_1(y; x, \alpha, e_{2,3}) = 0$ when three exist and $\psi(x)$ as the single real root when exactly one exists.

Theorem 3.3.1. *For a fixed location $x \in (0,1)$, the random variable $\Psi_n(x)$ converges pointwise as $n \to \infty$ almost surely to the following limits.*

$$\lim_{n\to\infty} \Psi_n(x) = \begin{cases} \psi(x), & \text{if } \alpha \geq -\frac{1}{2} \\ \psi(x), & \text{if } \alpha \in (-\frac{7}{8}, -\frac{1}{2}) \text{ and } x \notin \left[\frac{1}{2} - s, \frac{1}{2} + s\right] \\ \psi_1(x) \text{ or } \psi_3(x), & \text{if } \alpha \in (-\frac{7}{8}, -\frac{1}{2}) \text{ and } x \in \left[\frac{1}{2} - s, \frac{1}{2} + s\right] \\ \psi_1(x) \text{ or } \psi_3(x), & \text{if } \alpha \leq -\frac{7}{8} \end{cases}$$

where $s = \sqrt{\frac{-(1+2\alpha)^3}{108(\alpha+1)^2}}$.

Proof. By observation we see a phase transition at $\alpha = -\frac{1}{2}$. By solving $\frac{\partial}{\partial y}F_1(y; x, \alpha, e_{2,3}) = 0$ we calculate the turning points to be

$$\left(\frac{1}{2} + \sqrt{\frac{-1-2\alpha}{12}}, (\alpha+1)\left(x - \frac{1}{2}\right) + \frac{(-1-2\alpha)^{\frac{3}{2}}}{6\sqrt{3}}\right),$$
$$\left(\frac{1}{2} - \sqrt{\frac{-1-2\alpha}{12}}, (\alpha+1)\left(x - \frac{1}{2}\right) - \frac{(-1-2\alpha)^{\frac{3}{2}}}{6\sqrt{3}}\right).$$

The product of the vertical components of these turning points is negative if and only if there exists exactly three real roots.

$$0 > \left((\alpha+1)\left(x - \frac{1}{2}\right) - \frac{(-1-2\alpha)^{\frac{3}{2}}}{6\sqrt{3}}\right)\left((\alpha+1)\left(x - \frac{1}{2}\right) + \frac{(-1-2\alpha)^{\frac{3}{2}}}{6\sqrt{3}}\right)$$
$$0 > (\alpha+1)^2\left(x - \frac{1}{2}\right)^2 + \frac{(1+2\alpha)^3}{108}$$

by rearranging we deduce

$$\sqrt{-\frac{(1+2\alpha)^3}{108(\alpha+1)^2}} > \left|x - \frac{1}{2}\right|$$

which the desired critical points of $\frac{1}{2} \pm s$ are concluded. In the situation when $\alpha \geq -\frac{1}{2}$, $F_1(y; x, \alpha, e_{2,3}) = 0$ does not possess turning, points therefore there exists exactly one real root to converge to which was previously defined to be $\psi(x)$. Therefore $\Psi_n(x)$ is almost surely continuous. As we have restricted x to the interval $[0, 1]$ if $\alpha \leq \frac{-7}{8}$ that for every $x \in [0, 1]$ our function has exactly three real roots. By solving $\sqrt{\frac{-(1+2\alpha)^3}{108(\alpha+1)^2}} = \frac{1}{2}$ we see that when $\alpha \in \left(-\frac{7}{8}, -\frac{1}{2}\right)$ there exists a value $s = \sqrt{\frac{-(1+2\alpha)^3}{108(\alpha+1)^2}}$ such that $F_1(y; x, \alpha, e_{2,3}) = 0$ has three real roots when $x \in \left[\frac{1}{2} - s, \frac{1}{2} + s\right]$ and one real root when $x \in \{[0, s) \cup (1-s, 1]\}$. When our function satisfies the conditions outlined after Lemma 3.2.1 we conclude convergence almost surely to one of the

stationary points given by $\psi_1(x)$ and $\psi_3(x)$. □

For the associated phase transition $\alpha = -\frac{1}{2}$, it is true that when $\alpha \geq -\frac{1}{2}$, Ψ is almost surely continuous as there are no discontinuities in the limit (as required for condensation.) When $\alpha < -\frac{1}{2}$ we observe that Ψ_n is a function following the lower root $\psi_1(x)$ until a random point in $\left[\frac{1}{2} - s, \frac{1}{2} + s\right]$ at which a jump happens before following the upper root $\psi_3(x)$. This represents a discontinuity in the limit giving us a point of condensation. If $\alpha \leq -\frac{7}{8}$ then $s \geq \frac{1}{2}$ which means the location of the "jump" has full support on $(0, 1)$.

Figure 3.7 below shows two simulations which under the same initial conditions, namely $\alpha = -\frac{3}{4} \in (-\frac{7}{8}, -\frac{1}{2})$. These two simulations provide evidence of two different types of condensation.

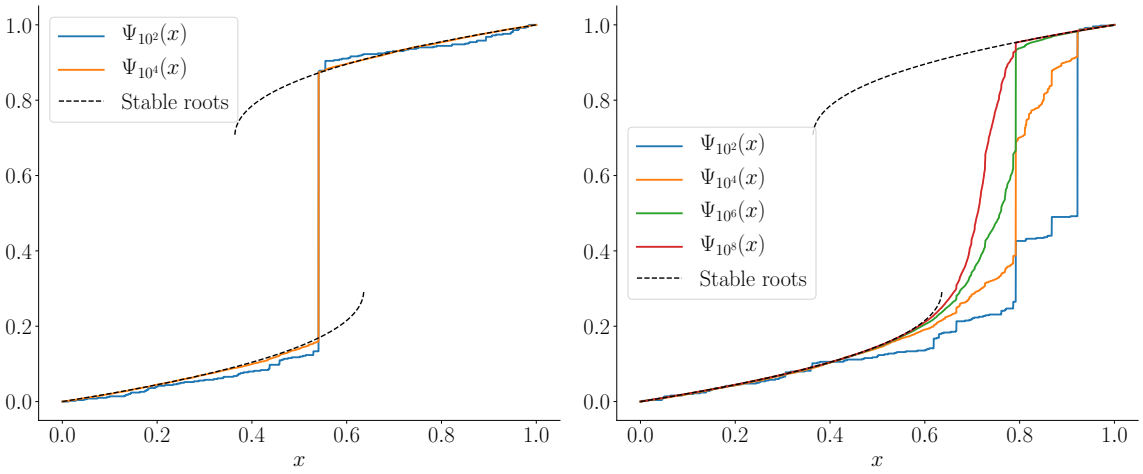

Fig. 3.7: Results from simulations for $\alpha = -\frac{3}{4}$. Diagrams here generated by simulations run by J.Haslegrave found in [HJY19].

Corollary 3.2.10 implies that if $\alpha \in (-\frac{7}{8}, -\frac{1}{2})$ then there is a positive probability that condensation could exist at a random location in the network and is caused by a persistent hub at a random location having full support on $(\frac{1}{2} - s, \frac{1}{2} + s)$. Evidence of this extensive condensation can be seen in Figure 3.7 (left). On the other hand, Lemma 3.2.4 tells us that there exists a non-zero probability of condensation

occurring at a touchpoint, though there is probability zero that a vertex joins the network (or is present from the start) which has location equal to this touchpoint. Therefore there is a positive probability condensation in the network is not down to a persistent hub. Evidence for this (slower convergence) can be seen in figure 3.7 (right) where new fitter vertices are joining the network with locations tending towards the upper touchpoint in this case at approximately $x \approx 0.62$. In the case wherer x is a touchpoint, there is a positive probability of a jump at the touch point. However there is probability zero of a vertex with this location. Therefore condensation cannot be down to a persistent hub.

By implementing conditions on $F_1(y; x, \alpha, e_{2,3})$ using x and α to control whether one or three roots exist, we solve

$$F_1(y; x, \alpha, e_{2,3}) = F_2(y, d; \alpha, e_{2,3}) = 0 \tag{3.12}$$

by assuming $F_1(y; x, \alpha, e_{2,3}) = 0$ has three real roots $\psi_1(x) \leq \psi_2(x) \leq \psi_3(x)$. We solve $F_2(\psi_i(x), d; \alpha, e_{2,3}) = 0$ for d to attain the solutions given by

$$\delta_j \in \left\{ 0, \frac{3}{4}(2\psi_i(x) - 1) \pm \frac{\sqrt{3}}{2}\sqrt{\psi_i(x) - \psi_i(x)^2 - \frac{7 - 8\alpha}{12}} \right\}.$$

We form solutions to equation (3.12) of the form $(\psi_i(x), \delta_j)$ where $i, j \in \{1, 2, 3\}$. By combining these components we form Figure 3.8. Figure 3.8 depicts the curve $F_1(y; x, \alpha, e_{2,3})$ in the domain $y \in [0, 1]$ at two different values of x producing touchpoints at $\psi_1(x)$ and $\psi_3(x)$. The upper solid curve is the higher limit of the region in which $\psi_2(x) = \psi_3(x)$, the lower solid curve is the lower value of x which produces $\psi_1(x) = \psi_2(x)$. In this same region we plotted $\lambda_1(y; \alpha, e_{2,3})$ (the parabola), $\lambda_2(y, \delta_2; \alpha, e_{2,3})$ and $\lambda_2(y, \delta_3; \alpha, e_{2,3})$ (dashed and dotted lines respectively). It is clear the two regions where the eigenvalues are both negative simultaneously overlap with where the roots of $F_1(y; x, \alpha, e_{k,r})$ would be as x increases from its lower limit to its upper limit.

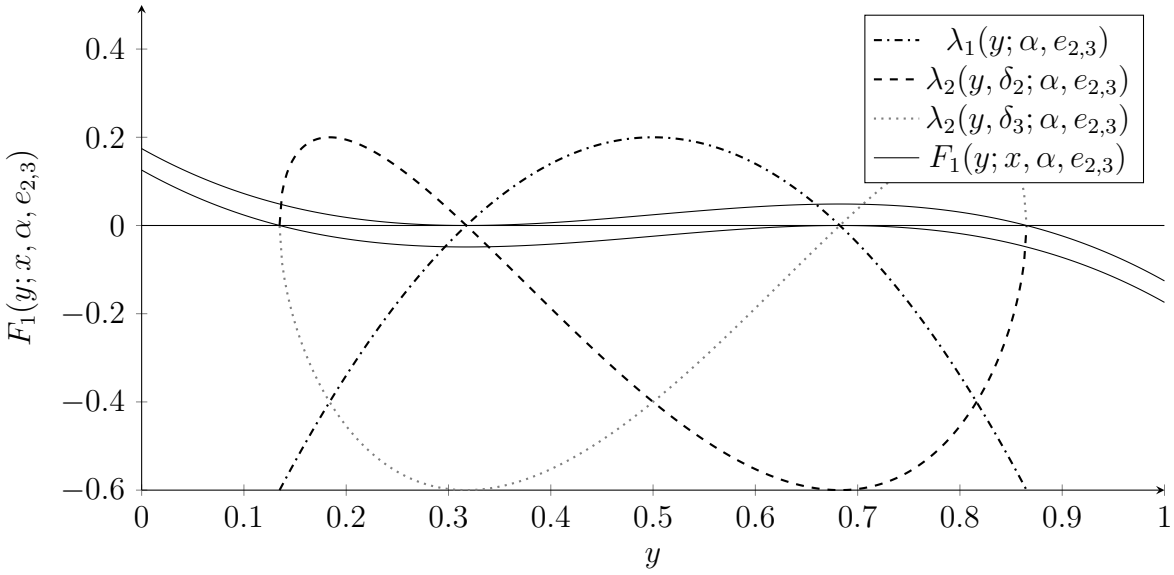

Fig. 3.8: Plot of eigenvalue domains evaluated at $\alpha = -\frac{7}{10}$.

From Theorem 3.2.11 we know that condensation can only occur at one location in the graphs and not in both regions where our eigenvalues are negative simultaneously.

Lemma 3.3.2. *Fix $x \in [0,1]$ and $\alpha < -\frac{1}{2}$ such that $\psi_1(x), \psi_2(x)$ and $\psi_3(x)$ are solutions to $F_1(y;x,\alpha,e_{2,3}) = 0$. There exists a positive probability of condensation occurring at only the stable point $(\psi_3(x), \delta_3) = (\psi_3(x), \psi_3(x) - \psi_1(x))$.*

Proof. As $\delta_j = \psi_i - \psi_j > 0$ we see from Lemma 3.2.9 that of the nine initial candidates for points of condensation only $(\psi_3(x), \psi_3(x) - \psi_2(x))$, $(\psi_3(x), \psi_3(x) - \psi_1(x))$ and $(\psi_2(x), \psi_2(x) - \psi_1(x))$ are viable. From Lemma 3.2.9 we see that $(\psi_i, \psi_i - \psi_j)$ is stable if $F_1'(\cdot) < 0$ for both y_i and y_j which is the gradient of $F_1(\cdot)$. Therefore the only viable candidate for condensation is $(\psi_3(x), \psi_3(x) - \psi_1(x))$ as Theorem 2.16 of [Pem07] states our process can only converge to a stable fixed point or touchpoint. Therefore our sequence of random variables must converge to $(\psi_3(x), \psi_3(x) - \psi_1(x))$ with positive probability. □

3.3.4 Second or sixth of seven

The final example we discuss utilizes the vector notation (Ξ) introduced in Section 3.1. In the middle of three and largest of r models we select the k^{th} from r for attachment. Theorem 3.2.11 proves there exists exactly one point of condensation in models of this type. The question we consider here is whether there can exist more than two stable roots for a given $x \in [0,1]$ or indeed two disjoint ranges in which there exist a point of condensation in each. This corresponds to multiple discontinuities in the limit of $\Psi_n(x)$ allowing for multiple points of condensation.

The vector notation indeed allows for multiple points of condensation to occur simultaneously in the network. In this context an example of when two points of condensation may be observed in the real world is that of a bipartisan election when two different candidates both attract an approximately constant proportion of the votes from different regions of the locations domain. Maybe if x represented the amount a candidate (vertex) cares for people who need governmental support. It is observable that a political party aligning itself with a caring ($x = 1$) or a lack of caring ($x = 0$) approach to supporting welfare programs can both attract votes (new edges) at a constant rate without dying out. A remark which we should make is that the vertices contained within the two condensates do not need to be growing at the same rate nor do they need to converge to the same limiting proportion. We consider a set of models asking questions relating to vertices of different types further in Chapter 6.

We chose the vector $\Xi = (0, \frac{1}{2}, 0, 0, 0, \frac{1}{2}, 0)$ as it is the simplest example we found which allows for two points of condensation. In short this states that from a sample of seven vertices, v_{n+1} forms an edge to the member of the sample with the second highest or second lowest locations each with probability $\frac{1}{2}$. We use this setting to construct an expression for $F_1(y; x, \alpha, \Xi)$ using Lemma 3.2.1 as

$$F_1(y; x, \alpha, \Xi) = \frac{1}{2}F_1(y; x, \alpha, e_{2,7}) + \frac{1}{2}F_1(y; x, \alpha, e_{6,7})$$

$$
\begin{aligned}
=&\frac{1}{2}\left(\sum_{i=2}^{7}\binom{7}{i}y^i\,(1-y)^{7-i}\right)+\frac{1}{2}\left(\sum_{i=6}^{7}\binom{7}{i}y^i\,(1-y)^{7-i}\right)\\
&-(2+\alpha)y+x(\alpha+1)\\
=&-6y^7+21y^6-42y^5+\frac{105}{2}y^4-35y^3+\frac{21}{2}y^2-(2+\alpha)y+x(\alpha+1)
\end{aligned}
$$

After plotting $F_1(y;x,\alpha,\Xi)$ in Figure 3.9 for four varying α values we see a similar behaviours as to Figure 3.4.

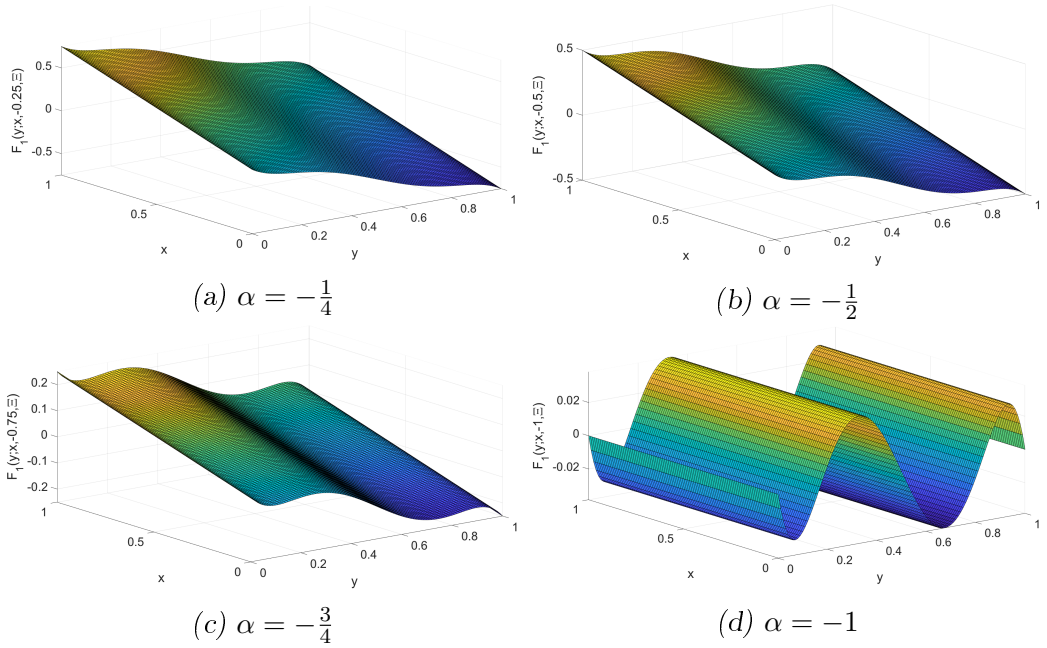

(a) $\alpha=-\frac{1}{4}$ (b) $\alpha=-\frac{1}{2}$

(c) $\alpha=-\frac{3}{4}$ (d) $\alpha=-1$

Fig. 3.9: The function $F_1(y;x,\alpha,\Xi)$ evaluated at four different values of α and x.

In the middle of three model discussed in section 3.3.3 we noticed that there were two phase transitions, one at $\alpha=-\frac{1}{2}$ and one at $\alpha=-\frac{7}{8}$. There exist phase transitions in this model too, however they are harder to calculate precisely due to the order seven polynomial. However, we show there exist four distinct phase transition points α_1, $\alpha_2\approx-0.876$, $\alpha_3\approx-0.931$ and $\alpha_4\approx-0.968$. The most important of these in our context is the phase transition between the condensation and non-condensation

phase α_1 given by

$$\alpha_1 = \inf\{\alpha : F_1'(y; x, \alpha, \Xi) \leq 0 \ \forall \ y \in (0,1)\} = \frac{35\sqrt{10} - 116}{9}.$$

If $\alpha \geq \alpha_1$, for any $x \in (0,1)$ there exists exactly one real solution to $F_1(\cdot)$ therefore no limit discontinuity. If $\alpha \in (\alpha_3, \alpha_1)$ there exist two separate ranges containing two stable roots and elsewhere only one. This implies there must be a jump from converging from $\psi_1(x)$ to $\psi_3(x)$ in the first range then from $\psi_3(x)$ to ψ_5 in the second range. When $\alpha < \alpha_3$ there can exist one or two points of condensation as there is a range with three stable roots. We know that the three roots $\psi_1(x), \psi_3(x)$ and $\psi_5(x)$ are stable in a given range. We use results found in Section 3.2 to show that a vertex with location in this range could attract condensation in three different ways, one with is a double jump which corresponds to the model only having condensation at one point. The phase transitions which occur at α_2 and α_4 are less important as they tell us where jumps can happen however not how many there are.

Lemma 3.3.3. *For a fixed location $x \in (0,1)$, as $n \to \infty$ the random variable $\Psi_n(x)$*

converges almost surely to a limit according to the following conditional equation:

$$\lim_{n\to\infty}\Psi_n(x)=\begin{cases}\psi(x), & \text{if } \alpha\geq\alpha_1,\ x\in[0,1],\\ \psi(x), & \text{if } \alpha\in(\alpha_2,\alpha_1),\ x\in\left[0,\frac{|F_1(\beta_2;x,\alpha,\Xi)|}{\alpha+1}\right),\\ \psi_1(x),\ \psi_3(x), & \text{if } \alpha\in(\alpha_2,\alpha_1),\ x\in\left[\frac{|F_1(\beta_2;x,\alpha,\Xi)|}{\alpha+1},\frac{|F_1(\beta_1;x,\alpha,\Xi)|}{\alpha+1}\right],\\ \psi(x), & \text{if } \alpha\in(\alpha_2,\alpha_1),\ x\in\left(\frac{|F_1(\beta_1;x,\alpha,\Xi)|}{\alpha+1},\frac{|F_1(1-\beta_1;x,\alpha,\Xi)|}{\alpha+1}\right),\\ \psi_1(x),\ \psi_3(x), & \text{if } \alpha\in(\alpha_2,\alpha_1),\ x\in\left[\frac{|F_1(1-\beta_1;x,\alpha,\Xi)|}{\alpha+1},\frac{|F_1(1-\beta_2;x,\alpha,\Xi)|}{\alpha+1}\right],\\ \psi(x), & \text{if } \alpha\in(\alpha_2,\alpha_1),\ x\in\left(\frac{|F_1(1-\beta_2;x,\alpha,\Xi)|}{\alpha+1},1\right],\\ \psi(x), & \text{if } \alpha\in[\alpha_3,\alpha_2),\ x\in\left(\frac{|F_1(\beta_1;x,\alpha,\Xi)|}{\alpha+1},\frac{|F_1(1-\beta_1;x,\alpha,\Xi)|}{\alpha+1}\right),\\ \psi_1(x),\ \psi_3(x), & \text{if } \alpha\in[\alpha_3,\alpha_2),\ x\notin\left(\frac{|F_1(\beta_1;x,\alpha,\Xi)|}{\alpha+1},\frac{|F_1(1-\beta_1;x,\alpha,\Xi)|}{\alpha+1}\right),\\ \psi_1(x),\ \psi_3(x),\ \psi_5(x), & \text{if } \alpha\in[\alpha_4,\alpha_3),\ x\in\left[\frac{|F_1(1-\beta_1;x,\alpha,\Xi)|}{\alpha+1},\frac{|F_1(\beta_1;x,\alpha,\Xi)|}{\alpha+1}\right],\\ \psi_1(x),\ \psi_3(x), & \text{if } \alpha\in[\alpha_4,\alpha_3),\ x\notin\left[\frac{|F_1(1-\beta_1;x,\alpha,\Xi)|}{\alpha+1},\frac{|F_1(\beta_1;x,\alpha,\Xi)|}{\alpha+1}\right],\\ \psi_1(x),\ \psi_3(x),\ \psi_5(x), & \text{if } \alpha\leq\alpha_4,\ x\in[0,1].\end{cases}$$

The function $F_1(y;x,\alpha,\Xi)$ *has at most four turning points denoted by* $(\beta_1,F_1(\beta_1;x,\alpha,\Xi))$, $(\beta_2,F_1(\beta_2;x,\alpha,\Xi))$, $(1-\beta_2,F_1(1-\beta_2;x,\alpha,\Xi))$ *and* $(1-\beta_1,F_1(1-\beta_1;x,\alpha,\Xi))$ *that satisfy* $\beta_1\leq\beta_2\leq1-\beta_2\leq1-\beta_1$, $F_1(\beta_1;x,\alpha,\Xi)\leq F_1(\beta_2;x,\alpha,\Xi)$ *and* $F_1(1-\beta_2;x,\alpha,\Xi)\leq F_1(1-\beta_1;x,\alpha,\Xi)$.

Plots of each of the four transition points can be seen in Figure 3.13 evaluated at (from bottom to top) $x=0$, $\frac{1}{2}$ and 1 respectively.

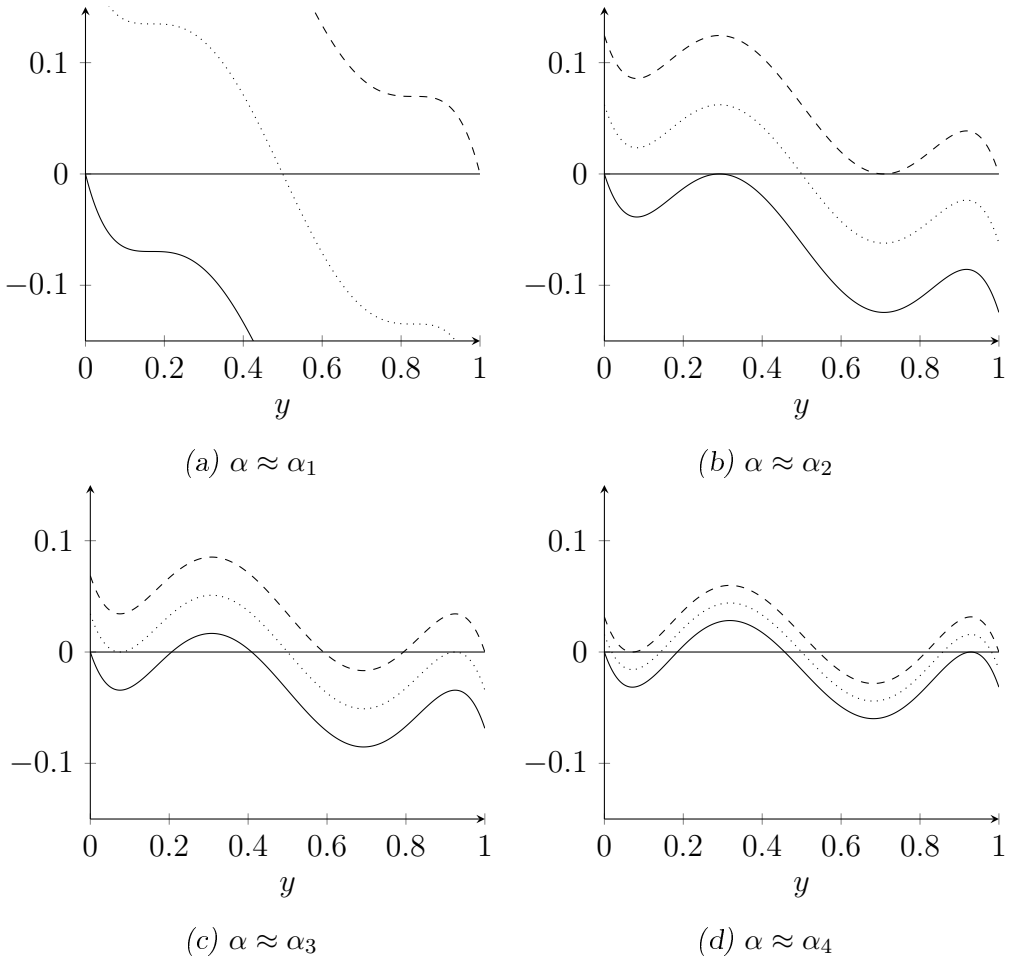

(a) $\alpha \approx \alpha_1$ (b) $\alpha \approx \alpha_2$

(c) $\alpha \approx \alpha_3$ (d) $\alpha \approx \alpha_4$

Fig. 3.10: $F_1(y; x, \alpha, \Xi)$ evaluated at values of α representing the phase transitions which appear for this choice of Ξ for $x \in \left\{0, \frac{1}{2}, 1\right\}$.

We examine further a particular value $\alpha = -0.85 \in (\alpha_2, \alpha_1)$ which produces a curve which lies between Figure 3.10a and Figure 3.10b. A plot of root frequency diagram of the curve in Figure 3.11. It is visible that x's interval is partitioned into five sections, three where there is exactly one real root and two where there exists three. The five partitions $[0, \beta_2]$, $[\beta_2, \beta_1]$, $[\beta_1, 1-\beta_1]$, $[1-\beta_1, 1-\beta_2]$ and $[1-\beta_2, 1]$. In this case $\beta_2 \approx 0.05$ and $\beta_1 \approx 0.275$.

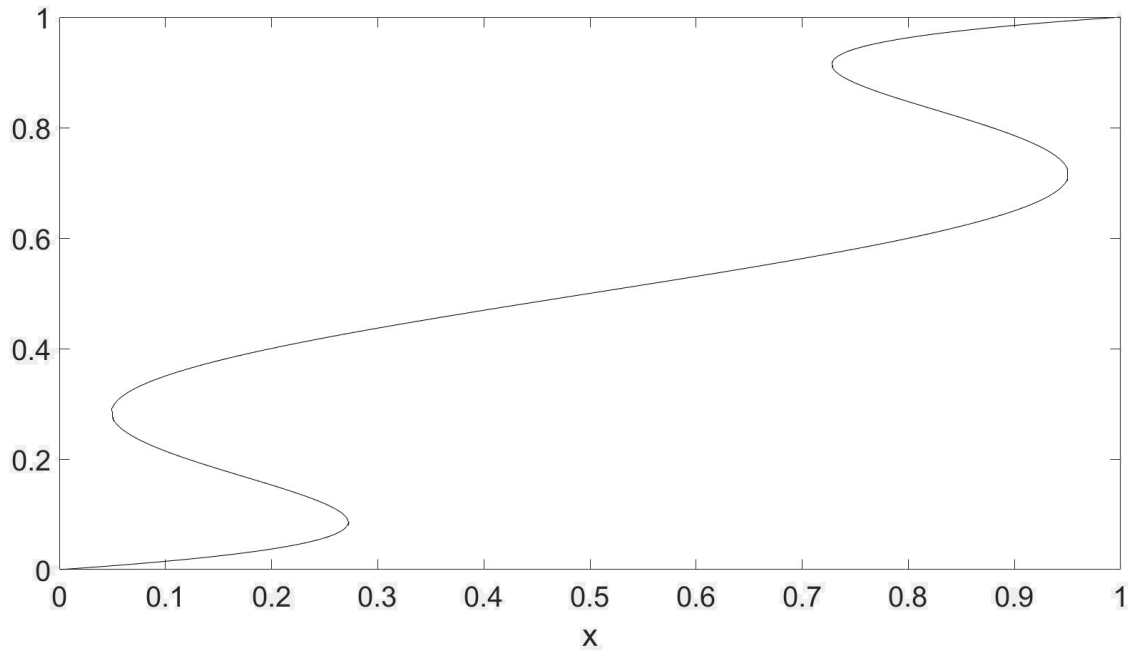

Fig. 3.11: Frequency of roots for values of $\alpha = -\frac{85}{100}$.

Figure 3.11 show that for $\alpha = -0.85$ that there almost surely exists two points of condensation. However Corollary 3.2.10 implies that this could be down to two separate persistent hubs forming in both feasible regions $[\beta_2, \beta_1]$ and $[1-\beta_1, 1-\beta_2]$, or by new fitter vertices joining the graph. Evidence of the former can be found below in Figure 3.12 (left) and the latter in Figure 3.12 (right) via simulations. We consider another particular value $\alpha = -0.95$ which lies between a different pair of phase transitions, (α_4, α_3). This value of α defines a curve between Figure 3.10c and Figure 3.10d.

In Figure 3.13 we run a similar simulation to that above based on $\alpha = -0.95$. It is shown that there exists a minimum of two stable roots for any $x \in (0, 1)$ therefore condensation can occur at any location in the graph.

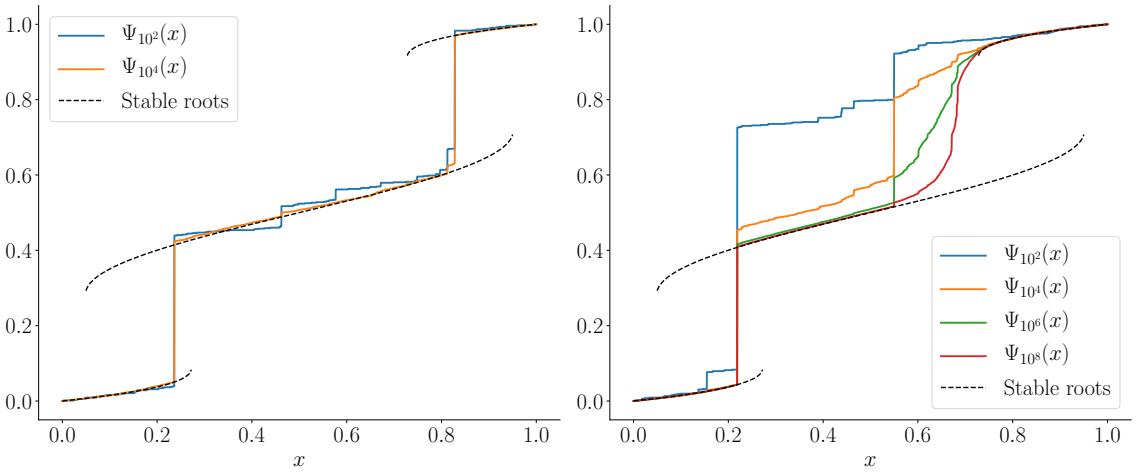

Fig. 3.12: The roots of $F_1(y; x, \alpha, \Xi)$ for $\alpha = -\frac{85}{100}$.

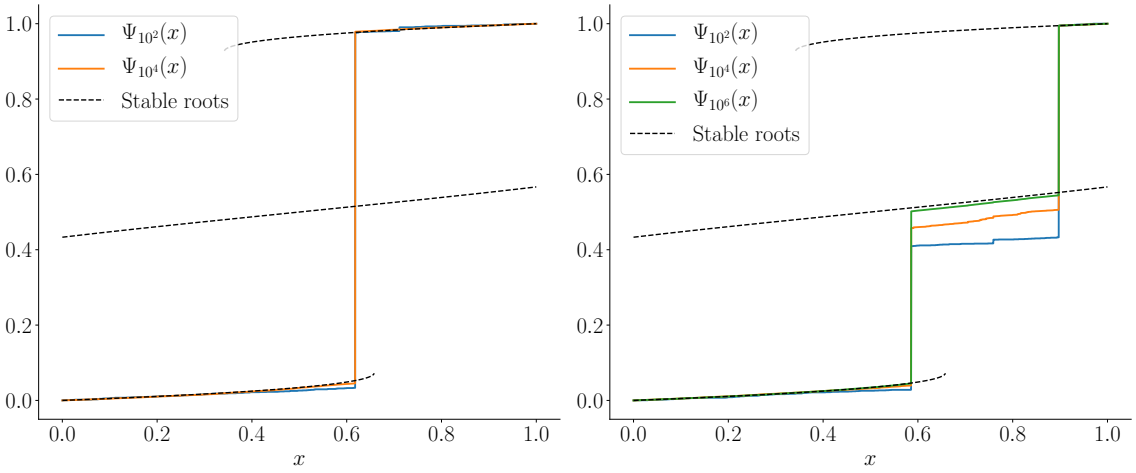

Fig. 3.13: Results from simulations for $\alpha = -\frac{95}{100}$. Diagrams here generated by simulations run by J.Haslegrave found in [HJY19].

4. LOCATION BASED CHOICE MODEL: DEGREE DISTRIBUTION

A common question asked as part of the study of growing networks is how the degree sequence behaves as the number of vertices grows. Chapter 3 focused on necessary conditions we must implement on the location based choice model to allow for condensation to occur in a network. This chapter focuses on the degree distribution of a specific subset of models discussed in Chapter 3.

This chapters' content is orientated around finding a power law degree distribution which models the middle of r set of location based choice models, specifically when r is odd. Section 4.1 sets out relevant definitions followed by key results. Section 4.2 discusses the middle of three model $\Xi = (0, 1, 0)$ from Section 3.3.3. Notation for this chapter remains consistent with that of Chapter 3.

This work was built upon in collaboration with Arne Grauer and Lukas Lüchtrath from the University of Köln resulting in [GLY20].

4.1 Results

Again we fix a parameter $r \in \mathbb{N}$ such that $r \geq 3$, imposing a further condition that r is odd. This condition on r is to ensure a definitive middle value of the $\mathbb{R}^r$ vector; more specifically this allows for the case where $\Xi = (0, \ldots, 0, 1, 0, \ldots, 0)$ such that the 1 is in the centre position.

Definition 4.1.1. *We define $P^{(n)}_{x_1,x_2}(k)$ as the proportion of vertices in G_n which have degree at most k and locations in the interval $[x_1, x_2] \subset [0, 1]$.*

Definition 4.1.2. *We define $\tau_{G_n}^{(k)}$ as the subset of vertices in G_n which have degree k and location in the interval $[x_1, x_2]$.*

Lemma 4.1.3. *The proportion of vertices in G_{n+1} with degree at most k with locations in the interval $[x_1, x_2]$ satisfies*

$$\frac{F_L}{n+n_0+1} \leq \mathbb{E}\left(P_{x_1,x_2}^{(n+1)}(k)\middle|\mathcal{F}_n\right) - P_{x_1,x_2}^{(n)}(k) \leq \frac{F_U}{n+n_0+1}. \tag{4.1}$$

Here $\mathcal{F}_n = \sigma(G_i, x_j; i, j \leq n)$ is the filtration generated by the sequence of graphs and

$$\begin{aligned} F_L =& - f_U(\Psi_n(x_1), \Psi_n(x_2)) \left(P_{x_1,x_2}^{(n)}(k) - P_{x_1,x_2}^{(n)}(k-1)\right) \frac{k+\alpha}{2+\alpha} - P_{x_1,x_2}^{(n)}(k) + (x_2 - x_1), \\ F_U =& - f_L(\Psi_n(x_1), \Psi_n(x_2)) \left(P_{x_1,x_2}^{(n)}(k) - P_{x_1,x_2}^{(n)}(k-1)\right) \frac{k+\alpha}{2+\alpha} - P_{x_1,x_2}^{(n)}(k) + (x_2 - x_1). \end{aligned}$$

Here the functions $f_U(y_1, y_2)$ and $f_L(y_1, y_2)$ are defined as

$$f_U(y_1, y_2) = \left(\sum_{j=0}^{\frac{r-1}{2}} \sum_{i=\frac{r+1}{2}}^{r} \binom{r}{i}\binom{i}{j} y_1^j \left(y_2 - y_1\right)^{i-j-1} \left(1 - y_2\right)^{r-i}\right)$$

and

$$f_L(y_1, y_2) = \frac{r+1}{2}\binom{r}{\frac{r+1}{2}} y_1^{\frac{r-1}{2}} \left(1 - y_2\right)^{\frac{r-1}{2}}.$$

Proof. We begin by finding the expected increase in the number of vertices with degree at most k and location inside the interval $[x_1, x_2]$ at the point in which v_{n+1} joins the graph with location x_{n+1}. This is expressed by

$$\begin{aligned} \mathbb{E}\left((n+n_0+1)P_{x_1,x_2}^{(n+1)}(k)\middle|\mathcal{F}_n\right) =& (n+n_0)P_{x_1,x_2}^{(n)}(k) - \mathbb{P}\left(v_{n+1} \sim \tau_{G_n}^{(k)}\right) \\ &+ \mathbb{P}(x_{n+1} \in [x_1, x_2]). \end{aligned} \tag{4.2}$$

The first term here counts the number of vertices in G_n with degree at most k which have locations in the interval $[x_1, x_2]$. The final term is the probability the location of the new vertex v_{n+1} is in the same interval. Given vertex locations are i.i.d.

uniform this is written as $\mathbb{P}(x_1 \leq x_{n+1} \leq x_2) = x_2 - x_1$. The second term here is the probability our new vertex forms an edge to a vertex in G_n with degree k in location $[x_1, x_2]$. The probability of this event is

$$\mathbb{P}\left(v_{n+1} \sim \tau_{G_n}^{(k)}\right) \leq \frac{(k+\alpha)(n+n_0)}{(2+\alpha)(n+n_0)-2}\left(P_{x_1,x_2}^{(n)}(k) - P_{x_1,x_2}^{(n)}(k-1)\right) f_U(\Psi_n(x_1), \Psi_n(x_2)).$$

and

$$\mathbb{P}\left(v_{n+1} \sim \tau_{G_n}^{(k)}\right) \geq \frac{(k+\alpha)(n+n_0)}{(2+\alpha)(n+n_0)-2}\left(P_{x_1,x_2}^{(n)}(k) - P_{x_1,x_2}^{(n)}(k-1)\right) f_L(\Psi_n(x_1), \Psi_n(x_2)).$$

The first term here describes the probability a degree k vertex is selected from G_n by v_{n+1} as a candidate for attachment; the second term describes the number of degree k vertices in G_n with locations in the interval $[x_1, x_2]$; the final term expresses the probability the vertex selected from G_n for attachment has location which lies in the interval $[x_1, x_2]$ given that one exists in our sample. We are able to reformulate equation (4.2) giving the expected number of vertices with degree at most k in G_{n+1} with locations in $[x_1, x_2]$ as

$$\begin{aligned}\mathbb{E}\left((n+n_0+1)P_{x_1,x_2}^{(n+1)}(k)\middle|\mathcal{F}_n\right) =& \frac{f(\Psi_n(x_1), \Psi_n(x_2))\left(P_{x_1,x_2}^{(n)}(k) - P_{x_1,x_2}^{(n)}(k-1)\right)(k+\alpha)}{(2+\alpha)-\frac{2}{n+n_0}} \\ &+ (n+n_0)P_{x_1,x_2}^{(n)}(k) + (x_2 - x_1).\end{aligned} \tag{4.3}$$

Here $f(\Psi_n(x_1), \Psi_n(x_1))$ is bounded by $f_U(\cdot)$ and $f_L(\cdot)$ which we define as the probability of attaching to the correct vertex with respect to our model given a member of the r selected vertices has location in $[x_1, x_2]$. Given the number of vertices n in G_n is increasing we have that

$$\lim_{n\to\infty} \frac{2}{n+n_0} \to 0,$$

therefore for $n \gg 0$ equation (4.3) is bounded above by

$$\begin{aligned}\mathbb{E}\left((n+n_0+1)P^{(n+1)}_{x_1,x_2}(k)\middle|\mathcal{F}_n\right) \leq & f_L(\Psi_n(x_1),\Psi_n(x_2))\left(P^{(n)}_{x_1,x_2}(k)-P^{(n)}_{x_1,x_2}(k-1)\right)\frac{k+\alpha}{2+\alpha} \\ & + (n+n_0)P^{(n)}_{x_1,x_2}(k)+(x_2-x_1).\end{aligned}$$

and below by

$$\begin{aligned}\mathbb{E}\left((n+n_0+1)P^{(n+1)}_{x_1,x_2}(k)\middle|\mathcal{F}_n\right) \geq & f_L(\Psi_n(x_1),\Psi_n(x_2))\left(P^{(n)}_{x_1,x_2}(k)-P^{(n)}_{x_1,x_2}(k-1)\right)\frac{k+\alpha}{2+\alpha} \\ & + (n+n_0)P^{(n)}_{x_1,x_2}(k)+(x_2-x_1).\end{aligned}$$

The lower bound f_L is fairly trivial to calculate as

$$\begin{aligned}(y_2-y_1)f_L(y_1,y_2) &= \frac{r+1}{2}\binom{r}{\frac{r+1}{2}}y_1^{s-1}(y_2-y_1)\left(1-y_2\right)^{r-s}, \\ f_L(y_1,y_2) &= \frac{r+1}{2}\binom{r}{\frac{r+1}{2}}y_1^{\frac{r-1}{2}}\left(1-y_2\right)^{\frac{r-1}{2}}.\end{aligned}$$

The upper bound f_U is calculated in the same way by conditioning on the event a vertex is selected with location in $[x_1,x_2]$,

$$\begin{aligned}(y_2-y_1)f_U(y_1,y_2) &= \sum_{j=0}^{\frac{r-1}{2}}\sum_{i=\frac{r+1}{2}}^{r}\binom{r}{i}\binom{i}{j}y_1^j\left(y_2-y_1\right)^{i-j}\left(1-y_2\right)^{r-i}, \\ f_U(y_1,y_2) &= \sum_{j=0}^{\frac{r-1}{2}}\sum_{i=\frac{r+1}{2}}^{r}\binom{r}{i}\binom{i}{j}y_1^j\left(y_2-y_1\right)^{i-j-1}\left(1-y_2\right)^{r-i}.\end{aligned}$$

Here $y_1,y_2\in[0,1]$ and $y_2\geq y_1$. By rearranging equation (4.3) we substitute in our upper and lower bounds to attain the desired result. □

Definition 4.1.4. *We define the noise introduced in Lemma 4.1.3 as*

$$\xi_{n+1}=\gamma_{n+1}^{-1}\left(P^{(n+1)}_{x_1,x_2}(k)-\mathbb{E}\left(P^{(n+1)}_{x_1,x_2}(k)\middle|\mathcal{F}_n\right)\right),$$

where $\xi_{n+1} \in \{\xi^L_{n+1}, \xi^U_{n+1}\}$. It is clear to see that $\mathbb{E}\left(\xi^U_{n+1}|\mathcal{F}_n\right) = \mathbb{E}\left(\xi^L_{n+1}|\mathcal{F}_n\right) = 0$.

Theorem 4.1.5. *For a fixed $\alpha \in (-1, \infty)$ and sufficiently large k we have that the proportion of vertices with degree less than or equal to k in the region $[x_1, x_2]$ denoted by $P^{(n)}_{x_1,x_2}(k)$ satisfies both*

$$\liminf_{n\to\infty} P^{(n)}_{x_1,x_2}(k) \gtrsim (x_2 - x_1)\left(1 - \delta_U(f_U(\Psi_n(x_1), \Psi_n(x_2)))(\alpha + 1 + k)^{-\frac{2+\alpha}{f_U(\Psi_n(x_1),\Psi_n(x_2))}}\right)$$

and

$$\limsup_{n\to\infty} P^{(n)}_{x_1,x_2}(k) \lesssim (x_2 - x_1)\left(1 - \delta_L(f_L(\Psi_n(x_1), \Psi_n(x_2)))(\alpha + 1 + k)^{-\frac{2+\alpha}{f_L(\Psi_n(x_1),\Psi_n(x_2))}}\right)$$

where

$$\delta_L(f_L(y_1, y_2)) = \frac{\Gamma\left(\alpha + 1 + \frac{2+\alpha}{f_L(y_1,y_2)}\right)}{\Gamma(\alpha + 1)} \text{ and } \delta_U(f_U(y_1, y_2)) = \frac{\Gamma\left(\alpha + 1 + \frac{2+\alpha}{f_U(y_1,y_2)}\right)}{\Gamma(\alpha + 1)}$$

such that

$$\liminf_{n\to\infty} P^{(n)}_{x_1,x_2}(k) \leq \lim_{n\to\infty} P^{(n)}_{x_1,x_2}(k) \leq \limsup_{n\to\infty} P^{(n)}_{x_1,x_2}(k).$$

Proof. We start by solving both $0 = F_L$ and $0 = F_U$

$$\begin{aligned}
0 &= (x_2 - x_1) - P^{(n)}_{x_1,x_2}(k) - f_L(y_1, y_2)\left(P^{(n)}_{x_1,x_2}(k) - P^{(n)}_{x_1,x_2}(k-1)\right)\frac{(k+\alpha)}{(2+\alpha)},\\
0 &= (x_2 - x_1) - P^{(n)}_{x_1,x_2}(k) - f_U(y_1, y_2)\left(P^{(n)}_{x_1,x_2}(k) - P^{(n)}_{x_1,x_2}(k-1)\right)\frac{(k+\alpha)}{(2+\alpha)}.
\end{aligned}$$

Due to the similarity of these equations we need only solve

$$0 = (x_2 - x_1) - P^{(n)}_{x_1,x_2}(k) - f(y_1, y_2)\left(P^{(n)}_{x_1,x_2}(k) - P^{(n)}_{x_1,x_2}(k-1)\right)\frac{(k+\alpha)}{(2+\alpha)}. \tag{4.4}$$

We rearrange equation (4.4) to make $P^{(n)}_{x_1,x_2}(k)$ the subject:

$$\begin{aligned}
P^{(n)}_{x_1,x_2}(k) &= \frac{x_2 - x_1 + \frac{(k+\alpha)f(y_1,y_2)}{2+\alpha} P^{(n)}_{x_1,x_2}(k-1)}{1 + \frac{(k+\alpha)f(y_1,y_2)}{2+\alpha}} \\
&= \frac{(2+\alpha)(x_2 - x_1)}{2 + \alpha + (k+\alpha)f(y_1,y_2)} + \frac{1}{1 + \frac{2+\alpha}{(k+\alpha)f(y_1,y_2)}} P^{(n)}_{x_1,x_2}(k-1) \\
&= \beta_k + \gamma_k P^{(n)}_{x_1,x_2}(k-1)
\end{aligned}$$

By using a recursive method and observing the termination criteria $P^{(n)}_{x_1,x_2}(0) = 0$ deduced because G_n is connected we have

$$\begin{aligned}
P^{(n)}_{x_1,x_2}(k) =& \beta_k + \sum_{j=1}^{k-1} \left(\beta_j \prod_{i=j+1}^{k} \gamma_i \right) \\
=& \beta_k + \sum_{j=1}^{k-1} \beta_j \left(\frac{\Gamma(\alpha+k+1)\Gamma\left(\alpha+j+1+\frac{2+\alpha}{f(y_1,y_2)}\right)}{\Gamma(\alpha+j+1)\Gamma\left(\alpha+k+1+\frac{2+\alpha}{f(y_1,y_2)}\right)} \right) \\
=& \beta_k + \left(\frac{\Gamma\left(\alpha+1+k+\frac{2+\alpha}{f(y_1,y_2)}\right)(\alpha+k)}{\Gamma(\alpha+1+k)\left(a+k+\frac{2+\alpha}{f(y_1,y_2)}\right)} - \frac{\Gamma\left(\alpha+2+\frac{2+\alpha}{f(y_1,y_2)}\right)(\alpha+1)}{\Gamma(\alpha+2)\left(a+1+\frac{2+\alpha}{f(y_1,y_2)}\right)} \right) \\
& \times \frac{(x_2-x_1)\,\Gamma(\alpha+1+k)}{\Gamma\left(\alpha+1+k+\frac{2+\alpha}{f(y_1,y_2)}\right)} \\
=& \beta_k - \frac{(x_2-x_1)\,\Gamma(\alpha+1+k)\Gamma\left(\alpha+1+\frac{2+\alpha}{f(y_1,y_2)}\right)}{\Gamma(\alpha+1)\Gamma\left(\alpha+1+k+\frac{2+\alpha}{f(y_1,y_2)}\right)} + \frac{(x_2-x_1)\,(\alpha+k)}{\left(\alpha+k+\frac{2+\alpha}{f(y_1,y_2)}\right)} \\
=& (x_2-x_1)\left(1 - \frac{\Gamma\left(\alpha+1+\frac{2+\alpha}{f(y_1,y_2)}\right)\Gamma(\alpha+1+k)}{\Gamma\left(\alpha+1+k+\frac{2+\alpha}{f(y_1,y_2)}\right)\Gamma(\alpha+1)} \right) \\
=& (x_2-x_1)\left(1 - \delta(f(y_1,y_2)) \frac{\Gamma(\alpha+1+k)}{\Gamma\left(\alpha+1+k+\frac{2+\alpha}{f(y_1,y_2)}\right)} \right).
\end{aligned}$$

such that

$$\delta(f(y_1, y_2)) = \frac{\Gamma\left(\alpha + 1 + \frac{2+\alpha}{f(y_1,y_2)}\right)}{\Gamma(\alpha+1)}.$$

By using an approximation associated to the division of two gamma functions

$$\frac{\Gamma(\alpha+1+k)}{\Gamma(\alpha+1+k+\frac{2+\alpha}{f(y_1,y_2)})} \sim (\alpha+1+k)^{-\frac{2+\alpha}{f(y_1,y_2)}},$$

as $k \to \infty$ the proportion $P^{(n)}_{k,x_1,x_2}$ follows

$$\liminf_{n\to\infty} P^{(n)}_{k,x_1,x_2} \lesssim (x_2 - x_1)\left(1 - \delta(f_L(\Psi_n(x_1), \Psi_n(x_2)))(\alpha+1+k)^{-\frac{2+\alpha}{f_L(\Psi_n(x_1),\Psi_n(x_2))}}\right)$$

and

$$\limsup_{n\to\infty} P^{(n)}_{k,x_1,x_2} \gtrsim (x_2 - x_1)\left(1 - \delta(f_U(\Psi_n(x_1), \Psi_n(x_2)))(\alpha+1+k)^{-\frac{2+\alpha}{f_U(\Psi_n(x_1),\Psi_n(x_2))}}\right).$$

□

The degree distribution of our network should take into account all of the vertices in the network, not just those with locations in a particular region. We currently have a description of the degree distribution in the range $[x_1, x_2]$ and not $[0, 1]$.

Theorem 4.1.6. *For*

$$P_k = \lim_{x_1,x_2\to x} \lim_{n\to\infty} \frac{P^{(n)}_{x_1,x_2}(k)}{x_2 - x_1}$$

then as $k \to \infty$

$$P_k \sim 1 - \delta(f(\Psi(x)))(\alpha+1+k)^{-\frac{2+\alpha}{f(\Psi(x))}},$$

here we use $f(\Psi(x))$ *in replace of* $f(\Psi(x), \Psi(x))$.

Proof. As the number of vertices $n \to \infty$ the random variable $\Psi_n(x)$ tends to the limit $\Psi(x)$. As the interval $[x_1, x_2]$ narrows to a point x such that $x_1 \le x \le x_2$ the

upper and lower limits on the probability converge to

$$\lim_{\substack{x_1\to x\\ x_2\to x}} f_L(\Psi_n(x_1),\Psi_n(x_2)) = \frac{r+1}{2}\binom{r}{\frac{r+1}{2}}\Psi_n(x_1)^{\frac{r-1}{2}}\left(1-\Psi_n(x_2)\right)^{\frac{r-1}{2}},$$
$$\lim_{\substack{x_1\to x\\ x_2\to x}} f_U(\Psi_n(x_1),\Psi_n(x_2)) = \frac{r+1}{2}\binom{r}{\frac{r+1}{2}}\Psi_n(x_1)^{\frac{r-1}{2}}\left(1-\Psi_n(x_2)\right)^{\frac{r-1}{2}}.$$

We denote this limit as

$$f(\Psi(x)) = \frac{r!}{\left(\frac{r-1}{2}\right)!\left(\frac{r-1}{2}\right)!}\Psi(x)^{\frac{r-1}{2}}\left(1-\Psi(x)\right)^{\frac{r-1}{2}}.$$

In conjunction with Theorem 4.1.5 we see the upper and lower bound on $f(\Psi_n(x_1),\Psi_n(x_2))$ converge to the same limit given by $f(\Psi_n(x))$. This means

$$\limsup_{n\to\infty} P^{(n)}_{k,x_1,x_2} - \liminf_{n\to\infty} P^{(n)}_{k,x_1,x_2} \to 0$$

thus the proportion of vertices with degree at most k in the interval $[x_1,x_2]$, P_k follows

$$P_k \le \max_{x_1,x_2}\limsup_{n\to\infty}\left((x_2-x_1)\left(1-\delta(f(\Psi(x)))(\alpha+1+k)^{-\frac{2+\alpha}{f(\Psi(x))}}\right)\right).$$

and

$$P_k \ge \min_{x_1,x_2}\liminf_{n\to\infty}\left((x_2-x_1)\left(1-\delta(f(\Psi(x)))(\alpha+1+k)^{-\frac{2+\alpha}{f(\Psi(x))}}\right)\right).$$

Therefore the functions $F_L(\cdot)$ and $F_U(\cdot)$ given in Lemma 4.1 converge sandwiching our stochastic approximation equation. By dividing by the length of the interval in question, x_2-x_1, we deduce a statement for the whole range our location values can take as

$$P_k \to \left(1-\delta(f(\Psi(x)))(\alpha+1+k)^{-\frac{2+\alpha}{f(\Psi(x))}}\right). \tag{4.5}$$

for $k\to\infty$. □

Theorem 4.1.7. *For a vertex $v_i \in V(G_n)$ selected uniformly at random with location*

in $[x_1, x_2]$*, the asymptotic degree distribution follows*

$$\lim_{x_1,x_2\to x}\lim_{n\to\infty}\mathbb{P}(\deg(v_i)\geq k|x_i\in[x_1,x_2])\to\frac{\Gamma\left(\alpha+1+\frac{2+\alpha}{f(\Psi(x))}\right)}{\Gamma(\alpha+1)}(\alpha+k)^{-\frac{2+\alpha}{f(\Psi(x))}},$$

where x_i *is the location of vertex* v_i*.*

Proof. The proof of this is a consequence of substituting (4.5) into $\mathbb{P}(\deg(V_i)\geq k) = 1-P_{k-1}$. □

We examine the behaviour of the degree distribution as α approaches the phase transition regarding condensation. Theorem 2.6 in [HJY19] states that in the case where the new vertex selects r vertices for attachment forming an edge between the new vertex and the member of the selection with the s^{th} highest location with probability 1 the phase transition α_c occurs at

$$\alpha_c = s\binom{r}{s}\left(\frac{s-1}{r-s}\right)^{s-1}\left(\frac{r-s}{r-1}\right)^{r-1}-2. \tag{4.6}$$

Precisely, condensation occurs in the model almost surely if $\alpha<\alpha_c$ and almost surely does not occur if $\alpha\geq\alpha_c$.

By applying equation (4.6) to the middle of r model we found this critical phase transition regarding condensation occurs at

$$\alpha_c = \frac{r!2^{1-r}}{\left(\frac{r-1}{2}\right)!\left(\frac{r-1}{2}\right)!}-2.$$

Given that $f(y)$ is maximized at $y=\frac{1}{2}$ found by using

$$\frac{df}{dy} = \binom{r-1}{2}y^{\frac{r-3}{2}}(1-y)^{\frac{r-3}{2}}(1-2y)=0$$

we have that $\mathbb{P}(\deg(v_i)\geq k)$ has the heaviest tail at $y=\frac{1}{2}$. This is seen below in Figure 4.1.

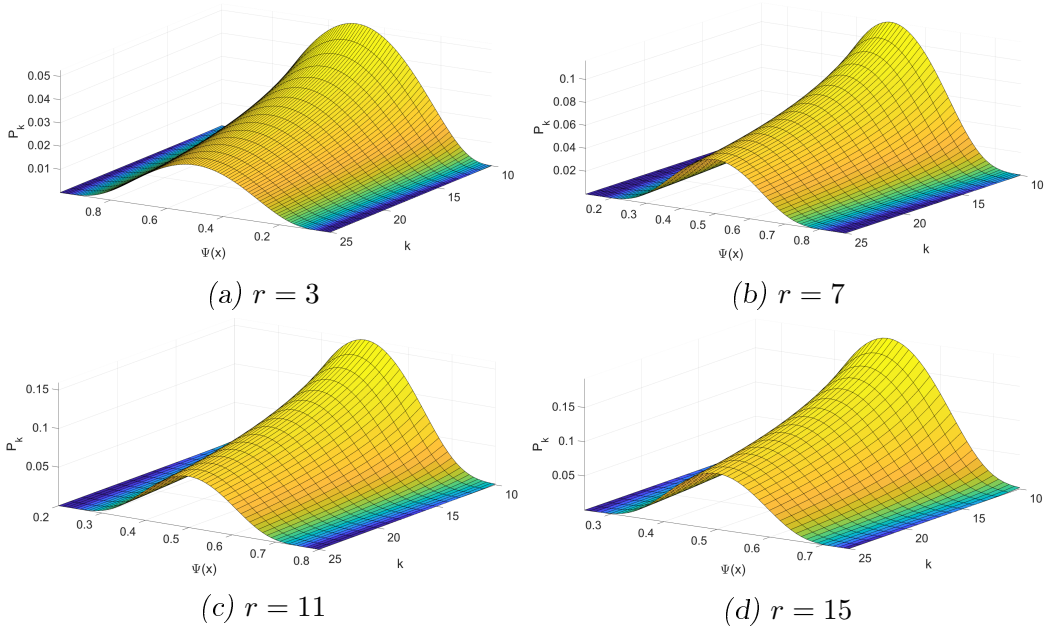

(a) $r = 3$ (b) $r = 7$

(c) $r = 11$ (d) $r = 15$

Fig. 4.1: Our degree distribution for $r \in \{3, 7, 11, 15\}$ and $K = \{10, 11, \ldots, 25\}$.

This makes sense, in middle of r model as new vertices favour those in G_n with locations closer to the centre of the range. We show that that at this point $f\left(\frac{1}{2}\right) = 2 + \alpha$ leads to the power law distribution associated to the point where the tail is heaviest is described by

$$\mathbb{P}(\deg(V_i) \geq k) = \frac{\frac{r!2^{1-r}}{\left(\frac{r-1}{2}\right)!\left(\frac{r-1}{2}\right)!} - 1}{k - 2 + \frac{r!2^{1-r}}{\left(\frac{r-1}{2}\right)!\left(\frac{r-1}{2}\right)!}} = 1 - \frac{k-1}{k - 2 + \frac{r!2^{1-r}}{\left(\frac{r-1}{2}\right)!\left(\frac{r-1}{2}\right)!}}.$$

4.2 Comparison to Barabási-Albert

Theorem 4.1.7 is evident when considering Barabási-Albert preferential attachment [BA99]. It is well known that the degree distribution of [BA99] follows

$$\mathbb{P}_{BA}(\deg(V_i) = k) = \frac{2m(m+1)}{k(k+1)(k+2)}. \tag{4.7}$$

Shown using (4.7), when $m = 1$ the degree distribution of the Barabási-Albert model follows

$$\mathbb{P}_{BA}(\deg(V_i) \geq k) = 1 - \sum_{n=1}^{k-1} \frac{4}{n(n+1)(n+2)} = 1 - 4\left(\frac{k(k+1)-2}{4k(k+1)}\right). \tag{4.8}$$

As $k \to \infty$ equation (4.8) converges to

$$\lim_{k\to\infty} 1 - 4\left(\frac{k(k+1)-2}{4k(k+1)}\right) = 2k^{-2}.$$

We consider how our model detailed in Section 3.1 relates to the Barabási-Albert model; we set $r = 1$ and the biasing coefficient $\alpha = 0$. To include the lack of vertex location in their model we set $x = 1$ leading to $\Psi_n(1) = 1$, leading to $f(\Psi(1)) = 1$ using equation (4.1.6). By combining this information using Theorem 4.1.7 we form

$$\mathbb{P}(\deg(V_i) \geq k) = \frac{\Gamma\left(0 + 1 + \frac{2+0}{1}\right)}{\Gamma(0+1)}(0+k)^{-\frac{2+0}{1}} = 2k^{-2},$$

verifying the asymptotic equivalence of the two models giving credence to our result.

5. LOCATION BASED CHOICE MODEL: DIMENSION EXTENSION

There are a number of extensions which could be explored concerning the location based choice model discussed in Chapter 3. Freeman and Jordan [FJ18] studied a variation allowing for a random sample size, r. They did however impose the restriction that the new edge always forms between v_{n+1} and the member of the sample with the highest location. An issue arising from applying this generalisation to the location based choice model is how we define Ξ. As described in Section 3.1, Ξ is a fixed parameter of the model.

This chapter focuses on an extension which allows for the vertex location to possess multiple components. This extension reflects real world systems more accurately in that the choice of where edges (hyperlinks, citations, friendships, etc) form is typically based on a multitude of different attributes, not just one. Due to the computational complexity of this model we discuss a few simplified examples exploring this multidimensional fitness model which discretises the problem onto a low dimensional lattice.

5.1 Model description

Notation and terminology remains mostly consistent with previous chapters. Given the premise of this chapter we redefine the notion of a vertex's location to fit our model. Specifically, for a vertex $v_i \in V(G_n)$ we define its location as $x_i = \left(x_i^{(1)}, x_i^{(2)}, \ldots, x_i^{(k)}\right)$ such that $x_i \sim \text{Uni}[0,1]^k$.

As a starting point we reduce our model so that every vertex has a two dimensional location, $k = 2$. Given this extended definition of location it is no longer appropriate to use the definition of $\Psi_n(x)$ from Chapters 3-4 as $\Psi_n(x)$ is fundamentally a one dimensional concept with no direct analogue into higher dimensions. As the nature of the model is to examine the effect an extension in the location has on the occurrence of condensation we cannot simply take the Euclidean norm of a vertex's location, as this simply reduces our model to the one dimensional case discussed in Chapter 3.

Comparing two high dimensional vectors in an way which preserves the aspects we are interested in which is analogous to $\Psi_n(x)$ in previous chapters is hard. An example why is if we have two vertices v_a and v_b with locations $x_a = (0, 1)^T$ and $x_b = (0.6, 0.8)^T$ respectively, we see that $|x_a| = |x_b| = 1$ and both $x_a^{(1)} \leq x_b^{(1)}$ and $x_a^{(2)} \geq x_b^{(2)}$ are satisfied. Though this first condition occurs with probability zero, the second is relatively common. We require a comparison method which not only works in this case but ideally in higher dimensions.

As we are more interested in the effect k has on the model opposed to r, we begin by looking at a reduced model whereby three existing vertices are sampled from G_n at time $n + 1$. This model begins with an initial graph G_0 on n_0 vertices labelled $\{v_{1-n_0}, v_{2-n_0}, \ldots, v_{-1}, v_0\}$. For simplicity we maintain the tree structure assumed in earlier chapters. The graph G_{n+1} is formed from the addition of vertex v_{n+1} to G_n. Preferential attachment as outlined by equation (2.4) is used to sample three vertices from G_n. There are a number of options for us to consider when deciding which of these three selected vertices v_{n+1} attaches to, for example:

1. The vertex of the three which is closest to the centre of mass of the three.
2. The vertex of the subset corresponding to the largest angle of the triangle.

It is fairly straightforward to see that in the $r = 3$ case both of these options result in the selection of the same vertex. We use option one as it is less computationally time consuming when simulating and extends well to a higher number of sampled vertices. Option two breaks down when concerning convexity when more than three vertices are sampled. Using option one the new vertex v_{n+1} forms an edge between itself and

the member of the selection which is closest to the centre of mass $M = (M_1, M_2)^T$ of the convex hull created by the locations of the selected vertices according to $M_s = \frac{1}{k}\sum_{r=1}^{k} x_r^{(s)}$ for $M_s \in \{M_1, M_2\}$. A visual representation of how this model behaves is given below in figure 5.1 below.

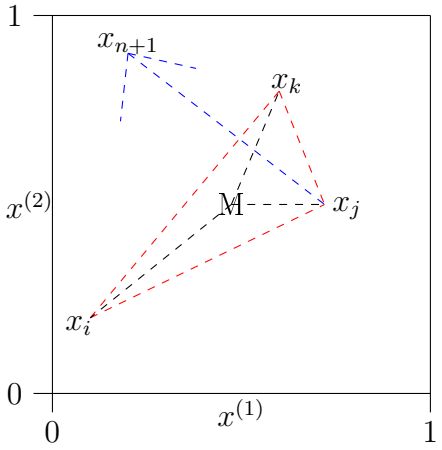

Fig. 5.1: Two dimensional location model involving three sampled vertices.

We define $d(M, x_i)$ as the Euclidean distance between M and the location associated with v_i calculated using $d(M, x_i) = \sqrt{\sum_{s=1}^{k}\left(x_i^{(s)} - M_s\right)^2}$.

Lemma 5.1.1. *If vertex v_i is sampled more than once then $\mathbb{P}(v_{n+1} \sim v_i) = 1$.*

Proof. Clearly if v_i is sampled three times, the edge $v_{n+1} \sim v_i$ is formed. We assign the locations x_i to v_i and x_j to v_j which we use to calculate the components of M as

$$M_s = \frac{x_j^{(s)} + 2x_i^{(s)}}{3}$$

for $M_s \in \{M_1, M_2\}$. We compare the distances $d(x_i, M)$ and $d(x_j, M)$:

$$d(x_i, M) = |x_i - M| = \frac{1}{3}\sqrt{\left(x_i^{(1)} - x_j^{(1)}\right)^2 + \left(x_i^{(2)} - x_j^{(2)}\right)^2},$$

$$d(x_j, M) = |x_j - M| = \frac{2}{3}\sqrt{\left(x_i^{(1)} - x_j^{(1)}\right)^2 + \left(x_i^{(2)} - x_j^{(2)}\right)^2}.$$

Clearly $d(x_i, M) = 2d(x_j, M)$ therefore v_{n+1} forms an edge between itself and vertex v_i with probability one. □

5.1.1 2×2 lattice simplification

We examine an initial simplification by considering a 2×2 lattice configuration where new vertices are at one of four locations denoted by x_1, x_2, x_3 and x_4.

Let us define $X_{1,n}$, $X_{2,n}$, $X_{3,n}$ and $X_{4,n}$ as the proportion of edge ends at each of the four points x_1, x_2, x_3 and x_4 respectively in graph G_n. Using [Pem07] we formulate an appropriate set of stochastic approximation equations concerning each of $X_{1,n}$, $X_{2,n}$, $X_{3,n}$ and $X_{4,n}$ in the form

$$\mathbb{E}(X_{n+1,i}|\mathcal{F}_n) - X_{n,i} = \gamma_{n+1} F_i\left(\mathbf{X_n}; \alpha\right), \tag{5.1}$$

where $\mathbf{X_n} = (X_{1,n}, X_{2,n}, \ldots, X_{4,n})$ and $\gamma_{n+1}^{-1} = (n+n_0)(2+\alpha)+\alpha$ is the appropriate normalization factor. Here our set of four stochastic approximation equations are given by

$$\begin{aligned}
F_1\left(\mathbf{X_n}; \alpha\right) &= -2X_{1,n}^3 + 3X_{1,n}^2 + 6X_{4,n}X_{1,n}X_{2,n} - (2+\alpha)X_{1,n} + \frac{(1+\alpha)}{4}, \\
F_2\left(\mathbf{X_n}; \alpha\right) &= -2X_{2,n}^3 + 3X_{2,n}^2 + 6X_{1,n}X_{2,n}X_{3,n} - (2+\alpha)X_{2,n} + \frac{(1+\alpha)}{4}, \\
F_3\left(\mathbf{X_n}; \alpha\right) &= -2X_{3,n}^3 + 3X_{3,n}^2 + 6X_{2,n}X_{3,n}X_{4,n} - (2+\alpha)X_{3,n} + \frac{(1+\alpha)}{4}, \\
F_4\left(\mathbf{X_n}; \alpha\right) &= -2X_{4,n}^3 + 3X_{4,n}^2 + 6X_{3,n}X_{4,n}X_{1,n} - (2+\alpha)X_{4,n} + \frac{(1+\alpha)}{4}.
\end{aligned} \tag{5.2}$$

By observing our proportions must satisfy $X_{4,n} = 1 - \sum_{k=1}^{3} X_{k,n}$ we require only three of these equations to fully describe our model, deducing a complete set of solutions to the four equations.

Theorem 5.1.2. *If $\alpha \geq -\frac{1}{2}$ there is a positive probability of convergence to $\left(\frac{1}{4}, \frac{1}{4}, \frac{1}{4}, \frac{1}{4}\right)$.*

If $\alpha < -\frac{1}{2}$ there exists a positive probability of convergence to (18), (19), (24) or (25) of Table 5.1. Convergence to $\left(\frac{1}{4}, \frac{1}{4}, \frac{1}{4}, \frac{1}{4}\right)$ when $\alpha \leq -\frac{1}{2}$ or any of (18), (19), (24) or (25) when $\alpha > -\frac{1}{2}$ occurs with probability zero.

Proof. We use MatLab to solve our set of equations displaying the complete list of stationary points in exact form in Table 5.1.

	X_1	X_2	X_3	X_4
1)	$\frac{1}{4}$	$\frac{1}{4}$	$\frac{1}{4}$	$\frac{1}{4}$
2)	$\frac{1}{4} - b$	$\frac{1}{4} + b$	$\frac{1}{4} - b$	$\frac{1}{4} + b$
3)	$\frac{1}{4} + b$	$\frac{1}{4} - b$	$\frac{1}{4} + b$	$\frac{1}{4} - b$
4)	$\frac{1}{4} + c$	$\frac{1}{4} - c$	$\frac{1}{4} - c$	$\frac{1}{4} + c$
5)	$\frac{1}{4} + c$	$\frac{1}{4} + c$	$\frac{1}{4} - c$	$\frac{1}{4} - c$
6)	$\frac{1}{4} - c$	$\frac{1}{4} - c$	$\frac{1}{4} + c$	$\frac{1}{4} + c$
7)	$\frac{1}{4} - c$	$\frac{1}{4} + c$	$\frac{1}{4} + c$	$\frac{1}{4} - c$
8)	$\frac{1}{4} - c - d$	$\frac{1}{4} - c + d$	$\frac{1}{4} + c - d$	$\frac{1}{4} + c + d$
9)	$\frac{1}{4} - c - d$	$\frac{1}{4} + c + d$	$\frac{1}{4} + c - d$	$\frac{1}{4} - c + d$
10)	$\frac{1}{4} + c + d$	$\frac{1}{4} - c - d$	$\frac{1}{4} - c + d$	$\frac{1}{4} + c - d$
11)	$\frac{1}{4} + c + d$	$\frac{1}{4} + c - d$	$\frac{1}{4} - c + d$	$\frac{1}{4} - c - d$
12)	$\frac{1}{4} + c - d$	$\frac{1}{4} - c + d$	$\frac{1}{4} - c - d$	$\frac{1}{4} + c + d$
13)	$\frac{1}{4} + c - d$	$\frac{1}{4} + c + d$	$\frac{1}{4} - c - d$	$\frac{1}{4} - c + d$
14)	$\frac{1}{4} - c + d$	$\frac{1}{4} - c - d$	$\frac{1}{4} + c + d$	$\frac{1}{4} + c - d$
15)	$\frac{1}{4} - c + d$	$\frac{1}{4} + c - d$	$\frac{1}{4} + c + d$	$\frac{1}{4} - c - d$
16)	z_1	$\frac{1}{2} - z_1 - 2c$	z_1	$\frac{1}{2} - z_1 + 2c$
17)	z_1	$\frac{1}{2} - z_1 + 2c$	z_1	$\frac{1}{2} - z_1 - 2c$
18)	z_2	$\frac{1}{2} - z_2 - 2c$	z_2	$\frac{1}{2} - z_2 + 2c$
19)	z_2	$\frac{1}{2} - z_2 + 2c$	z_2	$\frac{1}{2} - z_2 - 2c$
20)	z_3	$\frac{1}{2} - z_3 - 2c$	z_3	$\frac{1}{2} - z_3 + 2c$
21)	z_3	$\frac{1}{2} - z_3 + 2c$	z_3	$\frac{1}{2} - z_3 - 2c$
22)	$\frac{1}{2} - z_1 - 2c$	z_1	$\frac{1}{2} - z_1 + 2c$	z_1
23)	$\frac{1}{2} - z_1 + 2c$	z_1	$\frac{1}{2} - z_1 - 2c$	z_1
24)	$\frac{1}{2} - z_2 - 2c$	z_2	$\frac{1}{2} - z_2 + 2c$	z_2
25)	$\frac{1}{2} - z_2 + 2c$	z_2	$\frac{1}{2} - z_2 - 2c$	z_2
26)	$\frac{1}{2} - z_3 - 2c$	z_3	$\frac{1}{2} - z_3 + 2c$	z_3
27)	$\frac{1}{2} - z_3 + 2c$	z_3	$\frac{1}{2} - z_3 - 2c$	z_3

Tab. 5.1: Solutions to the 2×2 lattice model for multidimensional location.

Here

$$b = \frac{1}{4}\sqrt{4\alpha + 5},\ c = \frac{1}{4}\sqrt{-1 - 2\alpha} \text{ and } d = \frac{1}{2}\sqrt{\frac{1-\alpha}{2}}$$

and

$$f(z;\alpha) = z^3 - \frac{3}{4}z^2 + \frac{1}{2}\left(\alpha + \frac{1}{2}\right)z + \frac{1}{16}(\alpha + 1) = (z - z_1)(z - z_2)(z - z_3)$$

where $z_1 \leq z_2 \leq z_3$ such that

$$\begin{aligned}
z_1 =& \frac{35184372088832\left(\sqrt{3}\mathrm{i} - 1\right)\left(2\sqrt{3}\sqrt{128\alpha^3 + 291\alpha^2 + 249\alpha + 61} - 54\alpha - 27\right)^{1/3}}{585491545649747} + \\
& \frac{1099511627776\left(1 + \sqrt{3}\mathrm{i}\right)(384\alpha + 48)}{608935746319847\left(2\sqrt{3}\sqrt{128\alpha^3 + 291\alpha^2 + 249\alpha + 61} - 54\alpha - 27\right)^{1/3}} + \frac{1}{4} \\
z_2 =& -\frac{1099511627776\left(\sqrt{3}\mathrm{i} - 1\right)(384\alpha + 48)}{608935746319847\left(2\sqrt{3}\sqrt{128\alpha^3 + 291\alpha^2 + 249\alpha + 61} - 54\alpha - 27\right)^{1/3}} - \\
& \frac{35184372088832\left(1 + \sqrt{3}\mathrm{i}\right)\left(2\sqrt{3}\sqrt{128\alpha^3 + 291\alpha^2 + 249\alpha + 61} - 54\alpha - 27\right)^{1/3}}{585491545649747} + \frac{1}{4} \\
z_3 =& \frac{70368744177664\left(2\sqrt{3}\sqrt{128\alpha^3 + 291\alpha^2 + 249\alpha + 61} - 54\alpha - 27\right)^{1/3}}{585491545649747} \\
& - \frac{2199023255552\,(384\alpha + 48)}{608935746319847\left(2\sqrt{3}\sqrt{128\alpha^3 + 291\alpha^2 + 249\alpha + 61} - 54\alpha - 27\right)^{1/3}} + \frac{1}{4}.
\end{aligned}$$

We use the definitions of b, c and d along with the structure of these solutions to narrow down the potential stable points. We first note that all components of a viable solution (X_1, X_2, X_3, X_4) must be real values between 0 and 1 inclusive for $\alpha > -1$ as they correspond to proportions. We see from solutions (2-3) in Table 5.1 that we must have

$$0 \leq b \leq \frac{1}{4},$$

which is only true when $-\frac{5}{4} \leq \alpha \leq -1$, therefore this pair are infeasible with respect to the definition of α. We use similar logic to show that $-\frac{1}{2} \geq \alpha \geq -1$ must hold in order for solutions (4-7) to be viable.

We plot the components of solutions (8-15) in Figure 5.2.

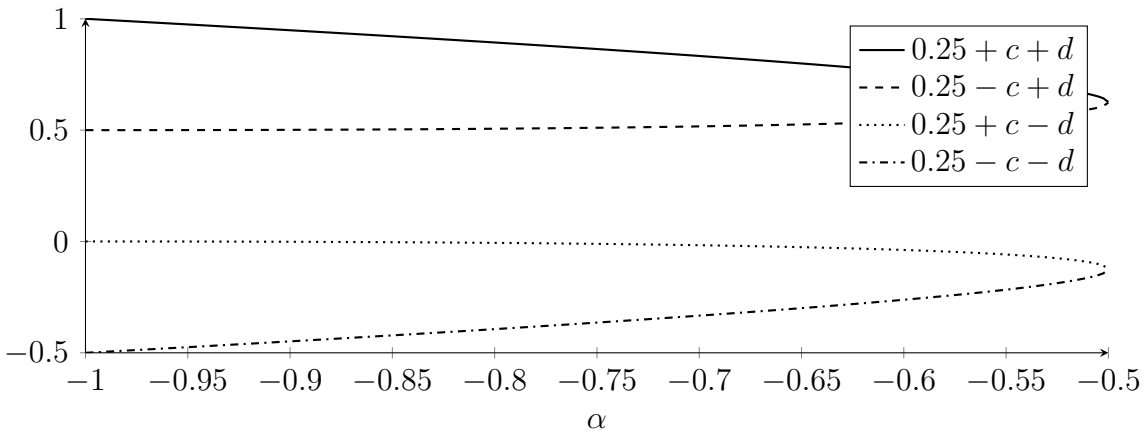

Fig. 5.2: Plot of solution components to entries (8-15) of Table 5.1.

We see $\frac{1}{4}-c-d$ is never in the interval $[0,1]$ implying all solutions (8-15) are infeasible.

In order to examine the stability of solutions (16-27) we must first take into consideration the possible values of z_1, z_2 and z_3. As we have shown above $-1 < \alpha \leq -\frac{1}{2}$ must hold for c to be real. We plot the function $f(z;\alpha)$ which generates z_1, z_2 and z_3 in Figure 5.3 for $\alpha \in (-1, -\frac{1}{2}]$. We display $f(z;-1)$ (bottom most curve) and $f(z;-0.5)$ (top curve) in black.

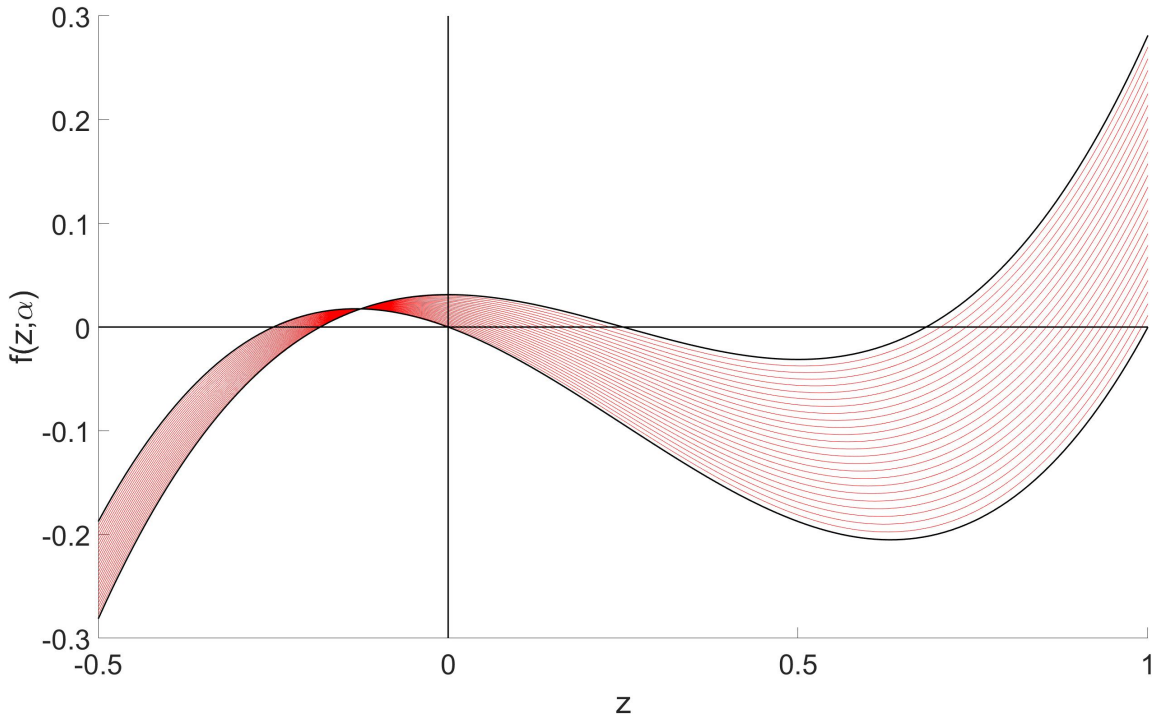

Fig. 5.3: A plot of $f(z;\alpha)$ depicting bounds on the roots generated by incremental values taken of $\alpha \in [-0.5, -1)$.

We see from Figure 5.3 that each of the roots are bounded above and below by the roots generated by $f(z;-0.5)$ and $f(z;-1)$. Moreover we see that

$$f(z;-1) = z(z-1)(z+0.25) \tag{5.3}$$

and

$$f(z;-0.5) = \left(z - \frac{1}{4}\right)\left(z^2 - \frac{z}{2} - \frac{1}{8}\right). \tag{5.4}$$

By using (5.3) and (5.4) we calculate exact values for the bounds on our roots as

$$z_1 \in \left(-\frac{1}{4}, \frac{1}{4} - \frac{\sqrt{3}}{4}\right], \; z_2 \in \left(0, \frac{1}{4}\right] \text{ and } z_3 \in \left[\frac{1}{4} + \frac{\sqrt{3}}{4}, 1\right). \tag{5.5}$$

Figure 5.4 evaluates the three roots of $f(z;\alpha)$ showing behaviour inside the intervals

given by (5.5).

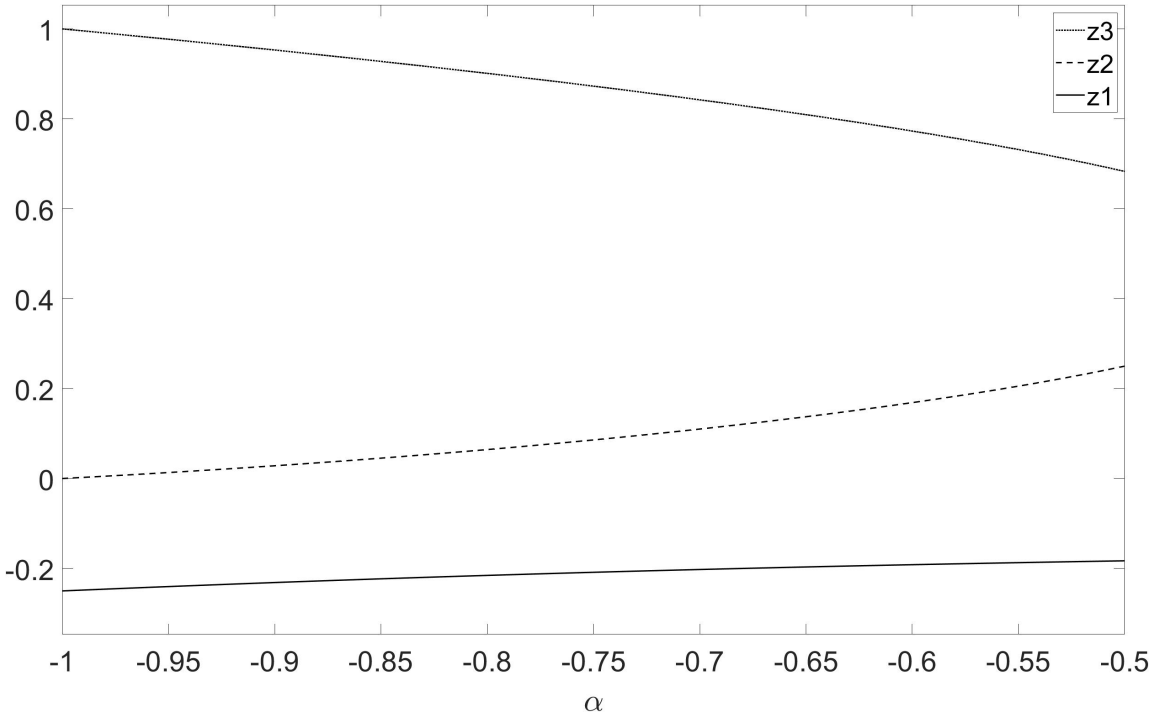

Fig. 5.4: A plot showing the effect a change in α has on z_1, z_2 and z_3.

We immediately see that any solutions with z_1 as a component are infeasible because $z_1 < 0$ for all α when $c \in \mathbb{R}$. We further see that as $z_3 > \frac{3}{5}$ and $c \geq 0$ it follows that $\frac{1}{2} - z_3 - 2c < 0$ ruling out any solutions with z_3 as a component. We plot the components of our solutions with higher complexity; namely $\frac{1}{2} + z_2 \pm 2c$ which has components plotted in Figure 5.5.

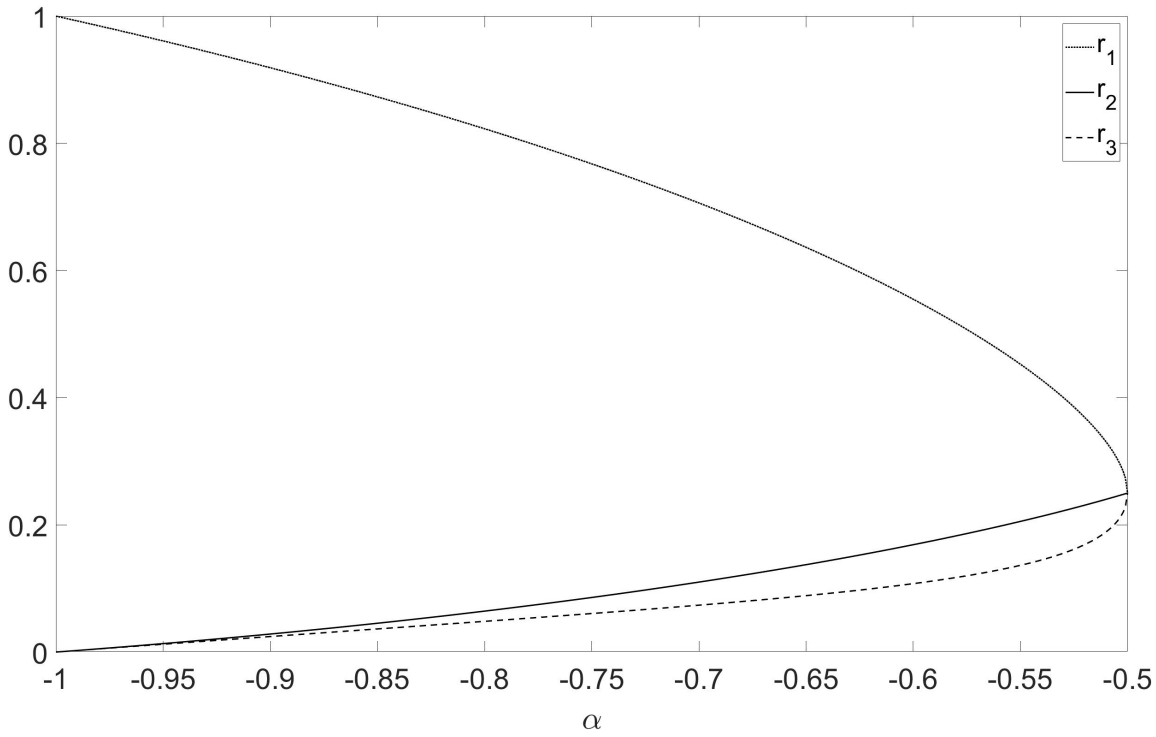

Fig. 5.5: A plot showing the effect a change in α has on the root components $r_1 = z_2 + \frac{1}{2} - 2c$, $r_2 = z_2$ and $r_3 = z_2 + \frac{1}{2} + 2c$.

Table 5.2 contains the feasible solutions of Table 5.1 and the corresponding range of α for which each is valid.

	X_1	X_2	X_3	X_4	Feasible Range
1)	$\frac{1}{4}$	$\frac{1}{4}$	$\frac{1}{4}$	$\frac{1}{4}$	Always
4)	$\frac{1}{4} + c$	$\frac{1}{4} - c$	$\frac{1}{4} - c$	$\frac{1}{4} + c$	$\alpha \leq -\frac{1}{2}$
5)	$\frac{1}{4} + c$	$\frac{1}{4} + c$	$\frac{1}{4} - c$	$\frac{1}{4} - c$	$\alpha \leq -\frac{1}{2}$
6)	$\frac{1}{4} - c$	$\frac{1}{4} - c$	$\frac{1}{4} + c$	$\frac{1}{4} + c$	$\alpha \leq -\frac{1}{2}$
7)	$\frac{1}{4} - c$	$\frac{1}{4} + c$	$\frac{1}{4} + c$	$\frac{1}{4} - c$	$\alpha \leq -\frac{1}{2}$
18)	z_2	$\frac{1}{2} - z_2 - 2c$	z_2	$\frac{1}{2} - z_2 + 2c$	$\alpha \leq -\frac{1}{2}$
19)	z_2	$\frac{1}{2} - z_2 + 2c$	z_2	$\frac{1}{2} - z_2 - 2c$	$\alpha \leq -\frac{1}{2}$
24)	$\frac{1}{2} - z_2 - 2c$	z_2	$\frac{1}{2} - z_2 + 2c$	z_2	$\alpha \leq -\frac{1}{2}$
25)	$\frac{1}{2} - z_2 + 2c$	z_2	$\frac{1}{2} - z_2 - 2c$	z_2	$\alpha \leq -\frac{1}{2}$

Tab. 5.2: Viable limiting proportions and conditions associated to Table 5.1.

Pemantle [Pem07] outlines conditions in which a random variables converge in a vector field to a stable (Theorem 2.8) attractor (Theorem 2.16) of the root set (Corollary 2.7) with positive probability and unstable with probability zero (Theorem 2.17). The stability associated to our system of stochastic approximation equations (5.2) requires the partial derivatives

$$\begin{aligned}
\frac{\partial}{\partial X_1}F_1\left(\mathbf{X_n};\alpha\right) &= 6(X_1+X_2)(X_3+X_4)-6X_2X_3-(a+2),\\
\frac{\partial}{\partial X_2}F_1\left(\mathbf{X_n};\alpha\right) &= 6X_1(X_4-X_2),\\
\frac{\partial}{\partial X_3}F_1\left(\mathbf{X_n};\alpha\right) &= -6X_1X_2,\\
\frac{\partial}{\partial X_1}F_2\left(\mathbf{X_n};\alpha\right) &= 6X_2X_3,\\
\frac{\partial}{\partial X_2}F_2\left(\mathbf{X_n};\alpha\right) &= 6X_2(1-X_2)+6X_1X_3-(a+2),\\
\frac{\partial}{\partial X_3}F_2\left(\mathbf{X_n};\alpha\right) &= 6X_1X_2,\\
\frac{\partial}{\partial X_1}F_3\left(\mathbf{X_n};\alpha\right) &= -6X_2X_3,\\
\frac{\partial}{\partial X_2}F_3\left(\mathbf{X_n};\alpha\right) &= 6X_3(X_4-X_2),\\
\frac{\partial}{\partial X_3}F_3\left(\mathbf{X_n};\alpha\right) &= 6(X_2+X_3)(X_1+X_4)-6X_1X_2-(a+2),
\end{aligned}$$

to fully describe. We use these to calculate the associated eigenvalues to this system as

$$\begin{aligned}
\lambda_1 &= 6(X_1+X_2)(X_3+X_4)-(\alpha+2),\\
\lambda_2 &= 6(X_1+X_4)(X_2+X_3)-(\alpha+2),\\
\lambda_3 &= 6(X_1X_3+X_2X_4)-(a+2).
\end{aligned}$$

Table 5.3 gives these evaluated at each of the solutions in Table 5.2.

Number	feasible proportion range	λ_1	λ_2	λ_3
1)	Always	$-\frac{1}{2}-\alpha$	$-\frac{1}{2}-\alpha$	$-\frac{5}{4}-\alpha$
4)	$\alpha \leq -\frac{1}{2}$	$-\frac{1}{2}-\alpha$	$1+2\alpha$	$-\frac{1}{2}+\frac{1}{2}\alpha$
5)	$\alpha \leq -\frac{1}{2}$	$1+2\alpha$	$-\frac{1}{2}-\alpha$	$-2-\frac{1}{2}\alpha$
6)	$\alpha \leq -\frac{1}{2}$	$1+2\alpha$	$-\frac{1}{2}-\alpha$	$-2-\frac{1}{2}\alpha$
7)	$\alpha \leq -\frac{1}{2}$	$-\frac{1}{2}-\alpha$	$1+2\alpha$	$-\frac{1}{2}+\frac{1}{2}\alpha$
18)	$\alpha \leq -\frac{1}{2}$	$1+2\alpha$	$-1+2\alpha$	$z_2^2-\frac{z_2}{2}+\frac{\alpha+1}{12}$
19)	$\alpha \leq -\frac{1}{2}$	$1+2\alpha$	$-1+2\alpha$	$z_2^2-\frac{z_2}{2}+\frac{\alpha+1}{12}$
24)	$\alpha \leq -\frac{1}{2}$	$1+2\alpha$	$-1+2\alpha$	$z_2^2-\frac{z_2}{2}+\frac{\alpha+1}{12}$
25)	$\alpha \leq -\frac{1}{2}$	$1+2\alpha$	$-1+2\alpha$	$z_2^2-\frac{z_2}{2}+\frac{\alpha+1}{12}$

Tab. 5.3: Each eigenvalue associated to the feasible solutions from Table 5.2.

In order for a solution to be stable all eigenvalues must be negative simultaneously. Table 5.4 combines the information found in the range column of Table 5.3 with the corresponding values of α for which each of the eigenvalues are negative. The final column of Table 5.4 combines all four columns to give the range for which each solution is a viable stable proportion.

Number	Range	λ_1	λ_2	λ_3	Stable when
1)	Always	$-\frac{1}{2}<\alpha$	$-\frac{1}{2}<\alpha$	$-\frac{5}{4}<\alpha$	$-\frac{1}{2}<\alpha$
4)	$-1<\alpha<-\frac{1}{2}$	$-\frac{1}{2}<\alpha$	$\alpha<-\frac{1}{2}$	$\alpha<1$	Never
5)	$-1<\alpha<-\frac{1}{2}$	$\alpha<-\frac{1}{2}$	$-\frac{1}{2}<\alpha$	$-4<\alpha$	Never
6)	$-1<\alpha<-\frac{1}{2}$	$\alpha<-\frac{1}{2}$	$-\frac{1}{2}<\alpha$	$-4<\alpha$	Never
7)	$-1<\alpha<-\frac{1}{2}$	$-\frac{1}{2}<\alpha$	$\alpha<-\frac{1}{2}$	$\alpha<1$	Never
18)	$-1<\alpha<-\frac{1}{2}$	$\alpha<-\frac{1}{2}$	$\alpha<\frac{1}{2}$	$z_2^2-\frac{z_2}{2}+\frac{\alpha+1}{12}<0$	$\alpha<-\frac{1}{2}$
19)	$-1<\alpha<-\frac{1}{2}$	$\alpha<-\frac{1}{2}$	$\alpha<\frac{1}{2}$	$z_2^2-\frac{z_2}{2}+\frac{\alpha+1}{12}<0$	$\alpha<-\frac{1}{2}$
24)	$-1<\alpha<-\frac{1}{2}$	$\alpha<-\frac{1}{2}$	$\alpha<\frac{1}{2}$	$z_2^2-\frac{z_2}{2}+\frac{\alpha+1}{12}<0$	$\alpha<-\frac{1}{2}$
25)	$-1<\alpha<-\frac{1}{2}$	$\alpha<-\frac{1}{2}$	$\alpha<\frac{1}{2}$	$z_2^2-\frac{z_2}{2}+\frac{\alpha+1}{12}<0$	$\alpha<-\frac{1}{2}$

Tab. 5.4: Stability conditions for each of the feasible limiting proportions for the 2×2 lattice model.

We see from Table 5.4 there exist a single phase transition in this model at $\alpha=-\frac{1}{2}$. When α is greater than this threshold the limiting proportion of edge ends at each of the four vertices is equal. Utilizing Theorem 2.16 of [Pem07] we show that when

$\alpha < -\frac{1}{2}$ our process converges to any of the four solutions (18, 19, 24 or 25) with positive probability and by Theorem 2.17 and non-convergence to these points when $\alpha > -\frac{1}{2}$. Similarly when $\alpha > -\frac{1}{2}$ Theorem 2.16 of [Pem07] allows us to conclude that this process converges to (1) and by Theorem 2.17 of [Pem07], non-convergence to (1) when $\alpha < -\frac{1}{2}$. □

5.1.2 3×3 *lattice simplification*

The natural extension to the model described in Section 5.1.1 is to increase the size of vertices in our network to $n \times n$. This is a complicated task; we first consider the case when we have nine vertices for new edges to be selected from.

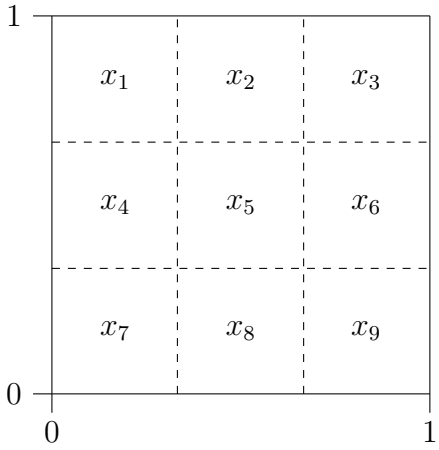

Fig. 5.6: A grid depicting the options for new vertices to attach to in the reduced 3×3 lattice model.

Using a similar method as we did in equation (5.1) we formulate the set of stochastic approximation equations:

$$\begin{aligned} F_1\left(\mathbf{X_n^{(9)}};\alpha\right) =& -2X_1^3 + 3X_1^2 - X_1(2+a) + \frac{1+\alpha}{9} \\ &+ 6X_1\left(X_2X_4 + X_3X_4 + X_2X_7 + X_3X_7 + \frac{1}{2}X_6X_7 + \frac{1}{2}X_3X_8\right) \\ F_2\left(\mathbf{X_n^{(9)}};\alpha\right) =& -2X_2^3 + 3X_2^2 - X_2(2+a) + \frac{1+\alpha}{9} + 6X_2(X_1X_3 + X_1X_9 + X_1X_5 \end{aligned}$$

$$
\begin{aligned}
&+ X_1X_6 + X_1X_8 + X_3X_4 + X_3X_5 + X_4X_6 + X_3X_7 + X_3X_8) \\
&+ 6X_2\left(\frac{1}{2}X_6X_7 + \frac{1}{2}X_4X_9\right) \\
F_3\left(\mathbf{X_n^{(9)}};\alpha\right) =& -2X_3^3 + 3X_3^2 - X_3(2+a) + \frac{1+\alpha}{9} \\
&+ 6X_3\left(X_1X_9 + X_1X_6 + X_2X_6 + X_2X_9 + \frac{1}{2}X_1X_8 + \frac{1}{2}X_4X_9\right) \\
F_4\left(\mathbf{X_n^{(9)}};\alpha\right) =& -2X_4^3 + 3X_4^2 - X_4(2+a) + \frac{1+\alpha}{9} + 6X_4(X_1X_5 + X_1X_6 + X_1X_7 \\
&+ X_1X_8 + X_1X_9 + X_2X_7 + X_2X_8 + X_3X_7 + X_5X_7 + X_6X_7) \\
&+ 6X_4\left(\frac{1}{2}X_2X_9 + \frac{1}{2}X_3X_8\right) \\
F_5\left(\mathbf{X_n^{(9)}};\alpha\right) =& -2X_5^3 + 3X_5^2 - X_5(2+a) + \frac{1+\alpha}{9} + 6X_5(X_1X_6 + X_1X_7 + X_1X_3 \\
&+ X_1X_8 + X_1X_9 + X_2X_4 + X_2X_7 + X_2X_8 + X_2X_9 + X_2X_6 + X_3X_4 \\
&+ X_3X_7 + X_3X_8 + X_3X_9 + X_4X_6 + X_4X_8 + X_4X_9 + X_6X_7 + X_6X_8 \\
&+ X_7X_9) \\
F_6\left(\mathbf{X_n^{(9)}};\alpha\right) =& -2X_6^3 + 3X_6^2 - X_6(2+a) + \frac{1+\alpha}{9} + 6X_6(X_1X_9 + X_2X_8 + X_2X_9 \\
&+ X_3X_4 + X_3X_7 + X_3X_8 + X_3X_9 + X_3X_5 + X_4X_9 + X_5X_9) \\
&+ 6X_6\left(\frac{1}{2}X_2X_7 + \frac{1}{2}X_1X_8\right) \\
F_7\left(\mathbf{X_n^{(9)}};\alpha\right) =& -2X_7^3 + 3X_7^2 - X_7(2+a) + \frac{1+\alpha}{9} \\
&+ 6X_7\left(X_1X_8 + X_1X_9 + X_4X_8 + X_4X_9 + \frac{1}{2}X_1X_6 + \frac{1}{2}X_2X_9\right) \\
F_8\left(\mathbf{X_n^{(9)}};\alpha\right) =& -2X_8^3 + 3X_8^2 - X_8(2+a) + \frac{1+\alpha}{9} + 6X_8(X_1X_9 + X_2X_7 + X_2X_9 \\
&+ X_3X_7 + X_4X_6 + X_4X_9 + X_5X_7 + X_5X_9 + X_6X_7 + X_7X_9) \\
&+ 6X_8\left(\frac{1}{2}X_1X_6 + \frac{1}{2}X_3X_4\right) \\
F_9\left(\mathbf{X_n^{(9)}};\alpha\right) =& -2X_9^3 + 3X_9^2 - X_9(2+a) + \frac{1+\alpha}{9}
\end{aligned}
$$

$$+ 6X_9 \left(X_3X_7 + X_3X_8 + X_6X_7 + X_6X_8 + \frac{1}{2}X_3X_4 + \frac{1}{2}X_2X_7 \right).$$

The analysis for this model is significantly more difficult due to the larger array of equations which requires solving simultaneously. When we had the four dimensional system we had $(4-1)^{4-1}$ solutions. In this situation we have $(9-1)^{9-1} = 2^{24}$ solutions for the 3×3 system. It follows immediately that if we were to use this method to solve the $n \times n$ system we have a maximum of

$$2^{\frac{\left(n^2-1\right)\ln\left|n^2-1\right|}{ln|2|}}$$

different solutions. We therefore must find a different method to solve this problem.

6. COMPETING TYPES WITH LOCATION MODEL: COEXISTENCE

In this chapter we introduce a natural extension of a model proposed by Antunović, Mossel and Rácz in [AMR16] discussed previously in Section 2.4. The AMR model applies a method of growth which allows for vertex choices to grow sequentially within the graph. The AMR model describes coexistence between types of vertices in a graph as the number of vertices grows. Here it is meant that vertices are classified by types where new vertices choose their type based on a sample of those taken from the current network. Coexistence in this situation is where no single type dominates. Our model extends the AMR type adoption framework to the geometric/community models discussed in [Jor13,HS18] by the introduction of vertex location. Under this new framework v_{n+1} is assigned a location upon its creation then deciding its type based on the m edges it forms with the current vertices using preferential attachment, equation (2.4).

An important change we make to definitions in previous chapters is vertex location. We categorise a vertex's type as either 1 or 2 and vertex location similarly as 1 or 2 for the most part, though we do define the basic model for any number of types and locations.

An analogy of this model is that of the US presidential primary election voting process. Here we might look for coexistence among voter sex (representing vertex location as it is chosen at birth) and political affiliation (as this is influenced by surrounding political views.) One would expect proportions of males and females affiliated to each party to be (probably) non equal quantities.

Work on this chapter was begun late in the process and therefore is potential for further work to extend the results.

6.1 Model description

We first define initial notation in terms of a general model involving any number of types T_j and locations L_i such that $i, j \in \mathbb{N}$. Following this we reduce the model to a specific case involving two types and two locations as this is enough to show our desired results involving coexistence we desire.

6.1.1 General model

Let $\{L_1, L_2, \ldots, L_l\}$ be the set of possible locations and $\{T_1, T_2, \ldots, T_t\}$ be the set of types. We define $v_k^{(i,j)}$ as a vertex in graph G_n with location L_i and type T_j, and μ_i as the probability a vertex is at location L_i.

Starting with an initial graph G_0 on n_0 vertices each of which has an assigned type and location, we denote these vertices by $\{v_{1-n_0}, v_{2-n_0}, \ldots, v_0\}$. For simplicity we assume that the average degree in G_0 is $2m$ (though as $n \to \infty$ this is not important.) We further assume there exist vertices in G_0 representing every combination of type and location. In a change to [AMR16] we introduce a constant $\theta \in [0, 1]$ which acts as a biasing constant during the type selection process. This value θ acts as the main feature of the model we are extending to. This is a version of the graph model from [Jor13, AMR16] however including the type allocation procedure from from [AMR16].

A question we ask is; in the situation when there exists is more than one limit in the model, is possible to get different limits at different locations? In order to examine this further we track the total degree weight at each combination of types and locations.

Definition 6.1.1. *Let $X_{i,j}^{(n)}$ be the proportion of degree mass at vertices with location i with type j in graph G_n.*

In order to form G_{n+1}, a new vertex $v_{n+1}^{(i)}$ joins G_n with its own location L_i chosen according to some distribution. A sample of m vertices are then taken from G_n with replacement by way of preferential attachment (2.4). This sampling is biased by θ when considering vertices with different locations than itself. If we assume the new vertex $v_{n+1}^{(i)}$ is at location L_i, of the m samples taken with replacement, a single edge from $v_{n+1}^{(i)}$ connects to an existing vertex of the same location with type T_j with probability

$$\frac{X_{i,j}^{(n)}}{\left(\sum_{k=1}^{t} X_{i,k}^{(n)}\right) + \left(\theta \sum_{\substack{r=1 \\ r\neq i}}^{l} \sum_{k=1}^{t} X_{r,k}^{(n)}\right)}.$$

A vertex not at location L_i forms an edge with a type T_j vertex with probability

$$\frac{\theta \sum_{\substack{k=1 \\ k\neq i}}^{l} X_{k,j}^{(n)}}{\left(\sum_{k=1}^{t} X_{i,k}^{(n)}\right) + \left(\theta \sum_{\substack{r=1 \\ r\neq i}}^{l} \sum_{k=1}^{t} X_{r,k}^{(n)}\right)}.$$

Combining both these probabilities we deduce the probability a new vertex forms an edge with a type T_j vertex as

$$\begin{aligned} Q_{i,j}^{(n)} &= \frac{X_{i,j}^{(n)} + \theta \sum_{\substack{k=1 \\ k\neq i}}^{l} X_{k,j}^{(n)}}{\left(\sum_{k=1}^{t} X_{i,k}^{(n)}\right) + \left(\theta \sum_{\substack{r=1 \\ r\neq i}}^{l} \sum_{k=1}^{t} X_{r,k}^{(n)}\right)} \\ &= \frac{X_{i,j}^{(n)} - \theta X_{i,j}^{(n)} + \theta \sum_{k=1}^{l} X_{k,j}^{(n)}}{\left(\sum_{k=1}^{t} X_{i,k}^{(n)}\right) - \theta \left(\sum_{k=1}^{t} X_{i,k}^{(n)}\right) + \left(\theta \sum_{r=1}^{l} \sum_{k=1}^{t} X_{r,k}^{(n)}\right)} \\ &= \frac{(1-\theta) X_{i,j}^{(n)} + \theta \sum_{k=1}^{l} X_{k,j}^{(n)}}{\theta + (1-\theta)\left(\sum_{k=1}^{t} X_{i,k}^{(n)}\right)}. \end{aligned} \tag{6.1}$$

Once type T_j has been allocated to $v_{n+1}^{(i)}$ it is redefined as $v_{n+1}^{(i,j)}$ though referred to in text as v_{n+1} for simplicity. We will choose the type of this new vertex later.

6.1.2 Reduced model

In order to explore this model further we restrict this model it to the lowest complexity in which we expect to see our desired results. This reduced model is where there exists exactly two locations $L_i \in \{L_1, L_2\}$ and two types $T_j \in \{T_1, T_2\}$. Vertices in our model have four combinations of locations and types. The probability associated to forming an edge to a vertex in these combinations given v_{n+1} is at location L_i is given by

$$Q_{i,j}^{(n)} = \frac{(1-\theta)X_{i,j}^{(n)} + \theta\left(X_{1,j}^{(n)} + X_{2,j}^{(n)}\right)}{\theta + (1-\theta)\left(X_{i,1}^{(n)} + X_{i,2}^{(n)}\right)}. \tag{6.2}$$

We define $\mathcal{F}_n$ as the σ-algebra generated by the sequence of graphs generated up to time n. Conditional on $\mathcal{F}_n$, the number of vertices of type T_j which v_{n+1} connects to is distributed binomially according to a binomial distribution given by

$$\text{Binomial}\left(m, Q_{i,j}^{(n)}\right).$$

Due to the nature of the model, a vertex is either T_1 or T_2, so we are able to fully describe vertex types as either T_1 or not T_1. Using this, the probability v_{n+1} is assigned type T_1 given $k \in \mathbb{N}$ edges are formed to vertices with type T_1 is $\rho_k \in [0,1]$. Using this type allocation criterion and equation (6.2) we formulate the probability v_{n+1} connects to k type T_1 vertices using the binomial distribution which is used to calculate the probability v_{n+1} is assigned T_1 as

$$\sum_{k=0}^{m} \rho_k \binom{m}{k} \left(Q_{i,1}^{(n)}\right)^k \left(1 - Q_{i,1}^{(n)}\right)^{m-k}$$

conditional on v_{n+1} being at location L_i. The probability v_{n+1} is at location L_i and of type T_1 is

$$\mu_i \sum_{k=0}^{m} \rho_k \binom{m}{k} \left(Q_{i,1}^{(n)}\right)^k \left(1 - Q_{i,1}^{(n)}\right)^{m-k}$$

where μ_i is the probability a vertex is at location L_i. This leads to the expected number of edges adjacent to v_{n+1} with type T_1 at location L_i as

$$G_{i,1}\left(\mathbf{X_n}; m, \theta, \mu_i\right) = m\mu_i \sum_{k=0}^{m} \rho_k \binom{m}{k} \left(Q_{i,1}^{(n)}\right)^k \left(1 - Q_{i,1}^{(n)}\right)^{m-k}. \tag{6.3}$$

where

$$\mathbf{X_n} = \begin{pmatrix} X_{1,1}^{(n)} & X_{1,2}^{(n)} & \dots & X_{1,t}^{(n)} \\ X_{2,1}^{(n)} & X_{2,2}^{(n)} & \dots & X_{2,t}^{(n)} \\ \vdots & \vdots & \ddots & \vdots \\ X_{l,1}^{(n)} & X_{l,2}^{(n)} & \dots & X_{l,t}^{(n)} \end{pmatrix}.$$

Remark 6.1.2. *We can write equation (6.3) in polynomial form with explicit coefficients as follows*

$$G_{i,1}\left(\mathbf{X_n}; m, \theta, \mu_i\right) = m\mu_i \sum_{k=0}^{m} \binom{m}{k} \left(\sum_{a=0}^{k} \binom{k}{a} (-1)^{a+k} \rho_a \right) \left(Q_{i,1}^{(n)}\right)^k.$$

The probability a single edge connects to a vertex at location L_i and type T_1 for any $i \in \mathbb{N}$ is expressed by

$$\frac{\mu_i X_{i,1}^{(n)}}{\sum_{k=1}^{t} X_{i,k}^{(n)} + \theta \sum_{k=1}^{t} \sum_{\substack{r=1 \\ r \neq i}}^{l} X_{r,k}^{(n)}} + \frac{\theta(1-\mu_i) X_{i,1}^{(n)}}{\theta \sum_{k=1}^{t} X_{i,k}^{(n)} + \sum_{k=1}^{t} \sum_{\substack{r=1 \\ r \neq i}}^{l} X_{r,k}^{(n)}}$$

which is rewritten as

$$\frac{\mu_i X_{i,1}^{(n)}}{\theta + (1-\theta) \sum_{k=1}^{t} X_{i,k}^{(n)}} + \frac{\theta(1-\mu_i) X_{i,1}^{(n)}}{1 - (1-\theta) \sum_{k=1}^{t} X_{i,k}^{(n)}}. \tag{6.4}$$

By restricting equation (6.4) to the setting where $l = t = 2$ we calculate the expected

number of edges which connect to a vertex at location L_i with type T_1 as

$$H_{i,1}\left(\mathbf{X_n}; m, \theta, \mu_i\right) = \frac{mX_{i,1}^{(n)}\mu_i}{\theta + (1-\theta)\left(X_{i,1}^{(n)} + X_{i,2}^{(n)}\right)} + \frac{\theta m X_{i,1}^{(n)}(1-\mu_i)}{1-(1-\theta)\left(X_{i,1}^{(n)} + X_{i,2}^{(n)}\right)}.$$

We define $G_{i,2}\left(\mathbf{X_n}; m, \theta, \mu_i\right)$ and $H_{i,2}\left(\mathbf{X_n}; m, \theta, \mu_i\right)$ analogously noting that the probability a new vertex is of type 2 given it has k type two neighbours is $1 - \rho_{m-k}$.

6.2 Approximation equation structure

By utilizing the form described by Pemantle in [Pem07] we formulate a stochastic approximation equation describing the expected change in the proportion of vertices of each type at each location.

Theorem 6.2.1. *For a fixed m we define the $i \times j$ set of stochastic approximation equations as*

$$X_{i,1}^{(n+1)} - X_{i,1}^{(n)} = \gamma_n \left(F_{i,1}\left(\mathbf{X_n}; m, \theta, \mu_i, \alpha\right) + \xi_{n+1}^{(i,1)}\right)$$

where

$$F_{i,1}\left(\mathbf{X_n}; m, \theta, \mu_i, \alpha\right) = G_{i,1}\left(\mathbf{X_n}; m, \theta, \mu_i\right) + H_{i,1}\left(\mathbf{X_n}; m, \theta, \mu_i\right) - (\alpha + 2m)X_{i,1}^{(n)}$$

and both $\mathbb{E}\left(\xi_{n+1}^{(i,1)} \middle| \mathcal{F}_n\right) = 0$ *and* $\gamma_n^{-1} = (\alpha + 2m)(n + 1 + n_0)$.

Proof. We set up an equation which describes the increase in the proportion of vertices at location i with type 1 using

$$X_{i,1}^{(n+1)} = \gamma_{n+1}\left(\gamma_n^{-1} X_{i,1}^{(n)} + G_{i,1}\left(\mathbf{X_n}; m, \theta, \mu_i\right) + H_{i,1}\left(\mathbf{X_n}; m, \theta, \mu_i\right) + \xi_{n+1}^{(i,1)}\right) \tag{6.5}$$

where $\gamma_{n+1}^{-1} = \alpha(n + n_0 + 1) + 2m(n+1) + 2mn_0$ is the total degree of G_{n+1}. By rearranging equation (6.5) we obtain the desired result. The associated noise of the

system is defined as

$$\xi_{n+1}^{(i,1)} = \gamma_{n+1}^{-1}\left(X_{i,1}^{(n+1)} - \mathbb{E}\left(X_{i,1}^{(n+1)}\middle|\mathcal{F}_n\right)\right)$$

which by definition has expectation zero. □

Theorem 6.2.2. *The four dimensional system of equations described by Theorem 6.2.1 for $i, j \in \{1, 2\}$ with variables*

$$\mathbf{X_n} = \left(X_{1,1}^{(n)}, X_{1,2}^{(n)}, X_{2,1}^{(n)}, X_{2,2}^{(n)}\right)$$

which satisfies

$$X_{i,1} + X_{i,2} \to p_i$$

as $n \to \infty$, where p_i gives the proportion of edge ends at location i.

Proof. We use an equation devised by Jordan [Jor13] containing μ_i and θ as arguments to calculate the limiting proportion of edge ends at location i, p_i, by solving

$$\mu_i\left(\frac{1}{p_i} + \frac{1-\theta}{p_i + \theta(1-p_i)}\right) = (1-\mu_i)\left(\frac{1}{1-p_i} + \frac{1-\theta}{1-p_i(1-\theta)}\right). \tag{6.6}$$

□

As we have restricted our model to $i \in \{1, 2\}$ we have that $\mu_2 = 1 - \mu_1$ and $p_2 = 1 - p_1$. In previous chapters we were able to reduce our system of equations using the knowledge that our limiting proportions should sum to one. Though we could do this again, we would be required to solve three equations simultaneously. Theorem 6.2.2 allows us to further simplify the process of solving our system. By utilizing Theorems 6.2.1 and 6.2.2 the stationary points of

$$F_{1,1}\left(\mathbf{X_n}; m, \theta, \mu_1, \alpha\right) = F_{2,1}\left(\mathbf{X_n}; m, \theta, \mu_2, \alpha\right) = 0 \tag{6.7}$$

we calculate limiting proportions corresponding to solutions to the four dimensional

stochastic approximation equations. Jordan [Jor13] proved convergence to a Lyapunov function describing a similar model to ours without vertex types. The Lyapunov function argument from [Jor13] allows us to deduce that a stable solution of equation (6.7) remains a stable solution with respect to the full model.

6.3 Specific attachment criteria for $\mu = \frac{1}{2}$

In this section we discuss a number of examples which occur based on different selection vectors $\rho = (\rho_0, \rho_1, \ldots, \rho_m)$ in the situation when $\mu_1 = \mu_2 = \frac{1}{2}$. For simplicity we set $\alpha = 0$ as we are interested in the phase transitions associated with θ. Using these conditions we factorize equation (6.6) as

$$4(\theta-1)^2\left(p-\frac{1}{2}\right)\left(p^2-p-\frac{\theta}{2(\theta-1)^2}\right)=0. \tag{6.8}$$

The solutions to equation (6.8) give the values

$$p^{(L)}=\frac{1}{2}-\frac{\sqrt{1+\theta^2}}{2(1-\theta)},\ p^{(M)}=\frac{1}{2} \text{ and } p^{(U)}=\frac{1}{2}+\frac{\sqrt{1+\theta^2}}{2(1-\theta)}.$$

It is clear that $p_U, p_L \notin (0,1)$ therefore $p^{(M)} = \frac{1}{2}$ is the only viable limiting proportion denoted by p going forward. Utilizing this value of p allows us to formulate the pair of ordinary differential equations

$$\begin{aligned} F_{1,1}\left(\mathbf{X_n}; m, \theta, \frac{1}{2}, 0\right) =& G_{1,1}\left(\mathbf{X_n}; m, \theta, \frac{1}{2}\right) - 2mX_{1,1}^{(n)} + H_{1,1}\left(\mathbf{X_n}; m, \theta, \frac{1}{2}\right) \\ =& \frac{m}{2}\sum_{k=0}^{m}\rho_k\binom{m}{k}\left(Q_{1,1}^{(n)}\right)^k\left(1-Q_{1,1}^{(n)}\right)^{m-k} - 2mX_{1,1}^{(n)} \\ &+ \frac{m}{2}\left(\frac{1}{\theta+(1-\theta)p_1}+\frac{\theta}{1-(1-\theta)p_1}\right)X_{1,1}^{(n)} \\ =& -mX_{1,1}^{(n)} + \frac{m}{2}\sum_{k=0}^{m}\rho_k\binom{m}{k}\left(Q_{1,1}^{(n)}\right)^k\left(1-Q_{1,1}^{(n)}\right)^{m-k} \end{aligned} \tag{6.9}$$

for $p_1 = \frac{1}{2}$, and

$$\begin{aligned} F_{2,1}\left(\mathbf{X_n}; m, \theta, \frac{1}{2}, 0\right) =& G_{2,1}\left(\mathbf{X_n}; m, \theta, \frac{1}{2}\right) + H_{2,1}\left(\mathbf{X_n}; m, \theta, \frac{1}{2}\right) - 2mX_{2,1}^{(n)} \quad (6.10) \\ =& \frac{m}{2}\sum_{k=0}^{m} \rho_k \binom{m}{k} \left(Q_{2,1}^{(n)}\right)^k \left(1 - Q_{2,1}^{(n)}\right)^{m-k} - 2mX_{2,1}^{(n)} \\ &+ \frac{m}{2}\left(\frac{1}{\theta + (1-\theta)p_2} + \frac{\theta}{1-(1-\theta)p_2}\right) X_{2,1}^{(n)} \\ =& -mX_{2,1}^{(n)} + \frac{m}{2}\sum_{k=0}^{m} \rho_k \binom{m}{k} \left(Q_{2,1}^{(n)}\right)^k \left(1 - Q_{2,1}^{(n)}\right)^{m-k} \end{aligned}$$

for $p_2 = \frac{1}{2}$ which describe our model. Using equation (6.2) evaluated at the appropriate parameters we formulate

$$Q_{1,1}^{(n)} = \frac{2\left(X_{1,1}^{(n)} + \theta X_{2,1}^{(n)}\right)}{1+\theta} \text{ and } Q_{2,1}^{(n)} = \frac{2\left(X_{2,1}^{(n)} + \theta X_{1,1}^{(n)}\right)}{1+\theta}. \quad (6.11)$$

We use Y to denote the set $(x_{1,1}, x_{1,2}, x_{2,1}, x_{2,2})$ such that all entries are positive values summing to one satisfying $p_i = x_{i,1} + x_{i,2}$. Further from this we say that the solutions to the ODE's given by (6.9) and (6.10) are restricted to Y.

6.3.1 Linear model

The linear model is where the choice of which type v_{n+1} is assigned varies linearly as the number of vertices sampled from G_{n+1} increases from 0 selections to m. More specifically the entries of the vector $\rho = (\rho_0, \rho_1, \ldots, \rho_m)$ follow $\rho_k = \frac{k}{m}$.

Theorem 6.3.1. *For $\rho_k = \frac{k}{m}$ it follows that*

$$G_{i,1}\left(\mathbf{X_n}; m, \theta, \mu_i, 0\right) = m\mu_i Q_{i,1}^{(n)}.$$

Proof. We use Remark 6.1.2 to calculate $G_{i,1}\left(\mathbf{X_n}; m, \theta, \mu_i, 0\right)$ as follows

$$\begin{aligned} G_{i,1}\left(\mathbf{X_n}; m, \theta, \mu_i, 0\right) &= m\mu_i \sum_{k=1}^{m} \binom{m}{k} \left(\sum_{a=0}^{k} \binom{k}{a} (-1)^{a+k} \frac{k}{m} \right) \left(Q_{i,1}^{(n)} \right)^k \\ &= \mu_i \sum_{k=1}^{m} \binom{m}{k} \left(k \sum_{a=1}^{k} \binom{k-1}{a-1} (-1)^{a+k} \right) \left(Q_{i,1}^{(n)} \right)^k \end{aligned}$$

Using the substitution $b = a - 1$

$$G_{i,1}\left(\mathbf{X_n}; m, \theta, \mu_i, 0\right) = \mu_i \sum_{k=1}^{m} \binom{m}{k} \left(k \sum_{b=0}^{k-1} \binom{k-1}{b} (-1)^{b-1+k} \right) \left(Q_{i,1}^{(n)} \right)^k.$$

By utilizing the series expansion

$$(1 + (-1))^{k-1} = \sum_{b=0}^{k-1} \binom{k-1}{b} (-1)^i = \begin{cases} 1, & \text{if } k = 1, \\ 0, & \text{otherwise,} \end{cases}$$

we reformulate $G_{i,1}\left(\mathbf{X_n}; m, \theta, \mu_i, 0\right)$ as

$$\begin{aligned} G_{i,1}\left(\mathbf{X_n}; m, \theta, \mu_i, 0\right) =& \mu_i \sum_{k=1}^{1} \binom{m}{k} \left(k \sum_{b=0}^{k-1} \binom{k-1}{b} (-1)^{b-1+k} \right) \left(Q_{i,1}^{(n)} \right)^k. \\ &+ \mu_i \sum_{k=2}^{m} \binom{m}{k} \left(k \sum_{b=0}^{k-1} \binom{k-1}{b} (-1)^{b-1+k} \right) \left(Q_{i,1}^{(n)} \right)^k. \\ =& m\mu_i Q_{i,1}^{(n)} \end{aligned}$$

as required. □

Lemma 6.3.2. *The solutions to the system of equations associated to the linear model when $\mu = \frac{1}{2}$ can be fully expressed by solving*

$$\begin{pmatrix} F_{1,1}\left(\mathbf{X_n}; m, \theta, \frac{1}{2}, 0\right) \\ F_{2,1}\left(\mathbf{X_n}; m, \theta, \frac{1}{2}, 0\right) \end{pmatrix} = \frac{m\theta}{\theta + 1} \begin{pmatrix} -1 & 1 \\ 1 & -1 \end{pmatrix} \begin{pmatrix} X_{1,1}^{(n)} \\ X_{2,1}^{(n)} \end{pmatrix}$$

restricted to the set Y.

Proof. We discussed in section 6.2 that the limiting proportions of our four dimensional system can be described fully by solving

$$F_{1,1}\left(\mathbf{X_n}; m, \theta, \frac{1}{2}, 0\right) = F_{2,1}\left(\mathbf{X_n}; m, \theta, \frac{1}{2}, 0\right) = 0$$

due to the proportions satisfying $X_{1,1} + X_{1,2} = \frac{1}{2}$ and $X_{2,1} + X_{2,2} = \frac{1}{2}$. Using this knowledge with the simplified form of G derived in Theorem 6.3.1 we need only solve both

$$F_{1,1}\left(\mathbf{X_n}; m, \theta, \frac{1}{2}, 0\right) = \frac{m}{2}Q_{1,1}^{(n)} - mX_{1,1}^{(n)},$$

and

$$F_{2,1}\left(\mathbf{X_n}; m, \theta, \frac{1}{2}, 0\right) = \frac{m}{2}Q_{2,1}^{(n)} - mX_{2,1}^{(n)},$$

simultaneously. This pair can be written in the required form as

$$\begin{pmatrix} F_{1,1}\left(\mathbf{X_n}; m, \theta, \frac{1}{2}, 0\right) \\ F_{2,1}\left(\mathbf{X_n}; m, \theta, \frac{1}{2}, 0\right) \end{pmatrix} = \frac{m\theta}{\theta + 1}\begin{pmatrix} -1 & 1 \\ 1 & -1 \end{pmatrix}\begin{pmatrix} X_{1,1}^{(n)} \\ X_{2,1}^{(n)} \end{pmatrix}. \tag{6.12}$$

□

Lemma 6.3.3. *For the linear case when $\mu = \frac{1}{2}$, all solutions are of the form $(\gamma, \frac{1}{2} - \gamma, \gamma, \frac{1}{2} - \gamma)$.*

Proof. We see from equation (6.12) that $X_{1,1}^{(n)} - X_{2,1}^{(n)} = 0$ which leads to solutions of the form $(\gamma, \frac{1}{2} - \gamma, \gamma, \frac{1}{2} - \gamma)$ such that $\gamma \in [0, \frac{1}{2}]$. □

We check whether this point is stable by using the stability matrix given by

$$\begin{vmatrix} \frac{\partial F_{1,1}\left(\mathbf{X_n}; m, \theta, \frac{1}{2}, 0\right)}{\partial X_{1,1}^{(n)}} - \lambda & \frac{\partial F_{1,1}\left(\mathbf{X_n}; m, \theta, \frac{1}{2}, 0\right)}{\partial X_{2,1}^{(n)}} \\ \frac{\partial F_{2,1}\left(\mathbf{X_n}; m, \theta, \frac{1}{2}, 0\right)}{\partial X_{1,1}^{(n)}} & \frac{\partial F_{2,1}\left(\mathbf{X_n}; m, \theta, \frac{1}{2}, 0\right)}{\partial X_{2,1}^{(n)}} - \lambda \end{vmatrix} = \begin{vmatrix} -c - \lambda & c \\ c & -c - \lambda \end{vmatrix} = \lambda\left(\lambda + 2c\right) = 0.$$

where $c = \frac{m\theta}{1+\theta}$. For a stable point to be stable we require all eigenvalues to be negative simultaneously. Clearly $-2c < 0$ however $\lambda = 0$ is ambiguous when it comes to concluding stability. Because of this we cannot deduce stability using these methods; there may be ways of doing it.

6.3.2 Coin flip model

The type selection for the coin flip model is described as follows: if a new vertex v_{n+1} forms edges between m vertices of one type then it chooses that type however if there is a mix of types in the selection then a coin is tossed to decide the type. This is written more precisely as

$$\rho_k = \begin{cases} 0, & \text{if } k = 0, \\ x, & \text{if } k \in \{1, 2, \ldots, m-1\}, \\ 1, & \text{if } k = m. \end{cases}$$

Here $x \in (0, 1)$ is the probability our new vertex assumes type one. By using this information we formulate the appropriate equations as:

$$F_{1,1}\left(\mathbf{X_n}; m, \theta, \frac{1}{2}, 0\right) = \frac{m}{2}\left((1-x)\left(Q_{1,1}^{(n)}\right)^m + x\left(1 - \left(1 - Q_{1,1}^{(n)}\right)^m\right)\right) - mX_{1,1}^{(n)}$$

and

$$F_{2,1}\left(\mathbf{X_n}; m, \theta, \frac{1}{2}, 0\right) = \frac{m}{2}\left((1-x)\left(Q_{2,1}^{(n)}\right)^m + x\left(1 - \left(1 - Q_{2,1}^{(n)}\right)^m\right)\right) - mX_{2,1}^{(n)},$$

where the solution set is restricted to Y.

Lemma 6.3.4. *When $\mu = \frac{1}{2}$ both $\left(\frac{1}{2}, 0, \frac{1}{2}, 0\right)$ and $\left(0, \frac{1}{2}, 0, \frac{1}{2}\right)$ are stable solutions to the system for any θ if $m \in \left(0, \frac{1}{x}\right)$ for $\left(\frac{1}{2}, 0, \frac{1}{2}, 0\right)$ or $m \in \left(0, \frac{1}{1-x}\right)$ for $\left(0, \frac{1}{2}, 0, \frac{1}{2}\right)$.*

We see later as part of a special case that these are the only solutions.

Proof. For $\mu = \frac{1}{2}$ we have that $p = \frac{1}{2}$ leading to

$$Q_{1,1}^{(n)} = \frac{2}{1+\theta}\left(X_{1,1}^{(n)} + \theta X_{2,1}^{(n)}\right)$$

and

$$Q_{2,1}^{(n)} = \frac{2}{1+\theta}\left(X_{2,1}^{(n)} + \theta X_{1,1}^{(n)}\right).$$

It is easy to check that both $\left(\frac{1}{2}, 0, \frac{1}{2}, 0\right)$ and $\left(0, \frac{1}{2}, 0, \frac{1}{2}\right)$ are solutions to

$$F_{1,1}\left(\mathbf{X_n}; m, \theta, \frac{1}{2}, 0\right) = F_{2,1}\left(\mathbf{X_n}; m, \theta, \frac{1}{2}, 0\right) = 0.$$

To check the stability we calculate the eigenvalues of the Jacobian matrix using

$$\begin{aligned}
\frac{\partial}{\partial X_{1,1}^{(n)}} F_{1,1}\left(\mathbf{X_n}; m, \theta, \frac{1}{2}, 0\right) =& \frac{(1-x)m^2}{1+\theta}(Q_{1,1}^{(n)})^{m-1} + \frac{xm^2}{1+\theta}(1-Q_{1,1}^{(n)})^{m-1} - m = Z_1 - m,\\
\frac{\partial}{\partial X_{2,1}^{(n)}} F_{1,1}\left(\mathbf{X_n}; m, \theta, \frac{1}{2}, 0\right) =& \frac{(1-x)\theta m^2}{1+\theta}(Q_{1,1}^{(n)})^{m-1} + \frac{x\theta m^2}{1+\theta}(1-Q_{1,1}^{(n)})^{m-1} = \theta Z_1,\\
\frac{\partial}{\partial X_{1,1}^{(n)}} F_{2,1}\left(\mathbf{X_n}; m, \theta, \frac{1}{2}, 0\right) =& \frac{(1-x)\theta m^2}{1+\theta}(Q_{2,1}^{(n)})^{m-1} + \frac{x\theta m^2}{1+\theta}(1-Q_{2,1}^{(n)})^{m-1} = \theta Z_2,\\
\frac{\partial}{\partial X_{2,1}^{(n)}} F_{2,1}\left(\mathbf{X_n}; m, \theta, \frac{1}{2}, 0\right) =& \frac{(1-x)m^2}{1+\theta}(Q_{2,1}^{(n)})^{m-1} + \frac{xm^2}{1+\theta}(1-Q_{2,1}^{(n)})^{m-1} - m = Z_2 - m.
\end{aligned}$$

By solving

$$\det\begin{vmatrix} Z_1 - m - \lambda & \theta Z_1 \\ \theta Z_2 & Z_2 - m - \lambda \end{vmatrix} = 0$$

we find the pair of eigenvalues as

$$\lambda = \frac{1}{2}(Z_1 + Z_2) - m \pm \frac{1}{2}\sqrt{(Z_1 - Z_2)^2 + 4Z_1 Z_2 \theta^2}.$$

These eigenvalues evaluated at $\left(\frac{1}{2}, 0, \frac{1}{2}, 0\right)$ result in $\lambda^+ = m(m(1-x)-1)$. We have $\lambda^+ < 0$ when $m \in \left(0, \frac{1}{1-x}\right)$. For $\lambda^- = m\left(\frac{m(1-x)(1-\theta)}{1+\theta} - 1\right)$ it follows that $\lambda^- < 0$ when $m \in \left(0, \frac{1+\theta}{(1-x)(1-\theta)}\right)$.

By evaluating our eigenvalues at $\left(0, \frac{1}{2}, 0, \frac{1}{2}\right)$ we have that $\lambda^+ = m(mx-1)$. Hence $\lambda^+ < 0$ holds true when $m \in \left(0, \frac{1}{x}\right)$. As $\lambda^- = m\left(\frac{mx(1-\theta)}{1+\theta} - 1\right)$ we solve $\lambda^- < 0$ to see that if $m \in \left(0, \frac{1+\theta}{x(1-\theta)}\right)$ then $\lambda^- < 0$.

For $\left(\frac{1}{2}, 0, \frac{1}{2}, 0\right)$ as $\theta \in (0,1)$ and $\frac{1+\theta}{1-\theta} > 1$ we see that $\frac{(1+\theta)}{(1-x)(1-\theta)} > \frac{1}{1-x}$ so the condition on λ^+ dominates. A similar result are found for $\left(0, \frac{1}{2}, 0, \frac{1}{2}\right)$ in that $m \in \left(0, \frac{1}{x}\right)$ dominates. □

6.3.2.1 *Coin flip model with $m = 3$, $x = \frac{1}{2}$*

We examine the coin flip model for the smallest value of m for which interesting results are expected, $m = 3$. We formulate the appropriate equations as:

$$F_{1,1}\left(\mathbf{X_n}; 3, \theta, \frac{1}{2}, 0\right) = \frac{3}{4}\left(Q_{1,1}^{(n)}\right)\left(2\left(Q_{1,1}^{(n)}\right)^2 - 3Q_{1,1}^{(n)} + 3\right) - 3X_{1,1}^{(n)}$$

and

$$F_{2,1}\left(\mathbf{X_n}; 3, \theta, \frac{1}{2}, 0\right) = \frac{3}{4}\left(Q_{2,1}^{(n)}\right)\left(2\left(Q_{2,1}^{(n)}\right)^2 - 3Q_{2,1}^{(n)} + 3\right) - 3X_{2,1}^{(n)}.$$

We solve this pair equal to zero using MatLab to attain the following table of solutions where the numbering in the left hand column are used throughout this section.

	$X_{1,1}$	$X_{2,1}$
1)	0	0
2)	$\frac{1}{2}$	$\frac{1}{2}$
3)	$\frac{1}{4}$	$\frac{1}{4}$
4)	$\frac{1}{4} - \frac{1}{4}\frac{1+\theta}{1-\theta}\sqrt{\frac{1+7\theta}{1-\theta}}$	$\frac{1}{4} + \frac{1}{4}\frac{1+\theta}{1-\theta}\sqrt{\frac{1+7\theta}{1-\theta}}$
5)	$\frac{1}{4} + \frac{1}{4}\frac{1+\theta}{1-\theta}\sqrt{\frac{1+7\theta}{1-\theta}}$	$\frac{1}{4} - \frac{1}{4}\frac{1+\theta}{1-\theta}\sqrt{\frac{1+7\theta}{1-\theta}}$
6)	$\frac{1}{4} - \alpha$	$\frac{1}{4} - \beta$
7)	$\frac{1}{4} + \alpha$	$\frac{1}{4} + \beta$
8)	$\frac{1}{4} - \beta$	$\frac{1}{4} - \alpha$
9)	$\frac{1}{4} + \beta$	$\frac{1}{4} + \alpha$

Tab. 6.1: A complete set of solutions to the coin flip model for $m = 3$, $\mu = \frac{1}{2}$ and $x = \frac{1}{2}$.

The components of our solutions are given by

$$\alpha = \frac{\sqrt{2}}{4}\sqrt{\frac{S+T(\theta^2-1)}{U}} \text{ and } \beta = \frac{\sqrt{2}}{4}\sqrt{\frac{S-T(\theta^2-1)}{U}}$$

for

$$S = 1+3\theta-15\theta^2+3\theta^3,\ U=(1-\theta)^3 \text{ and } T=\sqrt{(-55\theta^2+6\theta+1)}.$$

We use Table 6.1 and equations (6.11) to formulate a corresponding table of $Q_{1,1}^{(n)}$ and $Q_{2,1}^{(n)}$ values found in Table 6.2.

	$Q_{1,1}$	$Q_{2,1}$
1)	0	0
2)	1	1
3)	$\frac{1}{2}$	$\frac{1}{2}$
4)	$\frac{1}{2}-\frac{1}{2}\sqrt{\frac{1+7\theta}{1-\theta}}$	$\frac{1}{2}+\frac{1}{2}\sqrt{\frac{1+7\theta}{1-\theta}}$
5)	$\frac{1}{2}+\frac{1}{2}\sqrt{\frac{1+7\theta}{1-\theta}}$	$\frac{1}{2}-\frac{1}{2}\sqrt{\frac{1+7\theta}{1-\theta}}$
6)	$\frac{1}{2}-\frac{\sqrt{2}}{4(1+\theta)}(\alpha+\theta\beta)$	$\frac{1}{2}-\frac{\sqrt{2}}{4(1+\theta)}(\theta\alpha+\beta)$
7)	$\frac{1}{2}+\frac{\sqrt{2}}{4(1+\theta)}(\alpha+\theta\beta)$	$\frac{1}{2}+\frac{\sqrt{2}}{4(1+\theta)}(\theta\alpha+\beta)$
8)	$\frac{1}{2}-\frac{\sqrt{2}}{4(1+\theta)}(\beta+\theta\alpha)$	$\frac{1}{2}-\frac{\sqrt{2}}{4(1+\theta)}(\theta\beta+\alpha)$
9)	$\frac{1}{2}+\frac{\sqrt{2}}{4(1+\theta)}(\beta+\theta\alpha)$	$\frac{1}{2}+\frac{\sqrt{2}}{4(1+\theta)}(\theta\beta+\alpha)$

Tab. 6.2: The corresponding set of $Q_{1,1}$ and $Q_{2,1}$ values for each of the solutions found in Table 6.1.

The stability conditions of the three trivial solutions (1-3) are given by the following table.

	$X_{1,1}$	$X_{2,1}$	$Q_{1,1}$	$Q_{2,1}$	λ^+	$\lambda^+<0$	λ^-	$\lambda^-<0$
1)	0	0	0	0	$\frac{3}{2}$	never	$\frac{9}{2}\left(\frac{1-\theta}{1+\theta}\right)-3$	$\frac{1}{5}<\theta$
2)	$\frac{1}{2}$	$\frac{1}{2}$	1	1	$\frac{3}{2}$	never	$\frac{9}{2}\left(\frac{1-\theta}{1+\theta}\right)-3$	$\frac{1}{5}<\theta$
3)	$\frac{1}{4}$	$\frac{1}{4}$	$\frac{1}{2}$	$\frac{1}{2}$	$-\frac{3}{4}$	always	$\frac{9}{4}\left(\frac{1-\theta}{1+\theta}\right)-3$	always

Tab. 6.3: Stability conditions for the trivial solutions to the coin flip model where $m=3$, $\mu_1=\frac{1}{2}$ and $x=\frac{1}{2}$.

Here we see that neither (1) and (2) are stable due to λ^+. For any $\theta \in [0,1]$ the solution $\left(\frac{1}{4}, \frac{1}{4}, \frac{1}{4}, \frac{1}{4}\right)$ is stable with respect to both eigenvalues. By applying Theorem 2.16 from [Pem07] we conclude $\left(\frac{1}{4}, \frac{1}{4}, \frac{1}{4}, \frac{1}{4}\right)$ is a possible limit for the stochastic process. The pair of solutions given by (4) and (5) of Table 6.1 as

$$\left(\frac{1}{4} - \frac{1}{4}\sqrt{\frac{1+7\theta}{1-\theta}}, \frac{1}{4} + \frac{1}{4}\sqrt{\frac{1+7\theta}{1-\theta}}\right) \text{ and } \left(\frac{1}{4} + \frac{1}{4}\sqrt{\frac{1+7\theta}{1-\theta}}, \frac{1}{4} - \frac{1}{4}\sqrt{\frac{1+7\theta}{1-\theta}}\right)$$

are not viable solutions for our limiting proportions as $\sqrt{\frac{1+7\theta}{1-\theta}} > 1$ for all $\theta \in [0,1]$. Similarly solutions (6-9) are infeasible proportions of edge mass as there is no value $\theta \in [0,1]$ where both α or β satisfy $\alpha, \beta \in \left[0, \frac{1}{4}\right]$. This can be seen from Figure 6.1 below.

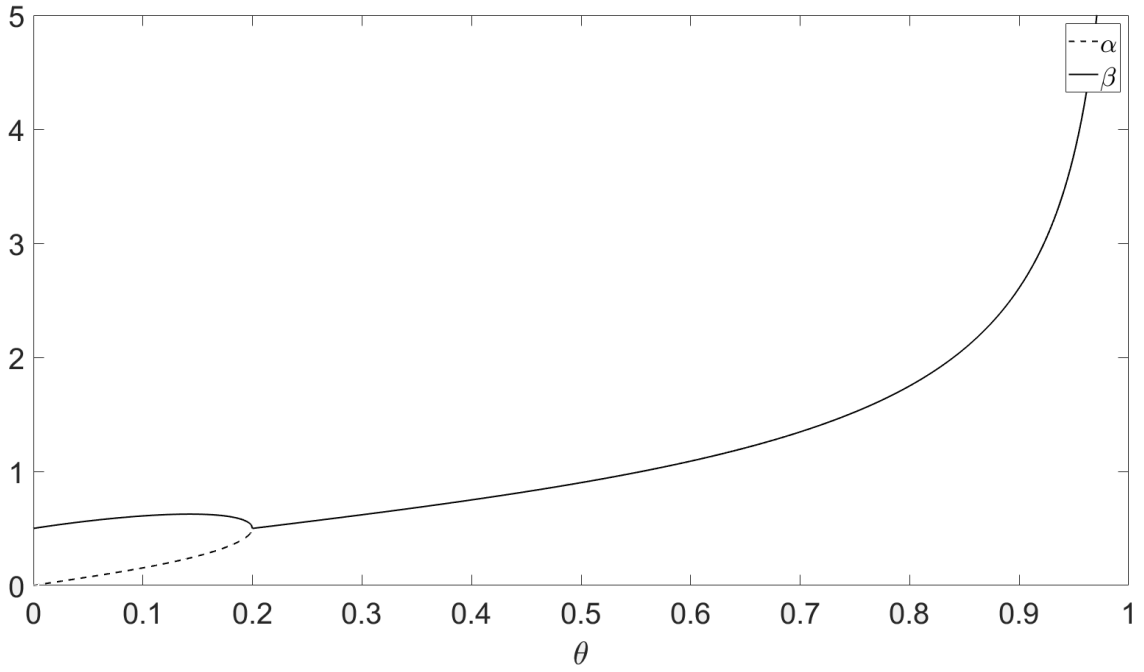

Fig. 6.1: A plot of α and β for $\theta \in [0,1]$ showing that there is no value of θ for which both $\alpha, \beta \in \left[0, \frac{1}{4}\right]$ simultaneously.

From analysing the stability conditions of the $m = 3$ coin flip model it is observable

there is only one stable limiting proportion. This is where all four proportions are equal in the limit.

6.3.3 Majority wins model

The majority wins model described by the vector $\rho = (0, 0, ..., 1, 1)$ specifies the type which v_{n+1} is assigned as the dominant type from the m vertices v_{n+1} is adjacent to. This selection criteria is expressed by

$$\rho_k = \begin{cases} 0, & \text{if } k = 0, 1, ..., \frac{m-1}{2}, \\ 1, & \text{if } k = \frac{m+1}{2}, \frac{m+3}{2}, ..., m, \end{cases}$$

if m is odd, and

$$\rho_k = \begin{cases} 0, & \text{if } k = 0, 1, ..., \frac{m}{2} - 1, \\ \frac{1}{2}, & \text{if } k = \frac{m}{2}, \\ 1, & \text{if } k = \frac{m}{2} + 1, \frac{m}{2} + 2, ..., m, \end{cases}$$

if m is even. Due to the complexity of this model we look into some specific values of m. There is no need to evaluate the $m = 2$ case in this context as in this situation the coin flip, majority wins and linear models all produce the same outcome. Using equations found in Section 6.3 we formulate the appropriate functions required to describe the associated four dimensional model as follows

$$F_{i,1}\left(\mathbf{X_n}; m, \theta, \frac{1}{2}, 0\right) = \begin{cases} -mX_{i,1}^{(n)} + \frac{m}{2}\sum_{k=\frac{m}{2}+1}^{m}\binom{m}{k}\left(Q_{i,1}^{(n)}\right)^k\left(1-Q_{i,1}^{(n)}\right)^{m-k} & \text{if } m \text{ even} \\ +\frac{m}{4}\binom{m}{m/2}\left(Q_{i,1}^{(n)}\right)^{\frac{m}{2}}\left(1-Q_{i,1}^{(n)}\right)^{\frac{m}{2}}, & \\ -mX_{i,1}^{(n)} + \frac{m}{2}\sum_{k=\frac{m+1}{2}}^{m}\binom{m}{k}\left(Q_{i,1}^{(n)}\right)^k\left(1-Q_{i,1}^{(n)}\right)^{m-k}, & \text{if } m \text{ odd.} \end{cases}$$

Theorem 6.3.5. *For any $s \in \mathbb{N}$ such that $s \geq 2$ it follows that*

$$F_{i,1}\left(\mathbf{X_n}; 2s, \theta, \frac{1}{2}, 0\right) = \frac{2s}{2s-1}F_{i,1}\left(\mathbf{X_n}; 2s-1, \theta, \frac{1}{2}, 0\right).$$

Proof. We prove this by calculating the difference between the two sides.

$$
\begin{aligned}
&(2s-1)F_{i,1}\left(\mathbf{X_n};2s,\theta,\frac{1}{2},0\right)-(2s)F_{i,1}\left(\mathbf{X_n};2s-1,\theta,\frac{1}{2},0\right)=\\
=&(2s-1)\left(-2sX_{i,1}^{(n)}+\frac{s}{2}\binom{2s}{s}\left(Q_{i,1}^{(n)}\right)^{s}\left(1-\left(Q_{i,1}^{(n)}\right)\right)^{s}+\left(s\sum_{k=s+1}^{2s-1}\binom{2s}{k}\left(Q_{i,1}^{(n)}\right)^{k}\left(1-\left(Q_{i,1}^{(n)}\right)\right)^{2s-k}\right)\right)\\
&-(2s)\left(-(2s-1)X+\frac{2s-1}{2}\sum_{k=s}^{2s-1}\binom{2s-1}{k}\left(Q_{i,1}^{(n)}\right)^{k}\left(1-Q_{i,1}^{(n)}\right)^{2s-1-k}\right)\\
=&s(2s-1)\left(\sum_{k=s+1}^{2s}\binom{2s}{k}\left(Q_{i,1}^{(n)}\right)^{k}\left(1-Q_{i,1}^{(n)}\right)^{2s-k}-\sum_{k=s}^{2s-1}\binom{2s-1}{k}\left(Q_{i,1}^{(n)}\right)^{k}\left(1-Q_{i,1}^{(n)}\right)^{2s-1-k}\right)\\
&+\frac{s(2s-1)}{2}\binom{2s}{s}\left(Q_{i,1}^{(n)}\right)^{s}\left(1-Q_{i,1}^{(n)}\right)^{s}\\
=&s(2s-1)\sum_{k=s}^{2s-1}\binom{2s-1}{k}\left(Q_{i,1}^{(n)}\right)^{k}\left(1-Q_{i,1}^{(n)}\right)^{2s-1-k}\left(\frac{k-2sQ_{i,1}^{(n)}}{2s-k}\right)\\
&+s(2s-1)\left(\left(Q_{i,1}^{(n)}\right)^{2s}-\frac{1}{2}\binom{2s}{s}\left(Q_{i,1}^{(n)}\right)^{s}\left(1-Q_{i,1}^{(n)}\right)^{s}\right)\\
=&s(2s-1)\left(Q_{i,1}^{(n)}\right)^{s}\left(1-Q_{i,1}^{(n)}\right)^{s}\left(\binom{2s-1}{s}-\frac{1}{2}\binom{2s}{s}\right)=0
\end{aligned}
$$

completing the proof. □

Theorem 6.3.5 links the odd and even case meaning we simply require a minor alteration to the odd cases to infer the solutions to the even cases.

6.3.3.1 *Majority wins model with $m = 3$*

We calculate the appropriate functions for the majority wins $m = 3$ case as

$$
\begin{aligned}
F_{1,1}\left(\mathbf{X_n};3,\theta,\frac{1}{2},0\right)&=-3X_{1,1}^{(n)}-3\left(Q_{1,1}^{(n)}\right)^{3}+\frac{9}{2}\left(Q_{1,1}^{(n)}\right)^{2} \qquad (6.13)\\
F_{2,1}\left(\mathbf{X_n};3,\theta,\frac{1}{2},0\right)&=-3X_{2,1}^{(n)}-3\left(Q_{2,1}^{(n)}\right)^{3}+\frac{9}{2}\left(Q_{2,1}^{(n)}\right)^{2}
\end{aligned}
$$

where the solution set is restricted to Y. For simplicity we let

$$\begin{aligned} S &= 3\theta^3 - 9\theta^2 + 3\theta - 1, \\ R &= (\theta - 1)\sqrt{-(7\theta - 1)(\theta + 1)^3}, \\ T &= 2\theta(2\theta^2 - 3\theta + 3), \\ U &= (\theta - 1)^3. \end{aligned}$$

Using MatLab we solved

$$F_{1,1}\left(\mathbf{X_n}; 3, \theta, \frac{1}{2}, 0\right) = F_{2,1}\left(\mathbf{X_n}; 3, \theta, \frac{1}{2}, 0\right) = 0$$

summarizing the solutions in Table 6.13.

	$X_{1,1}$	$X_{2,1}$
1)	$\frac{1}{4} + \frac{(\theta+1)\sqrt{5\theta-1}}{4(\theta-1)\sqrt{\theta-1}}$	$\frac{1}{4} - \frac{(\theta+1)\sqrt{5\theta-1}}{4(\theta-1)\sqrt{\theta-1}}$
2)	$\frac{1}{4} - \frac{(\theta+1)\sqrt{5\theta-1}}{4(\theta-1)\sqrt{\theta-1}}$	$\frac{1}{4} + \frac{(\theta+1)\sqrt{5\theta-1}}{4(\theta-1)\sqrt{\theta-1}}$
3)	0	0
4)	$\frac{1}{2}$	$\frac{1}{2}$
5)	$\frac{1}{4}$	$\frac{1}{4}$
6)	$\frac{1}{4} + \frac{\sqrt{2}(S+R)}{8T}\sqrt{\frac{S-R}{U}}$	$\frac{1}{4} - \frac{\sqrt{2}}{8}\sqrt{\frac{S-R}{U}}$
7)	$\frac{1}{4} - \frac{\sqrt{2}(S+R)}{8T}\sqrt{\frac{S-R}{U}}$	$\frac{1}{4} + \frac{\sqrt{2}}{8}\sqrt{\frac{S-R}{U}}$
8)	$\frac{1}{4} + \frac{\sqrt{2}(S-R)}{8T}\sqrt{\frac{S+R}{U}}$	$\frac{1}{4} - \frac{\sqrt{2}}{8}\sqrt{\frac{S+R}{U}}$
9)	$\frac{1}{4} - \frac{\sqrt{2}(S-R)}{8T}\sqrt{\frac{S+R}{U}}$	$\frac{1}{4} + \frac{\sqrt{2}}{8}\sqrt{\frac{S+R}{U}}$

Tab. 6.4: A complete set of solutions to the stochastic approximation equations given by equations (6.13) describing the $m = 3$ majority wins model.

Lemma 6.3.6. *For any $\theta \in [0, 1]$ it is true that*

$$\sqrt{\frac{S^2 - R^2}{T^2}} = 1.$$

Proof.

$$\sqrt{\frac{S^2-R^2}{T^2}} = \sqrt{\frac{(3\theta^3-9\theta^2+3\theta-1)^2-\left((\theta-1)\sqrt{-(7\theta-1)(\theta+1)^3}\right)^2}{4\theta^2(2\theta^2-3\theta+3)^2}}$$
$$= \sqrt{\frac{4\theta^2\left(4\theta^4-12\theta^3+21\theta^2-18\theta+9\right)}{4\theta^2(2\theta^2-3\theta+3)^2}} = 1.$$

□

We apply Lemma 6.3.6 to simplify entries contained in Table 6.4 forming Table 6.5.

	$X_{1,1}$	$X_{2,1}$
1)	$\frac{1}{4}+\frac{(\theta+1)}{4(\theta-1)}\sqrt{\frac{5\theta-1}{\theta-1}}$	$\frac{1}{4}-\frac{(\theta+1)}{4(\theta-1)}\sqrt{\frac{5\theta-1}{\theta-1}}$
2)	$\frac{1}{4}-\frac{(\theta+1)}{4(\theta-1)}\sqrt{\frac{5\theta-1}{\theta-1}}$	$\frac{1}{4}+\frac{(\theta+1)}{4(\theta-1)}\sqrt{\frac{5\theta-1}{\theta-1}}$
3)	0	0
4)	$\frac{1}{2}$	$\frac{1}{2}$
5)	$\frac{1}{4}$	$\frac{1}{4}$
6)	$\frac{1}{4}+\frac{\sqrt{2}}{8}\sqrt{\frac{S+R}{U}}$	$\frac{1}{4}-\frac{\sqrt{2}}{8}\sqrt{\frac{S-R}{U}}$
7)	$\frac{1}{4}-\frac{\sqrt{2}}{8}\sqrt{\frac{S+R}{U}}$	$\frac{1}{4}+\frac{\sqrt{2}}{8}\sqrt{\frac{S-R}{U}}$
8)	$\frac{1}{4}+\frac{\sqrt{2}}{8}\sqrt{\frac{S-R}{U}}$	$\frac{1}{4}-\frac{\sqrt{2}}{8}\sqrt{\frac{S+R}{U}}$
9)	$\frac{1}{4}-\frac{\sqrt{2}}{8}\sqrt{\frac{S-R}{U}}$	$\frac{1}{4}+\frac{\sqrt{2}}{8}\sqrt{\frac{S+R}{U}}$

Tab. 6.5: Simplified entries found in Table 6.4 containing solutions to the approximation equations relating to the majority wins model with $m = 3$.

Similarly as to previous sections, we use the stability matrix formed from equations (6.13)

$$\det\begin{vmatrix} \frac{18Q_{1,1}^{(n)}}{1+\theta}\left(1-Q_{1,1}^{(n)}\right)-\lambda-3 & \frac{18\theta Q_{1,1}^{(n)}}{1+\theta}\left(1-Q_{1,1}^{(n)}\right) \\ \frac{18\theta Q_{2,1}^{(n)}}{1+\theta}\left(1-Q_{2,1}^{(n)}\right) & \frac{18Q_{2,1}^{(n)}}{1+\theta}\left(1-Q_{2,1}^{(n)}\right)-\lambda-3 \end{vmatrix} = 0 \tag{6.14}$$

to identify the stability conditions associated to each of the solutions found in Table 6.5. By using (6.14) we find the appropriate eigenvalues of our the majority wins model with $m = 3$ as

$$\lambda = -3 + \frac{9}{1+\theta}\left(J \pm \sqrt{J^2 - 4K}\right) \tag{6.15}$$

where

$$J = Q_{1,1}\left(1 - Q_{1,1}\right) + Q_{2,1}\left(1 - Q_{2,1}\right)$$

and

$$K = Q_{1,1}Q_{2,1}\left(1 - Q_{1,1}\right)\left(1 - Q_{2,1}\right)\left(1 - \theta^2\right).$$

Lemma 6.3.7. *For any $\theta \in (0,1)$ both solutions $(0, \frac{1}{2}, 0, \frac{1}{2})$ and $(\frac{1}{2}, 0, \frac{1}{2}, 0)$ are stable whereas $(\frac{1}{4}, \frac{1}{4}, \frac{1}{4}, \frac{1}{4})$ is unstable.*

Proof. Using the values in Table 6.5 and the eigenvalues found in (6.15) we generate the following table:

	$X_{1,1}$	$X_{2,1}$	$Q_{1,1}$	$Q_{2,1}$	λ^+	$\lambda^+ < 0$	λ^-	$\lambda^- < 0$
3)	0	0	0	0	-3	always	-3	always
4)	$\frac{1}{2}$	$\frac{1}{2}$	1	1	-3	always	-3	always
5)	$\frac{1}{4}$	$\frac{1}{4}$	$\frac{1}{2}$	$\frac{1}{2}$	$\frac{3}{2}$	never	$\frac{3}{2} - \frac{9\theta}{1+\theta}$	$\frac{1}{5} < \theta$

We see from rows one and two that the eigenvalues for $(0, \frac{1}{2}, 0, \frac{1}{2})$ and $(\frac{1}{2}, 0, \frac{1}{2}, 0)$ are both always negative. We see from table that λ^+ for (5) is always positive. Therefore, we conclude that $(0, \frac{1}{2}, 0, \frac{1}{2})$ and $(\frac{1}{2}, 0, \frac{1}{2}, 0)$ are stable points and $(\frac{1}{4}, \frac{1}{4}, \frac{1}{4}, \frac{1}{4})$ is unstable. □

Lemma 6.3.8. *For $\theta \in (0,1)$ the two solutions to (6.13) described by (1) and (2) from Table 6.5 are stable when $\theta \in \left[0, \frac{1}{7}\right)$ and unstable when $\theta > \frac{1}{7}$.*

Proof. We begin our proof by using (1) to calculate

$$Q_{1,1} = \frac{1}{2} - \frac{1}{2}\sqrt{\frac{1-5\theta}{1-\theta}} \text{ and } Q_{2,1} = \frac{1}{2} + \frac{1}{2}\sqrt{\frac{1-5\theta}{1-\theta}}.$$

We see by observation that both $Q_{1,1}$ and $Q_{2,1}$ are real and in the interval $[0,1]$ when $\theta \in \left[0, \frac{1}{5}\right]$. Using these we evaluate the separate components of our eigenvalues as

$$J = 2Q_{1,1}Q_{2,1} \text{ and } K = (1-\theta^2)\left(Q_{1,1}\right)^2\left(Q_{2,1}\right)^2.$$

By putting these components together we formulate our eigenvalues in the form

$$\lambda = -3 + \frac{18\theta}{(1-\theta)(1+\theta)}(1 \pm \theta)$$

We deduce the conditions necessary to impose on θ to ensure stability given by

$$\lambda^+ : 0 > -3 + \frac{18\theta}{(1-\theta)} \implies \frac{1}{7} > \theta,$$
$$\lambda^- : 0 > -3 + \frac{18\theta}{(1+\theta)} \implies \frac{1}{5} > \theta.$$

We conclude that λ^+ and λ^- are both negative simultaneously for $\theta \in \left[0, \frac{1}{7}\right)$. Finally, using Theorem 2.17 of [Pem07] we conclude that non-convergence occurs when $\theta > \frac{1}{7}$. □

Lemma 6.3.8 outlines the possibility of two different behaviours in the two different communities in the majority wins model when $\theta < \frac{1}{7}$. This seems to not be the case, based on the stability criteria, for the majority wins model when $\theta > \frac{1}{7}$, the linear model or the coin flip models.

Definition 6.3.9. *For two column vectors* $[a] = [a_1, a_2, ..., a_k]^T$ *and* $[b] = [b_1, b_2, ..., b_k]^T$*; we define array multiplication as* $[a][b] = [a_1b_1, a_2b_2, ..., a_kb_k]^T$ *and array addition as* $[a]+[b] = [a_1+b_1, a_2+b_2, ..., a_k+b_k]^T$*. Similar identities can be defined for subtraction and division.*

Lemma 6.3.10. *For $\theta \in [0,1]$, none of the solutions to (6.13) given by the following table are stable*

	$X_{1,1}$	$X_{2,1}$	$Q_{1,1}$	$Q_{2,1}$
6)	$\frac{1}{4}+\frac{\sqrt{2}}{8}\alpha$	$\frac{1}{4}-\frac{\sqrt{2}}{8}\beta$	$\frac{1}{2}+\frac{\sqrt{2}}{4(1+\theta)}(\alpha-\beta\theta)$	$\frac{1}{2}+\frac{\sqrt{2}}{4(1+\theta)}(\alpha\theta-\beta)$
7)	$\frac{1}{4}-\frac{\sqrt{2}}{8}\alpha$	$\frac{1}{4}+\frac{\sqrt{2}}{8}\beta$	$\frac{1}{2}-\frac{\sqrt{2}}{4(1+\theta)}(\alpha-\beta\theta)$	$\frac{1}{2}-\frac{\sqrt{2}}{4(1+\theta)}(\alpha\theta-\beta)$
8)	$\frac{1}{4}+\frac{\sqrt{2}}{8}\beta$	$\frac{1}{4}-\frac{\sqrt{2}}{8}\alpha$	$\frac{1}{2}+\frac{\sqrt{2}}{4(1+\theta)}(-\alpha\theta+\beta)$	$\frac{1}{2}+\frac{\sqrt{2}}{4(1+\theta)}(-\alpha+\beta\theta)$
9)	$\frac{1}{4}-\frac{\sqrt{2}}{8}\beta$	$\frac{1}{4}+\frac{\sqrt{2}}{8}\alpha$	$\frac{1}{2}-\frac{\sqrt{2}}{4(1+\theta)}(-\alpha\theta+\beta)$	$\frac{1}{2}-\frac{\sqrt{2}}{4(1+\theta)}(-\alpha+\beta\theta)$

such that $\alpha = \sqrt{\frac{S+R}{U}}$ *and* $\beta = \sqrt{\frac{S-R}{U}}$.

Proof. We begin by calculating the components of our eigenvalues, starting with J.

$$J = \begin{bmatrix} \frac{1}{2}+\frac{\sqrt{2}}{4(1+\theta)}\left(\sqrt{\frac{S+R}{U}}-\sqrt{\frac{S-R}{U}}\theta\right) \\ \frac{1}{2}-\frac{\sqrt{2}}{4(1+\theta)}\left(\sqrt{\frac{S+R}{U}}-\sqrt{\frac{S-R}{U}}\theta\right) \\ \frac{1}{2}+\frac{\sqrt{2}}{4(1+\theta)}\left(-\sqrt{\frac{S+R}{U}}\theta+\sqrt{\frac{S-R}{U}}\right) \\ \frac{1}{2}-\frac{\sqrt{2}}{4(1+\theta)}\left(-\sqrt{\frac{S+R}{U}}\theta+\sqrt{\frac{S-R}{U}}\right) \end{bmatrix} \begin{bmatrix} \frac{1}{2}-\frac{\sqrt{2}}{4(1+\theta)}\left(\sqrt{\frac{S+R}{U}}-\sqrt{\frac{S-R}{U}}\theta\right) \\ \frac{1}{2}+\frac{\sqrt{2}}{4(1+\theta)}\left(\sqrt{\frac{S+R}{U}}-\sqrt{\frac{S-R}{U}}\theta\right) \\ \frac{1}{2}-\frac{\sqrt{2}}{4(1+\theta)}\left(-\sqrt{\frac{S+R}{U}}\theta+\sqrt{\frac{S-R}{U}}\right) \\ \frac{1}{2}+\frac{\sqrt{2}}{4(1+\theta)}\left(-\sqrt{\frac{S+R}{U}}\theta+\sqrt{\frac{S-R}{U}}\right) \end{bmatrix} +$$

$$\begin{bmatrix} \frac{1}{2}+\frac{\sqrt{2}}{4(1+\theta)}\left(\sqrt{\frac{S+R}{U}}\theta-\sqrt{\frac{S-R}{U}}\right) \\ \frac{1}{2}-\frac{\sqrt{2}}{4(1+\theta)}\left(\sqrt{\frac{S+R}{U}}\theta-\sqrt{\frac{S-R}{U}}\right) \\ \frac{1}{2}+\frac{\sqrt{2}}{4(1+\theta)}\left(-\sqrt{\frac{S+R}{U}}+\sqrt{\frac{S-R}{U}}\theta\right) \\ \frac{1}{2}-\frac{\sqrt{2}}{4(1+\theta)}\left(-\sqrt{\frac{S+R}{U}}+\sqrt{\frac{S-R}{U}}\theta\right) \end{bmatrix} \begin{bmatrix} \frac{1}{2}-\frac{\sqrt{2}}{4(1+\theta)}\left(\sqrt{\frac{S+R}{U}}\theta-\sqrt{\frac{S-R}{U}}\right) \\ \frac{1}{2}+\frac{\sqrt{2}}{4(1+\theta)}\left(\sqrt{\frac{S+R}{U}}\theta-\sqrt{\frac{S-R}{U}}\right) \\ \frac{1}{2}-\frac{\sqrt{2}}{4(1+\theta)}\left(-\sqrt{\frac{S+R}{U}}+\sqrt{\frac{S-R}{U}}\theta\right) \\ \frac{1}{2}+\frac{\sqrt{2}}{4(1+\theta)}\left(-\sqrt{\frac{S+R}{U}}+\sqrt{\frac{S-R}{U}}\theta\right) \end{bmatrix}$$

$$J = \begin{bmatrix} \frac{1}{2}-\frac{\left(\sqrt{\frac{S+R}{U}}-\sqrt{\frac{S-R}{U}}\theta\right)^2+\left(\sqrt{\frac{S+R}{U}}\theta-\sqrt{\frac{S-R}{U}}\right)^2}{8(1+\theta)^2} \\ \frac{1}{2}-\frac{\left(\sqrt{\frac{S+R}{U}}-\sqrt{\frac{S-R}{U}}\theta\right)^2+\left(\sqrt{\frac{S+R}{U}}\theta-\sqrt{\frac{S-R}{U}}\right)^2}{8(1+\theta)^2} \\ \frac{1}{2}-\frac{\left(\sqrt{\frac{S+R}{U}}-\sqrt{\frac{S-R}{U}}\theta\right)^2+\left(\sqrt{\frac{S+R}{U}}\theta-\sqrt{\frac{S-R}{U}}\right)^2}{8(1+\theta)^2} \\ \frac{1}{2}-\frac{\left(\sqrt{\frac{S+R}{U}}-\sqrt{\frac{S-R}{U}}\theta\right)^2+\left(\sqrt{\frac{S+R}{U}}\theta-\sqrt{\frac{S-R}{U}}\right)^2}{8(1+\theta)^2} \end{bmatrix}$$

We see from here that all four solutions produced the same value of J simplified as

follows

$$\begin{aligned} J &= \frac{1}{2} - \frac{\left(\sqrt{\frac{S+R}{U}} - \sqrt{\frac{S-R}{U}}\theta\right)^2 + \left(\sqrt{\frac{S+R}{U}}\theta - \sqrt{\frac{S-R}{U}}\right)^2}{8\left(1+\theta\right)^2} \\ &= \frac{1}{2} - \frac{\left(\frac{S+R}{U} + \frac{S-R}{U}\right)\left(\theta^2+1\right) - 4\theta\sqrt{\frac{S+R}{U}}\sqrt{\frac{S-R}{U}}}{8(1+\theta)^2} \\ &= \frac{1}{2} - \frac{2S\left(\theta^2+1\right) + 4\theta\left(\sqrt{S^2-R^2}\right)}{8U(1+\theta)^2}. \end{aligned}$$

Applying Lemma 6.3.6, $\sqrt{S^2-R^2} = \sqrt{T^2}$ yields

$$\begin{aligned} J &= \frac{1}{2} - \frac{S\left(\theta^2+1\right) + 2\theta T}{4U(1+\theta)^2} \\ &= \frac{1}{2} - \frac{(\theta-1)^2(\theta+1)^2(3\theta-1)}{4(\theta-1)^3(1+\theta)^2} \\ &= \frac{1+\theta}{4(1-\theta)}. \end{aligned}$$

We compute K in a similar way:

$$K = \begin{bmatrix} \frac{1}{2} + \frac{\sqrt{2}}{4(1+\theta)}\left(\sqrt{\frac{S+R}{U}} - \sqrt{\frac{S-R}{U}}\theta\right) \\ \frac{1}{2} - \frac{\sqrt{2}}{4(1+\theta)}\left(\sqrt{\frac{S+R}{U}} - \sqrt{\frac{S-R}{U}}\theta\right) \\ \frac{1}{2} + \frac{\sqrt{2}}{4(1+\theta)}\left(-\sqrt{\frac{S+R}{U}}\theta + \sqrt{\frac{S-R}{U}}\right) \\ \frac{1}{2} - \frac{\sqrt{2}}{4(1+\theta)}\left(-\sqrt{\frac{S+R}{U}}\theta + \sqrt{\frac{S-R}{U}}\right) \end{bmatrix} \begin{bmatrix} \frac{1}{2} - \frac{\sqrt{2}}{4(1+\theta)}\left(\sqrt{\frac{S+R}{U}} - \sqrt{\frac{S-R}{U}}\theta\right) \\ \frac{1}{2} + \frac{\sqrt{2}}{4(1+\theta)}\left(\sqrt{\frac{S+R}{U}} - \sqrt{\frac{S-R}{U}}\theta\right) \\ \frac{1}{2} - \frac{\sqrt{2}}{4(1+\theta)}\left(-\sqrt{\frac{S+R}{U}}\theta + \sqrt{\frac{S-R}{U}}\right) \\ \frac{1}{2} + \frac{\sqrt{2}}{4(1+\theta)}\left(-\sqrt{\frac{S+R}{U}}\theta + \sqrt{\frac{S-R}{U}}\right) \end{bmatrix} \times$$

$$\begin{bmatrix} \frac{1}{2} + \frac{\sqrt{2}}{4(1+\theta)}\left(\sqrt{\frac{S+R}{U}}\theta - \sqrt{\frac{S-R}{U}}\right) \\ \frac{1}{2} - \frac{\sqrt{2}}{4(1+\theta)}\left(\sqrt{\frac{S+R}{U}}\theta - \sqrt{\frac{S-R}{U}}\right) \\ \frac{1}{2} + \frac{\sqrt{2}}{4(1+\theta)}\left(-\sqrt{\frac{S+R}{U}} + \sqrt{\frac{S-R}{U}}\theta\right) \\ \frac{1}{2} - \frac{\sqrt{2}}{4(1+\theta)}\left(-\sqrt{\frac{S+R}{U}} + \sqrt{\frac{S-R}{U}}\theta\right) \end{bmatrix} \begin{bmatrix} \frac{1}{2} - \frac{\sqrt{2}}{4(1+\theta)}\left(\sqrt{\frac{S+R}{U}}\theta - \sqrt{\frac{S-R}{U}}\right) \\ \frac{1}{2} + \frac{\sqrt{2}}{4(1+\theta)}\left(\sqrt{\frac{S+R}{U}}\theta - \sqrt{\frac{S-R}{U}}\right) \\ \frac{1}{2} - \frac{\sqrt{2}}{4(1+\theta)}\left(-\sqrt{\frac{S+R}{U}} + \sqrt{\frac{S-R}{U}}\theta\right) \\ \frac{1}{2} + \frac{\sqrt{2}}{4(1+\theta)}\left(-\sqrt{\frac{S+R}{U}} + \sqrt{\frac{S-R}{U}}\theta\right) \end{bmatrix} (1-\theta^2)$$

which simplifies to

$$K(\theta) = (1-\theta^2)\begin{bmatrix} \frac{1}{4} - \frac{\left(\sqrt{\frac{S+R}{U}} - \sqrt{\frac{S-R}{U}}\theta\right)^2}{8(1+\theta)^2} \\ \frac{1}{4} - \frac{\left(\sqrt{\frac{S+R}{U}} - \sqrt{\frac{S-R}{U}}\theta\right)^2}{8(1+\theta)^2} \\ \frac{1}{4} - \frac{\left(-\sqrt{\frac{S+R}{U}}\theta + \sqrt{\frac{S-R}{U}}\right)^2}{8(1+\theta)^2} \\ \frac{1}{4} - \frac{\left(-\sqrt{\frac{S+R}{U}}\theta + \sqrt{\frac{S-R}{U}}\right)^2}{8(1+\theta)^2} \end{bmatrix} \begin{bmatrix} \frac{1}{4} - \frac{\left(\sqrt{\frac{S+R}{U}}\theta - \sqrt{\frac{S-R}{U}}\right)^2}{8(1+\theta)^2} \\ \frac{1}{4} - \frac{\left(\sqrt{\frac{S+R}{U}}\theta - \sqrt{\frac{S-R}{U}}\right)^2}{8(1+\theta)^2} \\ \frac{1}{4} - \frac{\left(-\sqrt{\frac{S+R}{U}} + \sqrt{\frac{S-R}{U}}\theta\right)^2}{8(1+\theta)^2} \\ \frac{1}{4} - \frac{\left(-\sqrt{\frac{S+R}{U}} + \sqrt{\frac{S-R}{U}}\theta\right)^2}{8(1+\theta)^2} \end{bmatrix}.$$

This again reduces to the same equation. For $\alpha = \sqrt{\frac{S+R}{U}}$ and $\beta = \sqrt{\frac{S-R}{U}}$ we have

$$\begin{aligned} K &= (1-\theta^2)\left(\frac{1}{4} - \frac{(\alpha-\beta\theta)^2}{8(1+\theta)^2}\right)\left(\frac{1}{4} - \frac{(\alpha\theta-\beta)^2}{8(1+\theta)^2}\right) \\ &= (1-\theta^2)\left(\frac{1}{16} - \frac{(\alpha-\beta\theta)^2 + (\alpha\theta-\beta)^2}{32(1+\theta)^2} + \frac{(\alpha-\beta\theta)^2(\alpha\theta-\beta)^2}{64(1+\theta)^4}\right) \\ &= (1-\theta^2)\left(\frac{J}{4} - \frac{1}{16} + \frac{(\alpha-\beta\theta)^2(\alpha\theta-\beta)^2}{64(1+\theta)^4}\right) \\ &= (1-\theta^2)\left(\frac{1+\theta}{16(1-\theta)} - \frac{1}{16} + \frac{(\alpha-\beta\theta)^2(\alpha\theta-\beta)^2}{64(1+\theta)^4}\right). \end{aligned}$$

Using identities $\alpha\beta = -\sqrt{\frac{T^2}{U^2}} = -\frac{T}{U}$ and $\alpha^2 + \beta^2 = \frac{2S}{U}$ found in Lemma 6.3.7 we simplify this to

$$K = (1-\theta^2)\left(\frac{1+\theta}{16(1-\theta)} - \frac{1}{16} + \frac{\theta^2}{4(\theta-1)^2}\right) = \frac{\theta(\theta+1)^2}{2(1-\theta)}.$$

We formulate the appropriate eigenvalues as

$$\lambda = -3 + \frac{9}{1+\theta}\left(\frac{1+\theta}{4(1-\theta)} \pm \sqrt{\left(\frac{1+\theta}{4(1-\theta)}\right)^2 - \frac{\theta(\theta+1)^2}{2(1-\theta)}}\right),$$

which simplifies to give

$$0 > -3 + \frac{9}{4(1-\theta)}\left(1 \pm \sqrt{8\theta^2 - 8\theta + 1}\right)$$

which holds true for $\theta \in \left[\frac{2-\sqrt{2}}{4}, \frac{2+\sqrt{2}}{4}\right]$. For λ^+ we solve

$$\begin{aligned} \frac{1-4\theta}{3} &> \sqrt{8\theta^2 - 8\theta + 1} \\ -(7\theta - 1)(\theta - 1) &> 0. \end{aligned}$$

which is satisfied when $\theta \in \left(\frac{1}{7}, \frac{2-\sqrt{2}}{4}\right)$. The particular solutions $X_{1,1}^{(n)}$ and $X_{2,1}^{(n)}$ exist when $\theta \leq \frac{1}{7}$. Clearly this eigenvalue is never negative in the required domain leading to instability for all solutions in question. □

6.3.3.2 *Majority wins model with $m = 4$*

In order to examine the $m = 4$ case we utilize Theorem 6.3.5. This is not so important in the formulation of the approximation equations, but more so in the solving of them. Given the $m = 4$ case is merely a scaled $m = 3$ case they have the same solutions, found in Table 6.5. We use the equations associated to the $m = 3$ case

$$F_{1,1}\left(\mathbf{X_n}; 4, \theta, \frac{1}{2}, 0\right) = -4X_{1,1}^{(n)} - 4\left(Q_{1,1}^{(n)}\right)^3 + 6\left(Q_{1,1}^{(n)}\right)^2 = \frac{4}{3}F_{1,1}\left(\mathbf{X_n}; 3, \theta, \frac{1}{2}, 0\right)$$

and

$$F_{2,1}\left(\mathbf{X_n}; 4, \theta, \frac{1}{2}, 0\right) = -4X_{1,1}^{(n)} - 4\left(Q_{2,1}^{(n)}\right)^3 + 6\left(Q_{2,1}^{(n)}\right)^2 = \frac{4}{3}F_{2,1}\left(\mathbf{X_n}; 3, \theta, \frac{1}{2}, 0\right).$$

to calculate the associated eigenvalues using

$$\det \begin{vmatrix} \frac{24Q_{1,1}^{(n)}}{1+\theta}\left(1 - Q_{1,1}^{(n)}\right) - \lambda - 4 & \frac{24\theta Q_{1,1}^{(n)}}{1+\theta}\left(1 - Q_{1,1}^{(n)}\right) \\ \frac{24\theta Q_{2,1}^{(n)}}{1+\theta}\left(1 - Q_{2,1}^{(n)}\right) & \frac{24Q_{2,1}^{(n)}}{1+\theta}\left(1 - Q_{2,1}^{(n)}\right) - \lambda - 4 \end{vmatrix} = 0$$

as

$$\lambda\left(\mathbf{X_n}; 4, \theta, \frac{1}{2}, 0\right) = -4 + \frac{12}{1+\theta}\left(J \pm \sqrt{J^2 - 4K}\right) = \frac{4}{3}\lambda\left(\mathbf{X_n}; 3, \theta, \frac{1}{2}, 0\right).$$

It is therefore clear to see that due to a similar property given by Theorem 6.3.5 the same limiting proportions and stability conditions hold as were discussed in Section 6.3.3.1.

BIBLIOGRAPHY

[AMR16] Tonći Antunović, Elchanan Mossel, and Miklós Z Rácz. Coexistence in preferential attachment networks. *Combinatorics, Probability and Computing*, 25(6):797–822, 2016.

[AR03] K Austin and GJ Rodgers. Growing networks with two vertex types. *Physica A: Statistical Mechanics and its Applications*, 326(3-4):594–603, 2003.

[Arn15] Barry C Arnold. *Pareto Distributions Second Edition*. Chapman and Hall/CRC, 2015.

[BA99] Albert-László Barabási and Réka Albert. Emergence of scaling in random networks. *science*, 286(5439):509–512, 1999.

[BB01] Ginestra Bianconi and A-L Barabási. Competition and multiscaling in evolving networks. *EPL (Europhysics Letters)*, 54(4):436, 2001.

[BCDR07] Christian Borgs, Jennifer Chayes, Constantinos Daskalakis, and Sebastien Roch. First to market is not everything: an analysis of preferential attachment with fitness. In *Proceedings of the thirty-ninth annual ACM symposium on Theory of computing*, pages 135–144. ACM, 2007.

[BRST01] Béla Bollobás, Oliver Riordan, Joel Spencer, and Gábor Tusnády. The degree sequence of a scale-free random graph process. *Random Structures & Algorithms*, 18(3):279–290, 2001.

[CCL13] Andrea Collevecchio, Codina Cotar, and Marco LiCalzi. On a prefer-

ential attachment and generalized Pólya's urn model. *The Annals of Applied Probability*, 23(3):1219–1253, 2013.

[CDMG06] Fabio Clementi, Tiziana Di Matteo, and Mauro Gallegati. The power-law tail exponent of income distributions. *Physica A: Statistical Mechanics and its Applications*, 370(1):49–53, 2006.

[DM13] Steffen Dereich and Peter Mörters. Emergence of condensation in kingman's model of selection and mutation. *Acta Applicandae Mathematicae*, 127(1):17–26, 2013.

[DMM17] Steffen Dereich, Cécile Mailler, and Peter Mörters. Nonextensive condensation in reinforced branching processes. *The Annals of Applied Probability*, 27(4):2539–2568, 2017.

[DMS00] Sergey N Dorogovtsev, José Fernando F Mendes, and Alexander N Samukhin. Structure of growing networks with preferential linking. *Physical review letters*, 85(21):4633, 2000.

[DO14] Steffen Dereich and Marcel Ortgiese. Robust analysis of preferential attachment models with fitness. *Combinatorics, Probability and Computing*, 23(3):386–411, 2014.

[Dri08] John Drinane. Rate of convergence of Pólya's urn to the beta distribution. *Oregon State University*, 2008.

[ER59] P Erdős and A Rényi. On random graphs i. *Publ. Math. Debrecen*, 6:290–297, 1959.

[ER60] Paul Erdős and A Rényi. On the evolution of random graphs. *Publ. Math. Inst. Hungar. Acad. Sci*, 5:17–61, 1960.

[FJ18] Nic Freeman and Jonathan Jordan. Extensive condensation in a model of preferential attachment with fitnesses. *Preprint, arXiv:1812.06946*, 2018.

[Gil59] Edgar N Gilbert. Random graphs. *The Annals of Mathematical Statistics*, 30(4):1141–1144, 1959.

[GLY20] Arne Grauer, Lukas Lüchtrath, and Mark Yarrow. Preferential attachment with location-based choice: Degree distribution in the noncondensation phase. 2020.

[HJ16] John Haslegrave and Jonathan Jordan. Preferential attachment with choice. *Random Structures & Algorithms*, 48(4):751–766, 2016.

[HJ18] John Haslegrave and Jonathan Jordan. Non-convergence of proportions of types in a preferential attachment graph with three co-existing types. *Electronic Communications in Probability*, 23, 2018.

[HJY19] John Haslegrave, Jonathan Jordan, and Mark Yarrow. Condensation in preferential attachment models with location-based choice. *Random Structures and Algorithms*, 2019.

[HS18] Bruce Hajek and Suryanarayana Sankagiri. Community recovery in a preferential attachment graph. *Preprint, arXiv:1801.06818*, 2018.

[JCLX15] Winfried Just, Hannah Callender, M Drew LaMar, and Ying Xin. The preferential attachment model, 2015.

[JH03] James Holland Jones and Mark S Handcock. An assessment of preferential attachment as a mechanism for human sexual network formation. *Proceedings of the Royal Society of London B: Biological Sciences*, 270(1520):1123–1128, 2003.

[Jor13] Jonathan Jordan. Geometric preferential attachment in non-uniform metric spaces. *Electronic Journal of Probability*, 18, 2013.

[Jor18] Jonathan Jordan. Preferential attachment graphs with co-existing types of different fitnesses. *Journal of Applied Probability*, 55(4):1211–1227, 2018.

[KBM13] Jérôme Kunegis, Marcel Blattner, and Christine Moser. Preferential

attachment in online networks: measurement and explanations. In *Proceedings of the 5th Annual ACM Web Science Conference*, pages 205–214. ACM, 2013.

[KR14] PL Krapivsky and S Redner. Choice-driven phase transition in complex networks. *Journal of Statistical Mechanics: Theory and Experiment*, 2014(4):P04021, 2014.

[KW52] Jack Kiefer and Jacob Wolfowitz. Stochastic estimation of the maximum of a regression function. *The Annals of Mathematical Statistics*, 23(3):462–466, 1952.

[MP14] Yury Malyshkin and Elliot Paquette. The power of choice combined with preferential attachment. *Electronic Communications in Probability*, 19, 2014.

[MP15] Yury Malyshkin and Elliot Paquette. The power of choice over preferential attachment. *ALEA*, 12(2):903–915, 2015.

[Pem07] Robin Pemantle. A survey of random processes with reinforcement. *Probab. Surv*, 4(0):1–79, 2007.

[Pol14] Pollyanna. Pólya's Urn. *University of Southern California*, 2014.

[RM51] Herbert Robbins and Sutton Monro. A stochastic approximation method. *The annals of mathematical statistics*, pages 400–407, 1951.

[RTV07] Anna Rudas, Bálint Tóth, and Benedek Valkó. Random trees and general branching processes. *Random Structures & Algorithms*, 31(2):186–202, 2007.

[Sim55] Herbert A Simon. On a class of skew distribution functions. *Biometrika*, 42(3/4):425–440, 1955.

[Yul25] George Udny Yule. Ii.- a mathematical theory of evolution, based on the conclusions of Dr. JC Willis, FRS. *Philosophical transactions of*

the Royal Society of London. Series B, containing papers of a biological character, 213(402-410):21–87, 1925.